Nasa CR 65366

DEVELOPMENT OF PASSIVE TEMPERATURE CONTROL COATINGS FOR USE ON THE APOLLO VEHICLE ABLATIVE THERMAL PROTECTION SYSTEM

FINAL REPORT

Contract No. NAS 9-3406

AVSSD-0012-66-RR

April 1966

GPO PRICE $ ____

CFSTI PRICE(S) $ ____

Hard copy (HC) 4.00

Microfiche (MF) 1.00

ff 653 July 65

Prepared by

T. S. Laszlo
R. E. Gannon
C. T. Hughes
M. Rand

Prepared for

NASA MANNED SPACECRAFT CENTER
Structures and Mechanics Division/ES3
Houston, Texas

SPACE SYSTEMS DIVISION
AVCO CORPORATION
Wilmington, Massachusetts

DEVELOPMENT OF PASSIVE TEMPERATURE CONTROL COATINGS FOR USE ON THE APOLLO VEHICLE ABLATIVE THERMAL PROTECTION SYSTEM

FINAL REPORT

Contract No. NAS 9-3406

AVSSD-0012-66-RR

April 1966

Prepared by

T. S. Laszlo
R. E. Gannon
C. T. Hughes
M. Rand

Prepared for

NASA MANNED SPACECRAFT CENTER
Structures and Mechanics Division/ES3
Houston, Texas

SPACE SYSTEMS DIVISION
AVCO CORPORATION
Wilmington, Massachusetts

PREFACE

On 25 January 1965 a contract was awarded to Avco/RAD by the NASA Manned Spacecraft Center, Houston, Texas. The task specified in the contract was to perform the necessary experiments and analysis required in the development of passive temperature control coatings for use on the Apollo vehicle ablative thermal protection system to alleviate the low and high temperature extremes.

The work was performed at the Research and Development Division of Avco Corporation, Wilmington, Massachusetts, by the following scientists and engineers: Tibor S. Laszlo, (project manager) C. Chicklis, R.E. Gannon, R.J. Hill, C.T. Hughes, F. Mansur, M. Rand and F.J. Sheehan. The technical monitor during the first half of the contract time was Robert A. Vogt and during the second half, Edward Chimenti, NASA, MSC. The work was completed in January 1966 and the draft of the final report submitted on 15 February 1966.

(Page iv is intentionally blank).

CONTENTS

(Page vi is intentionally blank).

ILLUSTRATIONS

ILLUSTRATIONS (Concl'd)

TABLES

TABLES (Concl'd)

I. INTRODUCTION

A program to develop a passive temperature control system for the Apollo vehicle was started by the Research and Development Division of AVCO for the NASA Manned Spacecraft Center on 29 January 1965. The purpose of the coating system is to alleviate the high and low temperature extremes of the vehicle during the hot and cold soak portions of the trajectory. The requirements for the Apollo thermal control coating, as stated at the start of the program, specify that in addition to the essential vacuum and ultraviolet stability the coating system must:

1) have a low thermal emittance (ϵ) to limit the temperature decline during periods in the Earth's shadow,

2) have a low solar absorptance/thermal emittance ratio (α/ϵ) to limit the temperature increase due to solar irradiation,

3) withstand ascent heating without protection with no degradation of its optical properties,

4) allow the escape of gaseous decomposition products generated by the degassing and/or thermal degradation of the Apollo heat shield material.

As the program proceeded, however, additional information from the various phases of the Apollo Project became available, necessitating certain changes in the original requirements. For example, a reduction in the allowable maximum temperature of the heat shield led to further restriction in the optical properties of the thermal control system. To maintain the heat shield temperature below the revised maximum it was stipulated than an α/ϵ less than 0.4 and ϵ less than 0.5 would be required.

Recent Pegasus flights have indicated still another requirement. These flights have shown that the exhaust of the S-I retro and/or the abort tower jettison motor contaminates the thermal control coating. Consequently it was considered mandatory to protect the thermal control coating from such contamination to altitudes of approximately 600,000 feet. Since a protection system designed to be effective to 600,000 feet will also protect the thermal control coating during ascent heating a revision in the refractoriness requirement of the coating was possible.

During the third quarter of the contract, therefore, the program was redirected toward the accomplishment of two major tasks.

Task I. The development of a stable thermal control system with an α/ϵ of less than 0.4 and an ϵ of less than 0.5. Since this coating has to be protected up to an altitude of 600,000 feet, the original ascent heating stability requirement became unnecessary. The protection against the retrorocket exhaust contamination also limits the temperature rise in the heat shield material during ascent. This limits the degassing and thermal degradation of the heat shield material and alleviates the problem of providing escape paths for large volumes of gaseous decomposition products.

Task II. The development of a coating to protect the thermal control system to an altitude of 600,000 feet. This coating must be functional until the danger of contamination by the exhaust of retrorockets, fired to separate the abort tower and the third stage is past. After its function has been fulfilled this must be removed or disappear of its own volition without damage to the thermal control surface.

This report describes the entire program including screening tests, selection criteria, process developments and simulated environmental tests of both the thermal control coating and rocket exhaust protection system.

II. CONCLUSIONS

The work to develop a passive temperature control coating for the Apollo heat shield was based on the idea that no single material has the required optical properties. The judicious blending of two materials with different optical properties, however, is likely to give the desired results. Six different approaches were explored for blending optically diverse materials:

- Macro-Checkerboard Pattern
- Paint
- Conversion Coating
- Metallized Fabrics
- Multilayer Systems
- Cermets.

Individually, none of these approaches were found to meet the specified requirements. Two combinations of three of the six approaches, however, were developed to satisfy the Apollo specifications. These systems are:

1) Textured aluminum foil covered with a noncontinuous layer of potassium metasilicate.

2) Textured aluminum foil covered with an openweave fiberglass cloth.

Both systems involve the metallized fabric approach in that the thin aluminum foil is rolled and bonded to a fiberglass fabric substrate. They also utilize the checkerboard approach in that their surfaces are heterogeneous and their overall optical properties are a mean value of the individual areas. Finally, they also incorporate the multi-layer approach because they are three-dimensional and their optical properties depend on the transparency of the upper layer.

The optical parameters of the two coatings as prepared before and after a simulated space exposure corresponding to the Apollo flight schedule, are as follows:

	Before Exposure			After Exposure			Change		
	α	ϵ	α/ϵ	α	ϵ	α/ϵ	α	ϵ	α/ϵ
Aluminum with K_2SiO_3	0.16	0.51	0.31	0.17	0.55	0.30	0.01	0.04	0.01
Aluminum with Glass Cloth	0.15	0.48	0.31	0.15	0.45	0.33	0.0	0.03	0.02

The maximum and minimum temperatures reached by these coatings when continuously exposed to simulated solar radiation and space heat sink effects are as follows:

	Maximum		Minimum	
	°F	Exposure Hours	°F	Exposure Hours
Aluminum with K_2SiO_3	+ 75	6	-30	6
Aluminum with Glass Cloth	+120	6	+20	6

These values are well within the specifications of +150 and -150°F respectively, indicating that the optical parameter values are very conservative. In addition both coatings are refractory; and would likely withstand ascent heating without deterioration. This property, however, would become insignificant, with application of a sublimable coating over the thermal control coating.

A sublimable coating was developed to protect the surface during ascent against thermal decomposition and against contamination from the retro and abort tower separation rocket exhaust. This coating consists of a ternary mixture of camphor (75 percent), camphene (24 percent) and benzoic acid (1 percent). The mixture is applied to the thermal control surface with a heated, airless gun. The thickness of this coating is designed so as to persist up until the abort tower is separated; at the maximum heat (location 48-68) it is 0.1 inch. The residual coating will volatilize quickly when the vehicle is exposed to space vacuum and solar radiation. The total weight is approximately 85 pounds.

Removal of contaminants during sublimation has not been verified by testing to date. This resolution is required before it can be established that the sublimable coating technique is a satisfactory solution to the contamination problem.

III. SYSTEMS DEVELOPMENT

In order to select candidate systems for consideration, a review was made of the properties of general classes of materials in light of the requirements. Polished metals have a low ϵ but a high α whereas nonmetals have a low α/ϵ but a high ϵ. To fulfill the requirement of a low α and a low α/ϵ, therefore, a composite of a metal and nonmetal, or an unpolished, roughened metal should be used. The original ascent heating requirements dictated that only materials with melting points above 1100°F be considered. Consequently, only metals or metal composites with suitable refractory qualities were included in the preliminary selection.

The feasibility of fabricating surfaces with the desired optical properties by mixing surfaces of different optical properties to obtain a weighted average was demonstrated by the following experiments: A surface composed of alternating strips of Dow 17 treated magnesium ($\alpha_1 = 0.87$, $\epsilon_1 = 0.85$) and Dow 15 treated magnesium ($\alpha_2 = 0.13$, $\epsilon_2 = 0.05$) was prepared. Assuming that the optical properties of the composite surface would be a weighted average of those of the components, $\bar{\alpha}$ and $\bar{\epsilon}$ were calculated by the equations

$$\bar{\alpha} = \alpha_1 \frac{A_1}{A} + \alpha_2 \frac{A_2}{A}$$

$$\bar{\epsilon} = \epsilon_1 \frac{A_1}{A} + \frac{A_2}{A} \epsilon_2$$

where $\bar{\alpha}$ and $\bar{\epsilon}$ are the optical properties of the composite surface α_1, ϵ_1, and A1/A refer to the optical properties and area ratio of component number 1 and α_2, ϵ_2, and A2/A the optical properties and area ratio of component number 2 respectively. Two patterns were prepared, one in which the area ratio of each component was 0.5, and one in which A1/A was 0.66 and A2/A 0.33. In the case where both area ratio were 0.5 the calculated values were $\bar{\alpha} = 0.50$ and $\bar{\epsilon} = 0.45$ and the measured values were $\bar{\alpha} = 0.47$ and $\bar{\epsilon} = 0.43$. In the second case, where A1 was twice A2, the calculated values were $\bar{\alpha} = 0.61$ and $\bar{\epsilon} = 0.58$ and the measured values were $\bar{\alpha} = 0.59$ and $\bar{\epsilon} = 0.54$.

Since the "averaging" principle should apply to all composite surfaces regardless of the size of individual area elements, these results support the correctness of the approach of mixing metals and nonmetals, either as discreet areas or as individual particles to obtain the desired optical properties.

Various approaches and techniques that are likely to yield the desired coating were analyzed and investigated. All subjects and considerations described in Avco/RAD Proposals B876-264 and B875-264 were investigated as possible approaches to the program objectives. The measurement of the optical properties, α and ϵ, was used as a preliminary screening test of samples prepared according to various approaches. When the preliminary measurements bore out the original concept, additional effort was expended by varying the components and other parameters. On the other hand, where the initial tests did not look promising, the program was curtailed to be continued only after the other approaches had been further explored. The following is a detailed discussion of work performed with each separate approach. Details of the materials and processes used in the preparation of each system appear in the separate material report which will be issued as an adjunct to this report.

A. MACRO-CHECKERBOARD PATTERN

The desired overall α/ϵ and ϵ values can be obtained by alternating two surfaces with different radiative parameters in a repeat pattern. The ratio of the areas of the two surfaces will determine the optical properties of the entire surface. This approach was used to satisfy the thermal control requirements of Explorer I[1]. For the Apollo thermal control system, it appears necessary to incorporate a polished metal surface with a low ϵ and a nonmetal surface with a low α/ϵ value. The low lateral heat transfer rate in a poor conductor such as the Apollo ablator requires a very small repeat pattern to avoid hot spots. For this reason, methods of applying small repeat patterns to large surfaces have been studied. In one technique, developed for this purpose, standard corss-hatch patterns were used in conjunction with the Kodak Photo Resist process to etch and/or anodize small repeat patterns into metal surfaces. The patterns that have been used are shown in Figure 1.

Several techniques of utilizing the principle of checkerboard surfaces to give the desired optical properties were evaluated (Table I). In one technique 30 percent of a gold plated FED teflon surface was covered by a sheet of clear FEP teflon. The use of the clear teflon cover effectively reduced the α/ϵ of the gold surface from 2.8 to 1.0 by increasing ϵ from 0.04 to 0.14 while only increasing α from 0.12 to 0.14.

A second macro checkerboard technique found to be promising involves the use of small repeat patterns etched into metallic surfaces. Portions of the etched pattern can then be selectively anodized and/or polished to give the desired optical properties. For example, a repeat pattern of 0.020-inch diameter circles spaced 0.020-inch apart etched into an aluminum sheet, which in the "as received" condition had an α of 0.42 and an ϵ of 0.06, reduced the α to 0.27 and only increased ϵ to 0.07. (CAO 59-5)* When this surface was then treated so that the holes were anodized to increase ϵ and the surface mechanically polished to decrease α, a composite surface (CAO 60-2) with an α of 0.21 and and ϵ of 0.21 resulted. On another sample (CAA 61-1) with the same pattern α and ϵ were further reduced to 0.11 and 0.09 respectively by chemically polishing the entire surface.

In utilizing the etching technique to control the optical properties of the more refractory metals, titanium and stainless steel, it was found that α was not so readily reduced as in the case of aluminum. In an attempt to reduce the α/ϵ, stainless steel and titanium samples were etched in the 4001 pattern by the Kodak Photo Resist process to increase α and subsequently gold plated to reduce α. The gold plated stainless steel sample had an α of 0.3 and an ϵ of 0.08. The surface of this sample was then mechanically polished until only the etched

* Identification number of the coating as listed in the tables.

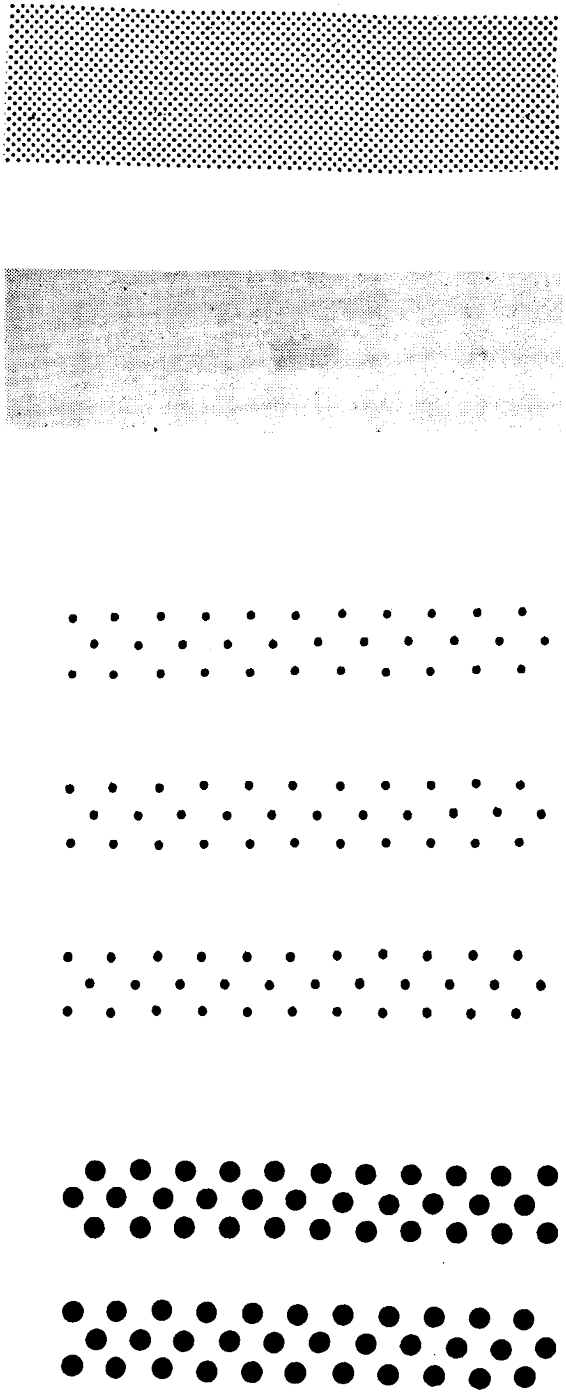

4001

4035

031

034

036

085

089

Figure 1 ETCH PATTERNS

TABLE I

MACRO-CHECKERBOARD SURFACES

Designation	Description	α	ϵ	α/ϵ
Magnesium Type A231B Sheet Stock 0. 125-Inch Thick				
CM048A	-Combination anodized and machined surfaces to give alternating strips of Dow 17 (green) and Dow 15 (silvery), each stripe 0. 06-inch wide.	0. 47	0. 43	1. 09
CM048B	-Same as above except Dow 17 stripes are 0. 12-inch and Dow 15 stripes are 0. 06-inch.	0. 59	0. 54	1. 09
Aluminum 0.010-Inch Thick				
CA059-5	-Hole pattern 4001 -- 0. 020-inch diameter holes spaced 0. 020-inch apart and etched to a depth of 0. 004- to 0. 005-inch.	0. 27	0. 07	3. 85
CAA66-5	-Hole pattern 4001 -- etched through aluminum foil (to form perforated foil) on Al Foil.	0. 23	0. 06	3. 8
CAB66-6	-Hole pattern 4001 -- etched through aluminum foil (to form perforated foil) On Black Paint.	0. 37	0. 18	2. 1
CA060-2	-Hole pattern 4001 -- bottom of holes anodized, surface polished.	0. 21	0. 21	1.00
CAA61-1	-Hole pattern 4001 -- bottom of holes and surface chemically polished.	0. 11	0. 09	1. 22
CAA59-3	-Hole pattern 4035 -- 0. 010-inch diameter holes spaced 0. 010-inch apart, etched to a depth of 0. 005-inch.	0. 28	0. 11	2. 55
CAA103-1	-Hole pattern 4001 surface anodized polished holes.	0. 30	0. 70	0. 43

TABLE I (Cont'd)

Designation	Description	a	ϵ	a/ϵ
	Titanium 99.7 Percent Pure Ti 0.010-Inch Sheet			
C1074-3	-Hole pattern 4001 -	0.49	0.12	4.1
C1176-5	-Hole pattern 4001 -- followed by chemical polishing	0.41	0.10	4.1
C1074-4	-Hole pattern 0.034	0.54	0.12	4.5
C1176-6	-Hole pattern 0.034 -- followed by chemical polishing	0.41	0.09	4.6
C1A74-5	-Hole pattern 4001 -- etched through to form perforated sheet. (Al Foil Substrate)	0.62	0.14	4.4
	Steel 302SS Sheet Stock			
CE067-2	-Hole pattern 4001 -- 0.020-inch diameter 0.020-inch apart, etched to depth of 0.005-inch.	0.57	0.16	3.56
CE061-3	-Hole pattern 031 -- 0.040-inch diameter, 3/16-inch apart, 0.010-inch deep	0.50	0.20	2.50
CE067-3	-Hole pattern 039 -- 0.040-inch diameter, 3/16-inch apart, 0.010-inch deep	0.47	0.17	2.77
CE067-4	-Hole pattern 036 -- 0.040-inch diameter, 3/16-inch apart, 0.005-inch deep	0.47	0.16	2.94
CE067-5	-Hole pattern 089 -- 0.090-inch diameter, 1/8-inch apart, 0.005-inch deep	0.47	0.17	2.77

TABLE I (Cont'd)

Designation	Description	α	ϵ	α/ϵ
Gold Patterns				
CTU27-3	-Gold coated FEP, 30 percent covered by clear FEP	0.14	0.14	1.00
CUA51-1	-Gold plated Rene' 41 metal cloth on aluminum foil	0.46	0.20	2.3
CUW51-1A	-Gold plated Rene' metal cloth on white paint	0.56	0.55	1.02
CIU76-13	-Hole pattern 4001, gold plated titanium field with etched titanium holes	0.32	0.10	3.2
CEU76-14A	-Hole pattern 4001, stainless steel field with gold plated holes	0.38	0.13	2.92
CEU76-14B	-Hole pattern 4001, gold plated field, stainless steel holes	0.30	0.08	3.75
CUA90-7A	-Gold plated expanded nickel on aluminum foil	0.30	0.07	4.3
CUA90-7D	-Gold plated expanded nickel on aluminum paint	0.23	0.66	0.35
CUR90-7E	-Gold plated expanded nickel on silver paint	0.32	0.58	0.55
CEA77A-1A	250 x 250-gage Mesh Stainless Steel Screen on Al Foil	0.65	0.32	2.0
CEA77A-2A	200 x 200-gage Mesh Stainless Steel Screen on Al Foil	0.60	0.29	2.0
CEA77A-3A	100 x 100 gage Mesh Stainless Steel Screen on Al Foil	0.65	0.27	2.4
CEA77A-4A	24 x 100 gage Mesh Stainless Steel Screen on Al Foil	0.73	0.42	1.7

TABLE I (Concl'd)

Designation	Description	α	ϵ	α/ϵ
CTA19-1	18 x 18 gage Mesh Al screen imbedded in FEP Teflon	0.50	0.40	1.25
Paint Patterns				
CZA101-4	11 percent Zn 0, 89 percent Al	0.26	0.28	0.93
CZA101-6	19 percent Zn 0, 81 percent Al	0.27	0.36	0.75
CZA101-5	28 percent Zn 0, 72 percent Al	0.28	0.54	0.52
CZA101-7	44 percent Zn 0, 56 percent Al	0.33	--	--

holes remained coated with gold. This composite gold-stainless steel surface exhibited an α of 0.38 and an ϵ of 0.13. A similar gold-titanium surface showed an α of 0.6 and ϵ of 0.2. By changing the plating and etching sequence, samples with gold fields and titanium or stainless steel holes were prepared. In the case of titanium this sample exhibited an α of 0.32 and an ϵ of 0.10 whereas the corresponding stainless steel checkerboard showed an α of 0.38 and an ϵ of 0.20.

The use of a wire mesh over the heat shield material to form a checkerboard appeared to be attractive for two reasons, (1) it would serve to reduce the ϵ of the surface, and (2) it would provide escape paths for any liberated gases from the ablator. To measure the optical properties of such composite surfaces, stainless steel screens were placed over white and black painted Apollo ablator samples. In the case of the white painted sample the addition of the wire mesh screen reduced ϵ from 0.89 to 0.54 but increased α from 0.14 to 0.70 and in the case of the black sample ϵ was reduced from 0.98 to 0.61 and α from 0.97 to 0.78. Four different mesh screens (250, 200, 100 and 24 x 110 mesh) were used but the difference in their effectiveness was negligible.

Using the same principle, a checkerboard pattern consisting of a piece of gold plated expanded nickel over a surface of white ZnO paint showed and α of 0.23 and an ϵ of 0.66. The same gold plated nickel over a mixed paint of 95 percent ZnO and 5 percent Ag showed an α of 0.32 and an ϵ of 0.58.

In the application of the checkerboard principle to an alternate pattern of aluminum and zinc oxide pigmented paints, $\bar{\alpha}$ has been observed to exceed both α_1 and α_2. These surfaces were prepared by painting a sample with one of the paints and then applying a predetermined pattern of the other paint on its surface. It is likely that the discrepancy between the calculated $\bar{\alpha}$ and the measured $\bar{\alpha}$ was due to either an increase in surface roughness in the areas of the second paint or to some transparency in the second paint. It has also been suggested that a difference in particle size between the two pigments might be the cause of the observed discrepancy.[2]

The interweaving of glass and metallic fibers should result in a checkerboard pattern with optical properties which are controlled by the choice of weave and metal fiber concentration. A survey was conducted on the commercial availability of metallized yarns and fabrics composed of aluminum, silver and gold. The commercial multi-colored yarns were found to be laminated ribbons (in varying widths) consisting of a thermoplastic polymer containing aluminum pigments. Colored effects (gold) were obtained by adding another pigment to the aluminum. In no case did any of these yarns possess suitable refractory properties.

B. PAINTS

The formulation of paints to achieve the required optical properties is an extension of the macro-checkerboard technique to microparticle size level. In this investigation, metallic pigment particles served as the areas of low ϵ whereas the continuous binder phase or added white pigment acted as areas of low α/ϵ. By control of the proportions of each component, pigment, and binder, as well as control of the processing techniques, paints with selected optical properties were formulated.

Numerous paints, using various pigments, mixed pigments and binders as well as process techniques were compounded or obtained from commercial manufacturers. In the intial experiments when the objective was to prepare a coating with both low α and low ϵ, metallic pigments, aluminum and silver were mixed with binders, such as, potassium and sodium silicate, methyl phenyl silicone resin or butyl titanate. Several paints with α and ϵ values less than 0.2 were prepared from these ingredients. A list of the paints tested, with the method of preparation is given in Table II. All paints were applied by spraying.

When it was specified that ϵ should be allowed to be as high as 0.5 in order to minimize the α/ϵ ratio, white pigments were added to the metallic pigments in order to increase ϵ. It appeared that if the linear mixing laws applied, a blend of about 60 percent metallic paint and 40 percent white paint should have the required optical properties. Mixtures of aluminum and silver paints (α = 0.2 and ϵ = 0.2) with zinc oxide, aluminum oxide, and potassium titanate paints (α = 0.1, ϵ = 0.9) were prepared. In all cases it was found that the α of the resulting mixture exceeded the α of either of the constituent paints. Processing variables, such as ball milling, homogenizing or changing the order in which the ingredients were added did not modify the results. Figure 2 shows the optical properties for a series of mixtures of silver and zinc oxide paints. The results are typical of the other mixtures investigated and indicate that simple mixing laws cannot be applied to the radiation properties of blended paints. This observation was recently substantiated in a paper by E. Schatz,[2] in which he concluded after an extensive investigation that the radiation properties of binary mixtures do not necessarily follow the proportionate composition.

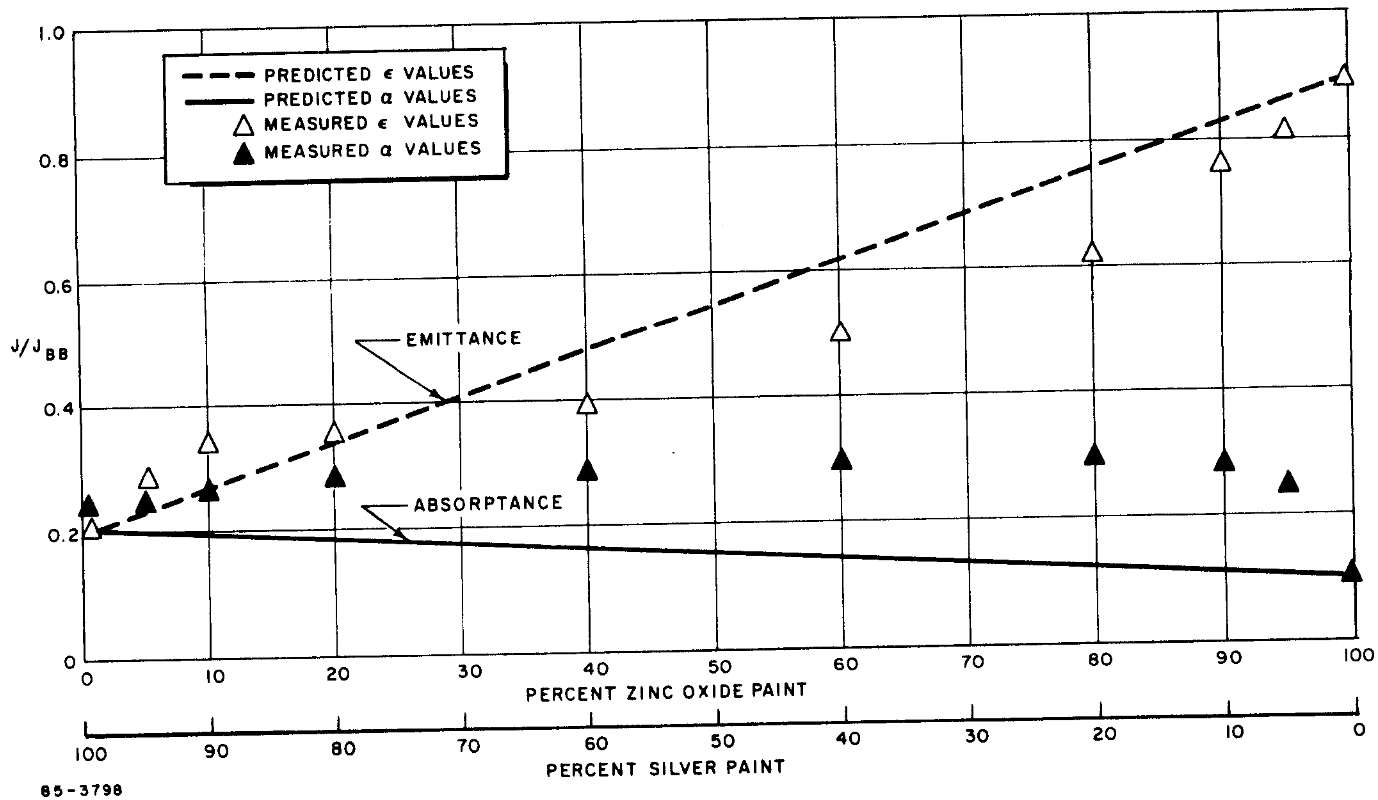

Figure 2 EFFECT OF COMPOSITION ON OPTICAL PROPERTIES OF MIXED PAINTS

TABLE II

PAINTS

Designation	Pigment	Binder	Process	Substrate	α	ϵ	α/ϵ
Aluminum-Silicone Systems							
PAS20-3	Al	Silicone	Fuller Paint Company	Copper	0.02	0.10	2.0
PAS22-7	Al	Silicone	Fuller Paint Company	Copper	0.21	0.21	1.0
PAS20-4	Al	Silicone	Fuller Paint Company	Copper	0.23	0.13	1.8
PAS22-8	Al	Silicone	Fuller Paint Company	Copper	0.20	0.19	1.05
PAS71-1	Al-830 (70 Percent)	DC803 30 Percent	Ball Milled	Copper	0.18	0.18	1.00
				Second Coat	0.20	0.18	1.10
PAS78-5A	Al-322 (70 Percent)	DC803 30 Percent	Ball Milled	Copper	0.20	0.20	1.00
PAS78-5B	Al-322 (70 Percent)	DC803 30 Percent	Ball Milled	116 Glass Cloth	0.26	0.29	0.90
PAS78-5C	Al-322 (70 Percent)	DC803 30 Percent	Ball Milled	EM-30 Glass Cloth	0.17	0.13	1.31
PAS78-7A	Al-830 (70 Percent)	DC803 30 Percent	Ball Milled	Copper	0.24	0.23	1.04
PAS78-7B	Al-830 (70 Percent)	DC803 30 Percent	Ball Milled	116 Glass Cloth	0.44	0.36	1.22
PAS78-7C	Al-830 (70 Percent)	DC803 30 Percent	Ball Milled	EM-30 Glass Cloth	0.30	0.26	1.15
PAS82-6A	Al-830 (70 Percent)	DC803 30 Percent	Ball Milled	5026	0.21	0.18	1.17
PAS96-8F	Al (Heatrem)	Silicone	Spec. Co.	Copper	0.23	0.26	0.88
Aluminum-Butyl Titanate Systems							
PAY31-5	0 Percent	100 Percent	Ball Milled	Al Foil	0.21	0.60	0.35
PAY31-1	70 Percent PL	30 Percent	Ball Milled	Copper	0.30	0.22	1.36
PAY31-2	80 Percent PL	20 Percent	Ball Milled	Copper	0.35	0.25	1.40
PAY31-3	90 Percent PL	10 Percent	Ball Milled	Copper	0.32	0.34	0.94
PAY31-4	0 Percent PL	100 Percent	Ball Milled	Copper	0.28	0.77	0.36
PAY33-4	70 Percent PL	30 Percent	Ball Milled	Copper	0.30	0.21	1.43
PAY33-5	80 Percent PL	20 Percent	Ball Milled	Copper	0.35	0.23	1.50
PAY33-6	90 Percent PL	10 Percent	Ball Milled	Copper	0.45	0.41	1.10
PAY33-7	70 Percent PL	30 Percent	Ball Milled	Copper	0.49	0.40	1.22
PAY33-8	80 Percent PL	20 Percent	Ball Milled	Copper	0.40	0.23	1.75
PAY 33-9	90 Percent PL	10 Percent	Ball Milled	Copper	0.52	0.46	1.14

TABLE II (Cont'd)

Designation	Pigment	Binder	Process	Substrate	α	ϵ	α/ϵ
PAY48-2	80 Percent 322	20 Percent	Ball Milled	Copper	0.26	0.28	0.92
PAY48-3	80 Percent 422	20 Percent	Ball Milled	Copper	0.40	0.33	1.21
PAY48-5	80 Percent 40-XD	20 Percent	Ball Milled	Copper	0.26	0.18	1.42
PAY82-7A	70 Percent A1-830	30 Percent	Ball Milled	5026	0.28	0.29	0.97
PAY97-4A	50 Percent A1-830	50 Percent	Ball Milled	Copper	0.44	0.41	1.07
Aluminum-Silicate Systems							
PAK48-1	70 Percent 830 A1	30 Percent K_2SiO_3*	Ball Milled	Copper	0.47	0.45	1.04
PAK78-6A	70 Percent 322 A1	30 Percent K_2SiO_3	Ball Milled	Copper	0.22	0.24	0.92
PAK78-6B	70 Percent 322 A1	30 Percent K_2SiO_3	Ball Milled	116 Glass Cloth	0.36	0.34	1.06
PAK78-6C	79 Percent 322 A1	30 Percent K_2SiO_3	Ball Milled	EM-30 Glass Cloth	0.29	0.21	1.38
PAK78-8A	70 Percent 830 A1	30 Percent K_2SiO_3	Ball Milled	Copper	0.36	0.37	0.97
PAK78-8B	70 Percent 830 A1	30 Percent K_2SiO_3	Ball Milled	116 Glass Cloth	0.44	0.39	1.13
PAK78-8C	70 Percent 830 A1	30 Percent K_2SiO_3	Ball Milled	EM-30 Glass Cloth	0.47	0.25	1.88
PAK97-7A	50 Percent 322 A1	50 Percent K_2SiO_3	Ball Milled	Copper	0.29	0.36	0.81
Silver-Silicone Systems							
PRS55-5	70 Percent 135	30 Percent DC805	Homogenized	Copper	0.23	0.18	1.26
				Second Coat	0.19	0.21	0.91
PRS56-4	70 Percent 135	30 Percent DC805	Ball Milled	Copper	0.21	0.24	0.87
PRS55-7	70 Percent 131	30 Percent DC805	Homogenized	Copper	0.25	0.21	1.18
				Second Coat	0.21	0.25	0.84
PRS65-2	70 Percent 131	30 Percent DC805	Ball Milled	Copper	0.25	0.32	0.78
PRS78-3A	70 Percent 131	30 Percent DC803	Ball Milled	Copper	0.28	0.37	0.76
PRS78-3B	70 Percent 131	30 Percent DC803	Ball Milled	116 Glass Cloth	0.31	0.29	1.07
PRS78-3C	70 Percent 131	30 Percent DC803	Ball Milled	EM-30 Glass Cloth	0.30	0.22	1.36
PRS82-3A	70 Percent 131	30 Percent DC803	Ball Milled	5026	0.43	0.43	1.00
Silver-Butyl Titanate Systems							
PRY55-2	70 Percent 131	30 Percent	Homogenized	Copper	0.21	0.13	1.6
				Second Coat	0.22	0.17	1.29

*30° Be Solution

TABLE II (Cont'd)

Designation	Pigment	Binder	Process	Substrate	α	ϵ	α/ϵ
PRY68-55-2	70 Percent 131	30 Percent	Ball Milled	Copper	0.38	0.36	1.06
PRY82-4B	70 Percent 131	30 Percent	Ball Milled	5026	0.25	0.34	0.74
Silver Silicate Systems							
PRK55-1	70 Percent 131	30 Percent K_2SiO_3	Homogenized	Copper	0.25	0.21	1.2
				Second Coat	0.18	0.29	0.62
PRK55-4	70 Percent 131	30 Percent K_2SiO_3	Ball Milled	Copper	0.24	0.18	1.3
				Second Coat	0.23	0.29	0.79
PRK55-6	70 Percent 131	30 Percent Na_2SiO_3	Homogenized	Copper	0.33	0.26	1.25
				Second Coat	0.41	0.59	0.70
PRK70-1	70 Percent 131	30 Percent K_2SiO_3	Ball Milled	Copper	0.24	0.21	1.1
				Second Coat	0.25	0.23	1.1
PRK78-4A	70 Percent 131	30 Percent K_2SiO_3	Ball Milled	Copper	0.29	0.22	1.32
PRK78-4B	70 Percent 131	30 Percent K_2SiO_3	Ball Milled	116 Glass Cloth	0.30	0.28	1.07
PRK78-4C	70 Percent 131	30 Percent K_2SiO_3	Ball Milled	EM-30 Glass Cloth	0.29	0.24	1.21
PRK82-5A	70 Percent 131	30 Percent K_2SiO_3	Ball Milled	5026	0.33	0.28	1.18
Zinc Oxide Paints							
PZS57-5	70 Percent 12	30 Percent DC805	Ball Milled	Copper	0.16	0.90	0.18
PZS57-9	70 Percent 500	30 Percent DC805	Ball Milled	Copper	0.15	0.88	0.17
PZY57-6	70 Percent 12	30 Percent Titanate	Ball Milled	Copper	0.12	0.89	0.13
PZY57-10	70 Percent 500	30 Percent Titanate	Ball Milled	Copper	0.23	0.93	0.25
PZK57-7	70 Percent 12	30 Percent K_2SiO_3	Ball Milled	Copper	0.12	0.95	0.13
PZK57-11	70 Percent 500	30 Percent K_2SiO_3	Ball Milled	Copper	0.11	0.98	0.11
PZK57-8	70 Percent 12	30 Percent Na_2SiO_3	Ball Milled	Copper	0.15	0.97	0.15
PZK57-12	70 Percent	30 Percent Na_2SiO_3	Ball Milled	Copper	0.10	0.97	0.10
PZS82-8A	70 Percent 500	30 Percent DC805	Ball Milled	5026	0.17	0.96	0.18
PZY82-9A	70 Percent 500	30 Percent Titanate	Ball Milled	5026	0.15	0.87	0.17
Al_2O_3 Paints							
PQS71-10	70 Percent A-14	30 Percent DC803	Ball Milled	Copper	0.13	0.83	0.15
				Second Coat	0.12	0.84	0.14
PQS78-1A	70 Percent T-61	30 Percent DC803	Ball Milled	Copper	0.39	0.89	0.44
PQS78-1B	70 Percent T-61	30 Percent DC803	Ball Milled	116 Glass Cloth	0.38	0.84	0.45

TABLE II (Cont'd)

Designation	Paint A	Paint B	Mixing Process	Substrate	α	ϵ	α/ϵ
PQS78-1C	70 Percent T-61	30 Percent DC803	Ball Milled	EM-30 Glass	0.40	0.72	0.56
PQK78-2A	70 Percent T-61	30 Percent K_2SiO_3	Ball Milled	Copper	0.25	0.90	0.28
PQK78-2B	70 Percent T-61	30 Percent K_2SiO_3	Ball Milled	116 Glass Cloth	0.26	0.78	0.33
PQK78-2C	70 Percent T-61	30 Percent K_2SiO_3	Ball Milled	EM-30 Glass Cloth	0.28	0.80	0.35
Mixed Paints $ZnO-K_2SiO_3$							
PRZS65-3	95 Percent PRS65-2	5 Percent PZS57-5	Ball Milled	Copper	0.30	0.39	0.77
PRZS65-4	90 Percent PRS65-2	10 Percent PZS57-5	Ball Milled	Copper	0.29	0.37	0.78
PRZS65-5	80 Percent PRS65-2	20 Percent PZS57-5	Ball Milled	Copper	0.28	0.39	0.72
PRZS68-3	60 Percent PRS65-2	40 Percent PZS57-5	Ball Milled	Copper	0.38	0.61	0.62
PRZS68-2	40 Percent PRS65-2	60 Percent PZS57-5	Ball Milled	Copper	0.42	0.64	0.66
PRZS68-1	20 Percent PRS65-2	80 Percent PZS57-5	Ball Milled	Copper	0.39	0.80	0.49
Mixed Paints (Silver-$ZnO-K_2SiO_3$)							
PRZK70-2A	95 Percent PRK55-4	5 Percent PZK57-7	Ball Milled	Copper	0.25	0.30	0.83
				Second Coat	0.25	0.28	0.89
PRZK70-3A	80 Percent PRK55-4	10 Percent PZK57-7	Ball Milled	Copper	0.26	0.33	0.79
				Second Coat	0.26	0.35	0.74
PRZK70-4A	80 Percent PRK55-4	20 Percent PZK57-7	Ball Milled	Copper	0.27	0.36	0.75
				Second Coat	0.30	0.32	0.94
PRZK70-5A	60 Percent PRK55-4	40 Percent PZK57-7	Ball Milled	Copper	0.34	0.52	0.65
				Second Coat	0.27	0.39	0.69
PRZK70-6A	40 Percent PRK55-4	60 Percent PZK57-7	Ball Milled	Copper	0.33	0.53	0.62
				Second Coat	0.29	0.49	0.59
PRZK70-7A	20 Percent PRK55-4	80 Percent PZK57-7	Ball Milled	Copper	0.37	0.78	0.47
				Second Coat	0.29	0.61	0.48
PRZK70-8A	10 Percent PRK55-4	90 Percent PZK57-7	Ball Milled	Copper	0.31	0.66	0.47
				Second Coat	0.27	0.75	0.36
PRZK70-9A	5 Percent PRK55-4	95 Percent PZK57-7	Ball Milled	Copper	0.23	0.77	0.30
				Second Coat	0.24	0.80	0.30
-With Butyl Titanate							
PRZY68-6	95 Percent PRY68-4A	5 Percent PZY57-6	Ball Milled	Copper	0.54	0.73	0.74
				Second Coat	0.71	0.82	0.87
PRZY68-7	90 Percent PRY68-4A	10 Percent PZY57-6	Ball Milled	Copper	0.53	0.54	0.98
				Second Coat	0.70	0.88	0.80
PRZY68-8	80 Percent PRY68-4A	20 Percent PZY57-6	Ball Milled	Copper	0.47	0.55	0.85
				Second Coat	0.57	0.70	0.81
PRZY68-9	60 Percent PRY68-4A	40 Percent PZY57-6	Ball Milled	Copper	0.60	0.78	0.77
				Second Coat	0.56	0.75	0.75

TABLE II (Concl'd)

Designation	Paint A	Paint B	Mixing Process	Substrate	α	ϵ	α/ϵ
PRZY68-10	40 Percent PRY68-4A	60 Percent PZY57-6	Ball Milled	Copper	0.51	0.82	0.62
				Second Coat	0.53	0.81	0.65
PRZY68-11	20 Percent PRY68-4A	80 Percent PZY57-6	Ball Milled	Copper	0.49	0.86	0.57
PAQS71-2A	95 Percent PAS71-1	5 Percent PQS71-10	Ball Mixed	Copper	0.24	0.25	0.96
				Second Coat	0.32	0.34	0.94
PAQS71-3A	90 Percent PAS71-1	10 Percent PQS71-10	Ball Mixed	Copper	0.31	0.35	0.89
				Second Coat	0.35	0.35	1.00
PAQS71-4A	80 Percent PAS71-1	20 Percent PQS71-10	Ball Mixed	Copper	0.34	0.35	0.97
				Second Coat	0.47	0.49	0.96
PAWS71-5A	60 Percent PAS71-1	40 Percent PQS71-10	Ball Mixed	Copper	0.38	0.40	0.95
				Second Coat	0.50	0.50	1.00
PAQS71-6A	40 Percent PAS71-1	60 Percent PQS71-10	Ball Mixed	Copper	0.57	0.63	0.91
				Second Coat	0.64	0.72	0.89
PAQS71-7A	20 Percent PAS71-1	80 Percent PQS71-10	Ball Mixed	Copper	0.51	0.59	0.86
				Second Coat	0.63	0.72	0.88
PAQS71-8A	10 Percent PAS71-1	90 Percent PQS71-10	Ball Mixed	Copper	0.58	0.70	0.83
				Second Coat	0.62	0.83	0.75
PAQS71-9A	5 Percent PAS71-1	95 Percent PQS71-10	Ball Mixed	Copper	0.53	0.78	0.68
				Second Coat	0.56	0.87	0.64
Miscellaneous Systems							
PAD97-1A	A1-803 (50 Percent)	Glass Resin (50 Percent)	Ball Milled	Copper	0.59	0.61	0.97
PKtD97-2A	K_2TiO_3 (50 Percent)	Glass Resin (50 Percent)	Ball Milled	Copper	0.08	0.96	0.08
PKtS92-1A	K_2TiO_3 (40 Percent)	Silicone (605)	Ball Milled	Copper	0.10	0.91	0.11
PKtK92-2A	K_2TiO_3 (40 Percent)	K_2SiO_3 (60 Percent)	Ball Milled	Copper	0.10	0.92	0.11
PKtS99-2A	K_2TiO_3 (12.5 Percent)	Silicone (87.5 Percent)	Ball Milled	5026	0.20	0.94	0.21
PAX81-6	Al (85 Percent)	Polyimide (15 Percent)	Stirred	Copper	0.66	0.50	1.32
PAX81-7	Al (82 Percent)	RC5034 Polyimide (18 Percent)	Stirred	Copper	0.71	0.67	1.06

C. CONVERSION COATINGS

A wide variety of chemical surface treatments was applied to the following metals:

Magnesium

Aluminum

Titanium

Steel

The treatments were designed to alter the chemical composition of the surface by such processes as anodizing, chromate and fluoride conversion. In some cases a combination of surface treatments was applied to the same specimen.

As shown in Table III, all the tested conversion coatings had either a high ϵ or a high α/ϵ which eliminated them from further consideration as control coatings. A conversion coating (Alodine 401) which lends itself to controlled variations in ϵ by additional etching was described by Pezdirtz and Wakelyn.[3] Variations in the optical properties of this coating, a mixture of chromium phosphate and aluminum phosphate, is exercised by control of the immersion time in a sodium hydroxide solution. For example, a 60 second immersion of an Alodine 401-45 coated piece of aluminum foil resulted in a change of ϵ from 0.2 to 0.4 while α remained nearly constant. It was attempted to tailor the α and ϵ of the alodine coating by NaOH etching treatments, as reported by Pezdirtz and Wakelyn. In isolated cases the optical properties were observed to approach the requirements (e.g. α =0.23 ϵ =0.49), but the reproducibility was rather poor. The difficulty in control of the optical properties is due very likely to the great sensitivity of ϵ to the etching time:

Pezdirtz and Wakelyn indicate a rate of change ϵ greater than 1 percent per second. Since reliable control of etching times to plus or minus a few seconds is not possible for large pieces, it would be necessary to decrease the rate of change of ϵ with etching to make this process practical. Since ϵ is also sensitive to other process variables the development of a process of the required precision appears to be beyond the scope of this program.

TABLE III

CONVERSION COATINGS

Designation	Description	α	ϵ	α/ϵ
Magnesium:	Type AZ31B Sheet Stock 0.125-inch Thick			
VMO 47-1	-Dow 17 - High Density Coating	0.87	0.85	1.03
VMO 47-7	-Dow 17 - Dark Coating	0.82	0.80	1.02
VMO 47-8	-Dow 17 - Light Coating	0.51	0.47	1.08
VMO 47-2	-Dow 15 - Bright Dip	0.13	0.05	2.60
VMO 47-9	-H. A. E. - Light Brown	0.44	0.09	4.90
VMO 47-3	-H. A. E. - Dark Brown	0.57	0.51	1.12
VMO 47-4	-H. A. E. - Bifluoride Sealed and Post-Treat Dichromate	0.51	0.43	1.19
VMO 47-6	-H. A. E. - Black Anodize	0.69	0.57	1.21
VMO 41-5	-Dow 9 - Galvanic Anodize	0.88	0.81	1.09
VMO 80-2	-Dow 7 - Galvanic Anodize	0.74	0.55	1.35
Aluminum:	Type 6061 Sheet Stock, Thickness Varied from 0.250 to 0.62-inch			
VA 52-9	-Chemical Polishing	0.14	0.05	2.8
VAO 33-2	-Light Anodized	0.40	0.79	0.51
VAO 33-1	-Heavy Anodized	0.38	0.89	0.42
VAO 30-8	-Gold Plated	0.19	0.06	3.1
VAO 73-2	-Alodine 600 - Chromate Treatment	0.42	0.08	5.3
VAO 73-3	-Aldine 1200 - Chromate Treatment	0.34	0.09	3.7
VAO 73-1	-Iridite 14 - Chromate Treatment	0.33	0.09	3.6
Alodyne 407-41 (equivalent to 401-45)				
VAO106-1	30 second Alodyne immersion	0.24	0.08	3.0
VAO106-2	60 second Alodyne immersion	0.35	0.14	2.5
VAO106-3	90 second Alodyne immersion	0.45	0.32	1.4
VAO106-4	120 second Alodyne immersion	0.46	0.38	1.2
VAO106-5	150 second Alodyne immersion	0.46	0.48	0.96
VAO106-6	180 second Alodyne immersion	0.49	0.58	0.85

TABLE III (Concl'd)

Designation	Description	α	ϵ	α/ϵ
Sodium Hydroxide Treatment of Alodyne 407-41				
VAO101-14	10 seconds in 0.1N Na04	0.28	0.49	0.57
VAO101-15	20 seconds in 0.1N Na04	0.27	0.29	0.93
VAO101-16	30 seconds in 0.1N Na04	0.23	0.49	0.47
VAO101-17	40 seconds in 0.1N Na04	0.22	0.32	0.69
VAO101-18	60 seconds in 0.1N Na04	0.20	0.32	0.63
VAO105-3	1 minute in 0.025 Na04	0.32	0.41	0.78
VAO105-4	10 minutes in 0.025 Na04	0.26	0.56	0.46
VAO105-5	20 minutes in 0.025 Na04	0.32	0.54	0.59
VAO105-6	30 minutes in 0.025 Na04	0.31	0.45	0.69
Titanium				
VT78-15	Nitrided Titanium	0.57	0.18	3.17

D. FABRICS

The refractivity, porosity, flexibility and variability of optical properties make woven fiberglass fabrics likely candidates for thermal control systems. Potentially they could be used in one of three ways.

1) As a component of a multilayer system. Fine weaves, partially transparent to the solar spectrum with high ϵ values should be most effective in this application. This approach was supported by the fact that the α and ϵ of a fine weave glass cloth (No. 108) on a piece of Al foil were found to be 0.18 and 0.28 respectively, whereas the same cloth on a sample of white paint exhibited an α of 0.31 and an ϵ of 0.47. The multilayer systems using glass cloths as one of the layers are given in Table IV and discussed in Section III. F.

2) Fabrics as components in checkerboard pattern have been discussed in section III-A.

3) As a substrate for deposited metals or paints. Used in this way the thermal control surface would take the form of a textured metal surface due to the fabric substrate. For example, gold deposited on Refrasil glass cloth showed an α of 0.68 and an ϵ of 0.39. The metallized fabric systems that were tested are listed in Table V.

Utilized in the latter way, i.e. as a substrate for vapor deposited metals, the measurements showed that in all cases, α of the composite was too high. An extension of this approach, however, proved to be more useful. This involved bonding under pressure 0.0005 mil aluminum foil to the fabric surface, so that the foil assumed the texture of the cloth. The initial laminate of this type evaluated on the program consisted of a fine weave cotton fabric coated with 0.0005 mil aluminum. Its α and ϵ were measured to be 0.21 and 0.18 respectively. Since both the cotton fabric and adhesive used to bond the foil to the fabric were limited to low temperature applications, the manufacturer* was requested to prepare samples with better refractoriness. Fiberglass cloth as well as a high temperature adhesive, HT424Fwere supplied to the manufacturer for this purpose. Evaluation for the resulting laminate showed that much additional developmental work would be required to produce an effective bond between the foil and the fiberglass cloth.

In the meantime, it was found that the 3M Company had developed an aluminum fiberglass laminate in the form of a tape using a high temperature silicone adhesive. Measurement of the optical properties of the tape indicated that its ϵ was low (0.06). Methods of increasing its ϵ to satisfactory levels are discussed in Section F on Multilayer Composites.

* Archer Aluminum Company

TABLE IV

MULTILAYER SYSTEMS

Designation	Top Layer	Under Layer	α	ϵ	α/ϵ
Silicone-Aluminum Systems					
LSA111-1	Clear MP Heatrem (Speco Mfg.) 1 pass	Al Tape (Y9050)	0.17	0.06	2.8
LSA111-2	Clear MP Heatrem (Speco Mfg.) 2 passes		0.17	0.14	1.2
LSA111-3	Clear MP Heatrem (Speco Mfg.) 3 passes		0.17	0.15	1.1
LSA111-4	Clear MP Heatrem (Speco Mfg.) 4 passes		0.17	0.18	0.94
LSA111-5	Clear MP Heatrem (Speco Mfg.) 5 passes		0.17	0.24	0.71
LSA111-6	Clear MP Heatrem (Speco Mfg.) 6 passes		0.16	0.28	0.57
LSA111-7	Clear MP Heatrem (Speco Mfg.) 7 passes		0.16	0.33	0.48
LSA111-8	Clear MP Heatrem (Speco Mfg.) 8 passes		0.16	0.37	0.43
LSA113-7A	Clear MP Heatrem (Speco Mfg.) 9 passes		0.15	0.39	0.38
LSA113-8A	Clear MP Heatrem (Speco Mfg.) 10 passes		0.17	0.42	0.40
LSA113-9A	Clear MP Heatrem (Speco Mfg.) 11 passes	Al Tape (Y9050)	0.19	0.46	0.41
Silicate-Aluminum Systems					
LKA116-1C	K_2SiO_3 (1 pass)	Al Tape (Y9050)	0.11	0.17	0.65
LKA116-2C	K_2SiO_3 (3 passes)		0.13	0.40	0.32
LKA116-3C	K_2SiO_3 (5 passes)		0.14	0.47	0.30
LKA116-4C	K_2SiO_3 (7 passes)		0.13	0.54	0.24
LKA116-6C	K_2SiO_3 (9 passes)		0.14	0.54	0.26
LKA116-7C	K_2SiO_3 (11 passes)		0.13	0.59	0.22
LKA116-8C	K_2SiO_3 (13 passes)		0.14	0.63	0.22
LKA116-9C	K_2SiO_3 (15 passes)	Al Tape (Y9050)	0.14	0.74	0.19

TABLE IV (Cont'd)

Designation	Top Layer	Under Layer	α	ϵ	α/ϵ
Fiberglass-Aluminum Systems					
LGA104B-1	No. 104 glass cloth	Al Foil	0.18	0.55	0.33
LGA16-2	No. 112 glass cloth		0.18	0.53	0.34
LGA104B-3	EM-10 glass cloth		0.21	0.59	0.36
LGA104B-4	EM-21 glass cloth		0.21	0.51	0.41
LGA104B-5	EM-32 glass cloth		0.19	0.39	0.49
LGA104B-6	EM-50 glass cloth		0.25	0.67	0.37
LGA104B-7	EM-51 glass cloth		0.21	0.76	0.28
LGA104B-8	EM-52 glass cloth		0.20	0.60	0.33
LGA104B-9	EM-63 glass cloth		0.20	0.77	0.26
LGA104B-10	EM-65 glass cloth		0.22	0.70	0.31
LGA17-2	EM-71 glass cloth		0.28	0.76	0.37
LGA104B-11	EM-77 glass cloth		0.30	0.88	0.34
LGA17-4	No. 120 glass cloth		0.20	0.57	0.35
LGA17-5	No. 181 glass cloth		0.20	0.71	0.28
LGA35-1	LTI glass cloth		0.21	0.60	0.35
LGA19-3	Refrasil glass cloth		0.17	0.77	0.22
LGA17-3	Woven Roving	Al Foil	0.21	0.64	0.33
LGA113A-1	EM-10 glass cloth	Y9050 Al Tape	0.18	0.68	0.26
LGA113A-2	EM-21 glass cloth		0.15	0.51	0.29
LGA113A-3	EM-32 glass cloth		0.14	0.49	0.29
LGA113A-4	No. 104 glass cloth		0.18	0.56	0.32
LGA113A-5	5614-A glass cloth	Y9050 Al Tape	0.20	0.62	0.32

TABLE IV (Concl'd)

Designation	Top Layer	Under Layer	α	ϵ	α/ϵ
Fiberglass-White Paint Systems					
LGW16-2	No. 112 glass cloth	White Paint	0.30	0.57	0.53
LGW16-3	918-30 glass cloth		0.26	0.72	0.36
LGW17-2	EM-71		0.31	0.64	0.48
LGW17-3	Woven Roving		0.26	0.64	0.41
LGW17-5	No. 181 glass cloth		0.24	0.77	0.31
LGW19-3	Refrasil		0.18	0.71	0.25
LGW35-1	LTI glass cloth	White Paint	0.20	0.66	0.30
Nylon Systems					
LNA45-7	No. 621 Nylon	Al Foil	0.28	0.54	0.52
LNW45-7	No. 621 Nylon	White Paint	0.37	0.72	0.51
LNB45-7	No. 621 Nylon	Black Paint	0.59	0.86	0.68
LNA45-8	No. 309 Nylon	Al Foil	0.28	0.45	0.62
LNW45-8	No. 309 Nylon	White Paint	0.33	0.56	0.59
LNB45-8	No. 309 Nylon	Black Paint	0.66	0.81	0.81
Miscellaneous Systems					
LTU29-1	FEP Teflon	Gold (deposited on underside)	0.32	0.59	0.54
LXA80-3	Skygard 700 Polyimide	Al	0.77	0.73	1.05
LXA80-4	SCP 5034 Polyimide	Al	0.74	0.76	0.97
LXwA101-7	Saran Wrap	Al Heatrem No. 170 Paint	0.22	0.55	0.40
LSiA101-8	Silicon Monoxide (Schjeldahl)	Aluminized Mylar	0.13	0.47	0.28
LSiA101-9	Silicon Monoxide (Schjeldahl)	Al Mylar Tape	0.11	0.43	0.25
LSiA101-10	Silicon Monoxide (Schjeldahl)	Al Foil	0.11	0.68	0.16
LSiA101-11	Alodyne (Schjeldahl)	Al Foil	0.18	0.25	0.72

TABLE V

METALLIZED FABRICS

Designation	Metal	Fabric	Deposition Process	α	ϵ	α/ϵ
FAG 25-1	Aluminum	No. 120 glass cloth	Vapor Dep.	0.38	0.28	1.36
FAG 25-2	Aluminum	Refrasil	Vapor Dep.	0.64	0.49	1.30
FAG 25B-1	Aluminum	Woven Roving	Vapor Dep.	0.35	0.21	1.68
FAG 28-1	Aluminum	EM-71	Spray Paint	0.43	0.32	1.34
FAN 45-1	Aluminum	Nylon No. 309 Sail Cloth	Vap. Dep.	0.39	0.18	2.16
FAN 45-2	Aluminum	Nylon No. 621 Sail Cloth	Vap. Dep.	0.56	0.32	1.75
FA 49A-1	Aluminum	Cotton	Rolled*	0.21	0.18	1.16
FA 57-9	Aluminum	Fiberglass	Rolled*	0.17	0.06	2.83
FGU 30-1	Gold	No. 120	Chemical Spray**	0.46	0.34	1.35
FGU 30-2	Gold	Refrasil	Chemical Spray**	0.68	0.43	1.59
FGU 30-4	Gold	Woven Roving	Chemical Spray**	0.57	0.29	1.98
FGU 35-5	Gold	L.T.I. glass cloth	Vapor Dep.	0.48	0.27	1.79
FGU 35-6	Gold	No. 120 glass cloth	Vapor Dep.	0.44	0.25	1.76
FAG 83A-1	Aluminum	No. 103 glass cloth filled with HT 424F Primer	Vapor Dep.	0.38	0.16	2.4
FAG 83A-5	Aluminum	EM-30 glass cloth filled with HT 424F Primer	Vapor Dep.	0.34	0.14	2.4
FAG 101-10	Aluminum	Fiberglass (Y9050)	Rolled***	0.12	0.06	2.00

*Foylon **Enthone Inc. ***3M

E. CERMETS

Another class of composite materials which exhibits good refractoriness and metal-non-metal surface is that of cermets. These can be applied to a surface by either flame spraying the metal powder in air and allowing it to form an oxide coat or arc spraying a mixture of a ceramic and metal powders in the process. Cermet coatings of nickel with aluminum oxide and of nickel with chromium oxide were obtained from the Industrial Products Division of AVCO. In each case, both α and ϵ were found to be exceedingly high.

Commercial sources of high metal content white oxide cermets were sought without success. The development of fabrication methods to prepare such composites were considered, but the scope of the entire program necessarily precludes such a basic, concentrated effort on a single approach. The results of the measurements made on those cermets tested are given in the following table.

TABLE VI

CERMETS

Designation	Description	α	ϵ	α/ϵ
	Sprayed on Aluminum Sheet Nickel-Alumina Cermet			
J62-1	as sprayed	0.86	0.77	1.11
J66-2	polished (100 grit)	0.84	0.83	1.01
J76-1	polished (240 grit)	0.84	0.76	1.11
	Nickel-Chromia Cermet			
J62-2	as sprayed	0.92	0.82	1.12
J66-3	polished (100 grit)	0.84	0.75	1.12
J76-2	polished (240 grit)	0.85	0.65	1.31
	Rod Stock			
J7 -2	Zircalloy-2: boron carbide (Nuclear Materials and Equipment Corporation)	0.71	0.29	2.44

F. MULTILAYER SYSTEMS

The use of multiple layers of materials with complementary optical parameters to achieve the desired thermal control properties for the layer structure was employed for the Vanguard I satellite.[4] For the Apollo problem this approach would consist of incorporating a thin layer of a material with a high ϵ and transparent to solar radiation over a substrate of a polished metal with a low ϵ. For such a composite the high ϵ of the outermost layer should serve to increase the ϵ of the metal without affecting its α. Control of the thickness of the outer layer should serve to regulate the increase in ϵ.

The feasibility of this approach was demonstrated by systematically increasing the thickness of a silicone resin coating on aluminum foil tape and measuring the change in optical properties. For this purpose, successive layers of Speco silicone resin (transparent to solar radiation but only semitransparent to infrared) was applied to 3M aluminum tape (Y9050). The α value of the coated foil was relatively insensitive to the thickness of the coating whereas ϵ increased linearly as a function of coating thickness (Figure 3). A description of the multilayer systems was investigated and their optical properties were given in Table IV.

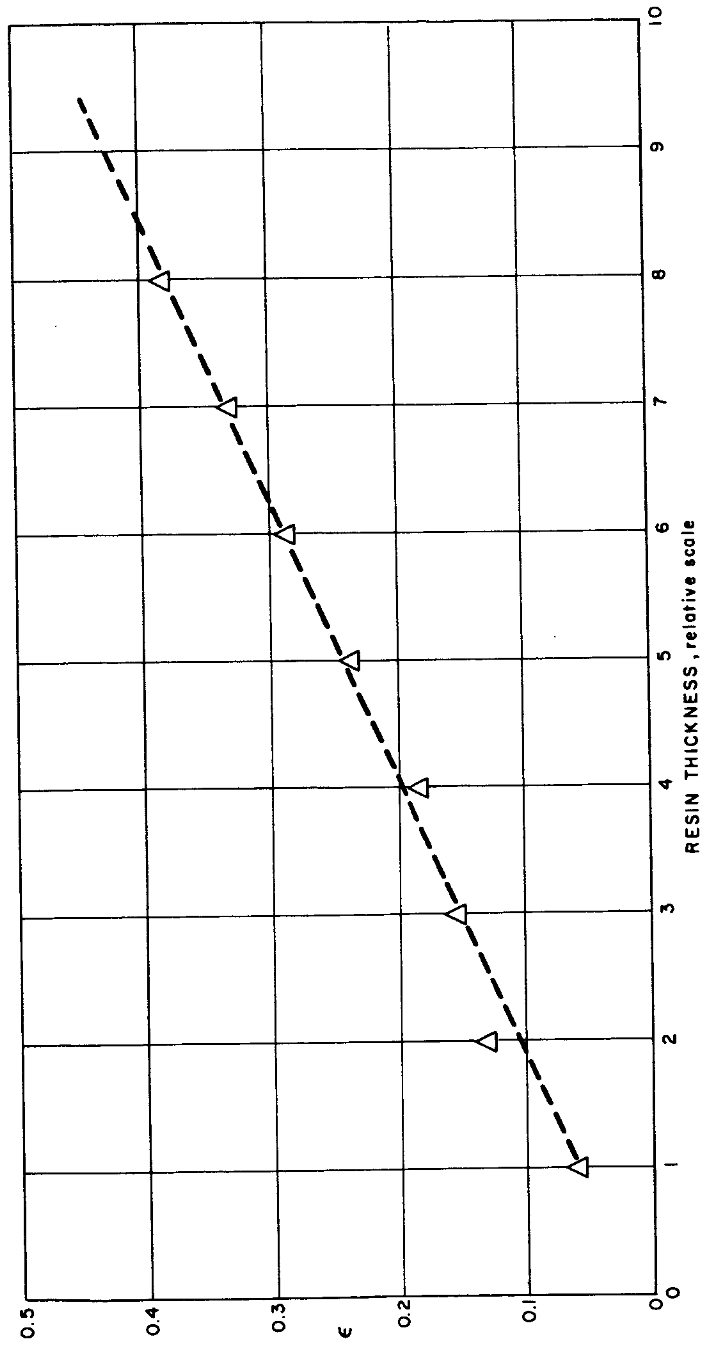

Figure 3 EFFECT OF RESIN THICKNESS ON THE OPTICAL PROPERTIES OF RESIN COATED ALUMINUM TAPE

(Page 32 is intentionally blank)

IV. TEST INSTRUMENTATION AND METHODS

A. Measurement of Solar Absorptance (α)

A Gier-Dunkle Solar Reflectometer (Figure 4) was used for the measurement of solar absorptance. This instrument consists of a detection head and a cabinet with its own power supply and readout system. In the detection head radiation from a high pressure Xenon lamp is filtered and directed into an integrating sphere. A sensor in the sphere registers this radiation as 100 percent. If however, a sample is placed over the port on the detection head, the radiation impinges on the sample and only the reflected radiation enters the integrating sphere. The sensor registers the reflected fraction of the solar spectrum. For an opaque sample

$$\alpha = 1 - R$$

where α is the solar absorptance

R is the solar reflectance.

The radiation source, the filters and the spectral response of the sensors are selected in such fashion that the recorded reflectance corresponds to the extra-terrestial solar reflectance.

Before each measurement the instrument is calibrated for 0 and 100 percent solar reflectance respectively by the use of built-in shutters and reflectors.

In addition to the measurement of total solar reflectance, it is possible by the use of built-in filters, to measure reflectance for the following high wavelength cut off spectra:

- 0.523μ
- 0.665μ
- 0.913μ
- 1.30μ

Reflectance (absorptance) for any waveband, defined by these cut-off numbers can be determined by difference.

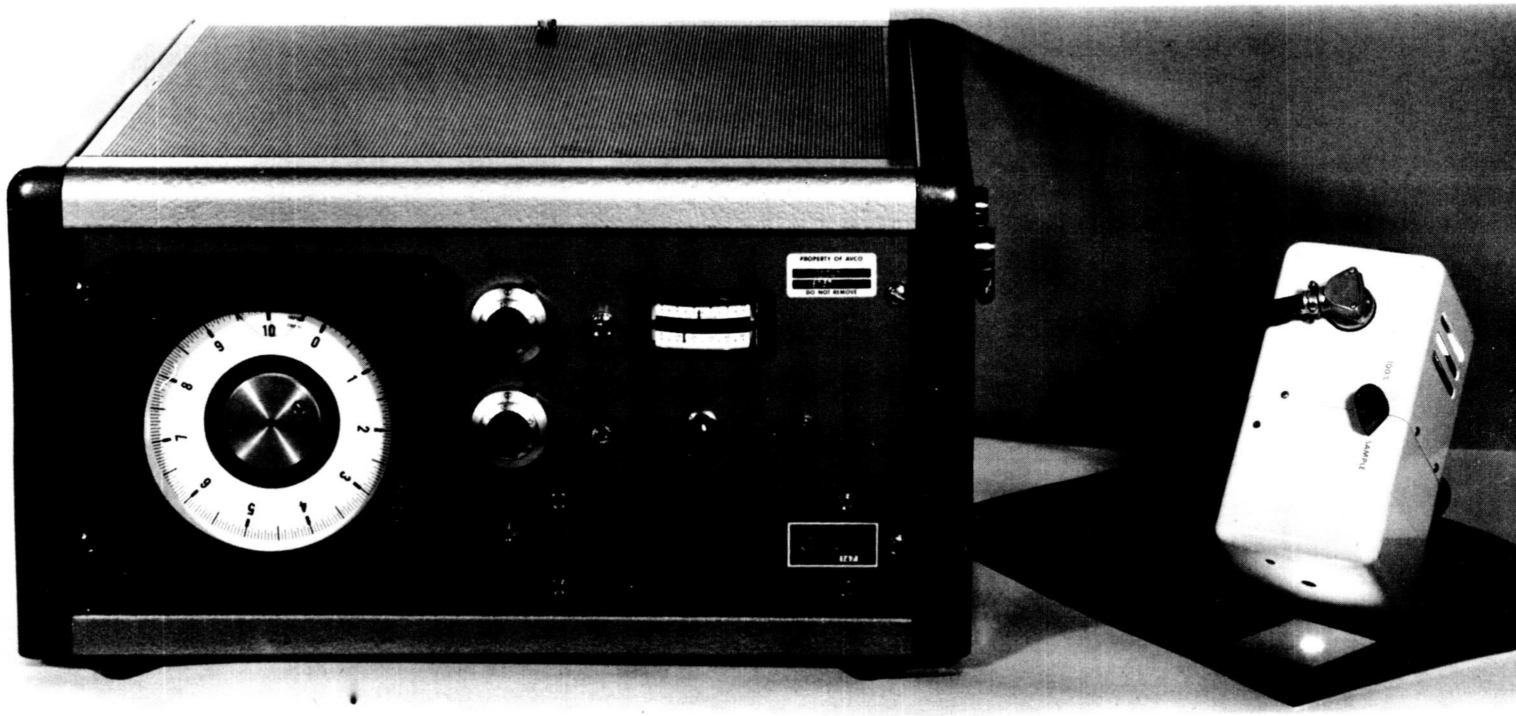

P-12517-B

Figure 4 GIER-DUNKLE SOLAR REFLECTOMETER

B. MEASUREMENT OF THERMAL EMITTANCE (ϵ)

A Barnes Model R4-F2 radiometer was used for the measurement of thermal emittance (Figure 5). The two radiation sensors, mounted in the radiometer head, are thermistor bolometers with KRS-5 windows. Thus the spectral range of this instrument is 0.5 - 40 μ. Radiation from a sample is directed through a paraboloidal and a hyperboloidal mirror alternately into two bolometers by the use of a rotating reflector-chopper (Figure 6). While one bolometer receives the unknown radiation, the other is focused on the reference blackbody. The output of the two bolometers senses only the total emitted radiation. The second bolometer is provided with the following filters:

SiO_2	4.5μ	long wave cut-off
Germanium	1.8μ	short wave cut-off
Kodak 210S	1.0μ	short wave cut-off
Kodak 220S	2.0μ	short wave cut-off
Kodak 230S	3.0μ	short wave cut-off

Spectral thermal emittance for any wave band corresponding to the combination made up with these filters can be determined.

The focal length of the instrument optics can be adjusted from 29 inches to infinity. When the instrument is precisely focused on a surface, a 3/8 inch diameter area is measured. Thus variations of the emittance of the surface can be detected with good resolution. By slightly defocusing it is possible to increase the viewed area to a 1 inch diameter without adversely affecting the sensitivity of the measurement. By this method the average emittance over a large area can be found.

For the determination of thermal emittance the sample as well as a high and a low emittance standard are heated to the same temperature slightly above ambient. This is accomplished by placing all samples on a large temperature controlled aluminum block. From measurements on the high and low emittance standards a calibration curve is obtained correlating the emf output of the bolometer with the thermal emittance. Values corresponding to the signal received from the sample are read from the calibration curve. To establish the precision of the α and ϵ measurements, ten determinations were made on a single specimen. The mean value and the standard deviation were calculated. The results showed that the precision of the α measurements was ± 0.65 percent and that of the ϵ measurements was ± 1.8 percent.

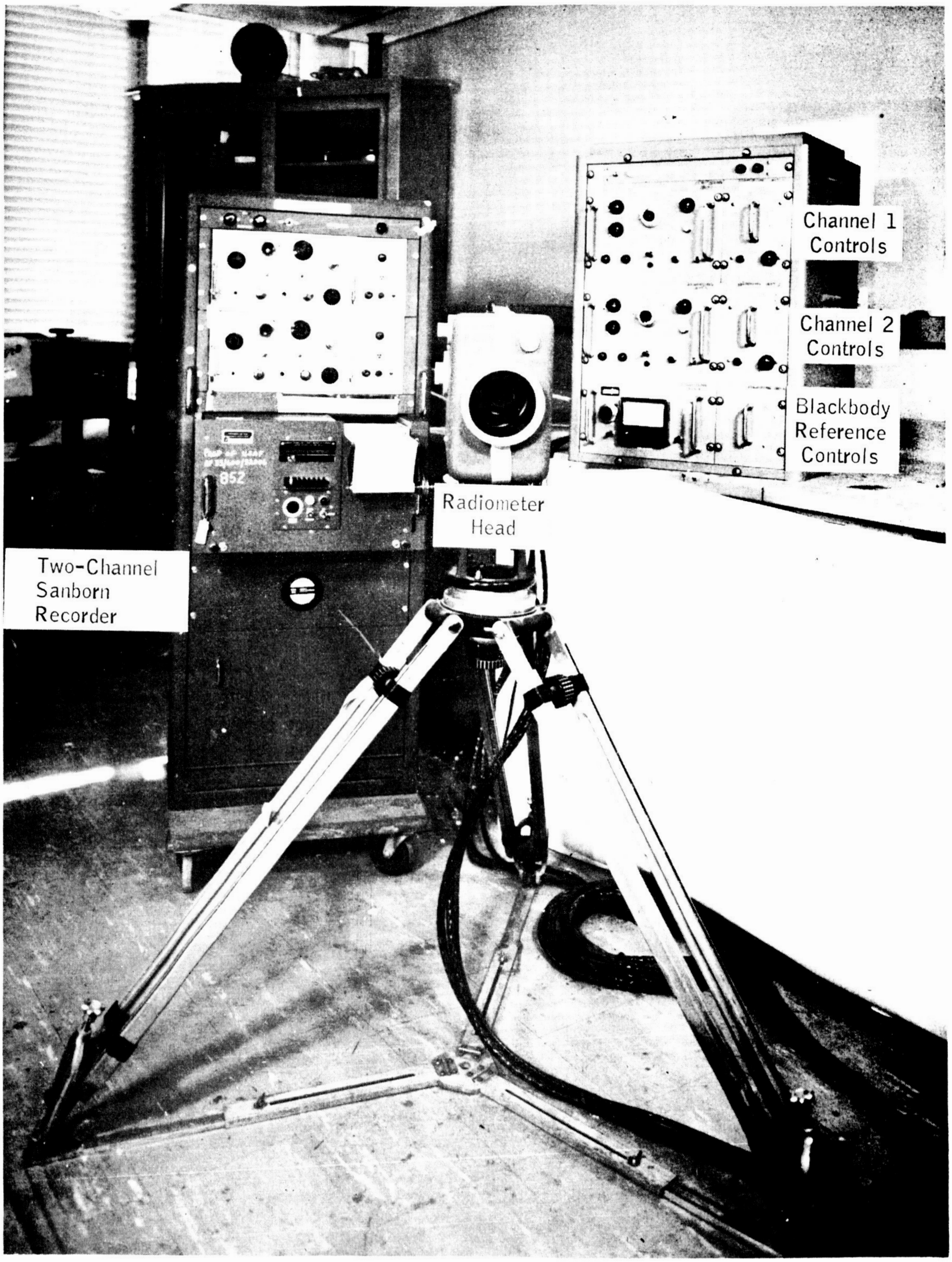

Figure 5 BARNES MODEL R4-F2 RADIOMETER

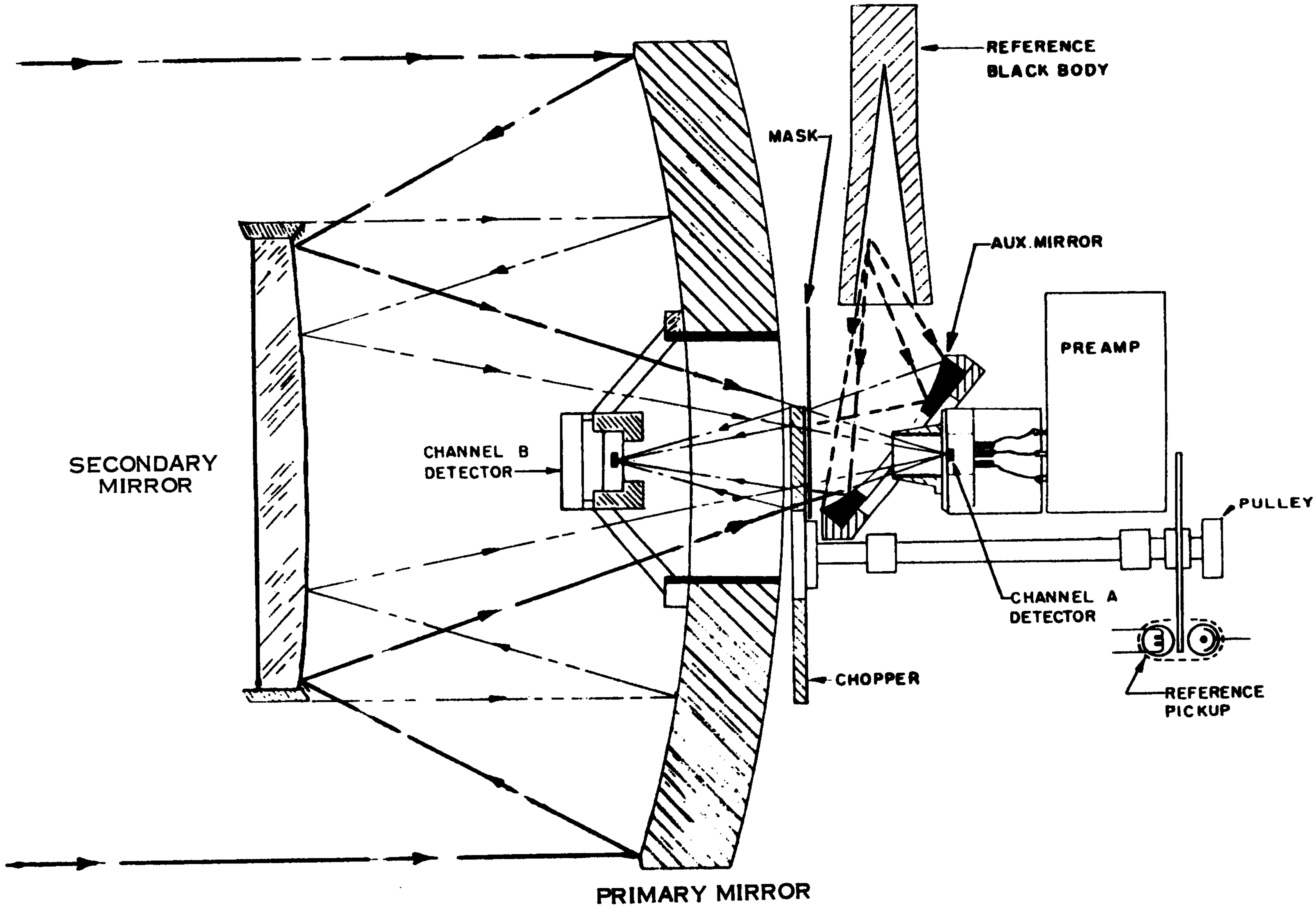

Figure 6 SCHEMATIC OF TOTAL NORMAL EMITTANCE APPARATUS

C. THE SPACE SIMULATION CHAMBER

In order to verify the effectiveness of any coating for the role of passive thermal control, it must be tested in an environment which simulates as closely as possible the conditions of its flights through space. To obtain these conditions a 200-liter space simulation chamber was used (Figure 7). The interior of the chamber is accessible through four 8 inch ports on its side and one 12 inch port at the top. The ports are sealed with Ultek flanges and metallic gaskets. Three cryogenic pumps incorporating zeolite molecular sieves are used for the initial pumpdown to avoid contamination of the system by oil vapors, and the pumping is continued with an ultevac 1000 liter/second sputter-ion pump. The baked out empty chamber has an ultimate vacuum of approximately 10^{-11} torr, but with a typical specimen in position 5×10^{-8} torr is attainable.

The construction of the entire system is shown in cross section in Figure 8. A cooling shroud constructed from square cross section copper tubing, lines the interior wall. The shroud is cooled with liquid nitrogen, and its inside is coated with a high emittance inorganic coating. An 8 inch diameter opening is cut in the shroud for admitting solar radiation to a sample suspended at the center. An 8 inch diameter fused silica window is attached to one port so that simulated solar radiation may be admitted to the system. The window consists of a 3/4 inch thick polished disc of fused silica clamped to an 8μ inch finish base plate using indium wire as gasket material. An entry lock is used to introduce or remove samples from the chamber without the loss of vacuum.

Although the coatings have been designed to operate as controls in the temperature range of 10 to 50°C, it is possible that temperature excursions could reach as high as 100°C under certain circumstances. A facility is available so that the control coatings can be subjected to simulated space effects at a temperature of 100°C.

A considerable time would be necessary to evacuate the 200-liter chamber particularly if the liquid nitrogen shroud were still cool when the vacuum was broken.

The time needed to change specimens was minimized by incorporating a 12 inch diameter ultra-high vacuum valve at the top of the chamber and by having a demountable entry lock system above this valve. The specimen and associated monitoring leads consisting of heater leads and seven thermocouples may be mounted on stainless steel chains which are wound on capstans. These capstans may be rotated and controlled in a very precise manner by external drive motors. The rotational motion is transmitted to the capstan shafts by glandless bellows-type rotation seals. Two chains are responsible for supporting the specimen and are controlled by the same shaft. A third chain mounted on a second shaft and attached to the bottom of the specimen provides an attitude control for the specimen. Thermocouples, heater wires, and any other control and recording connections are made via loosely coiled cables consisting of thin

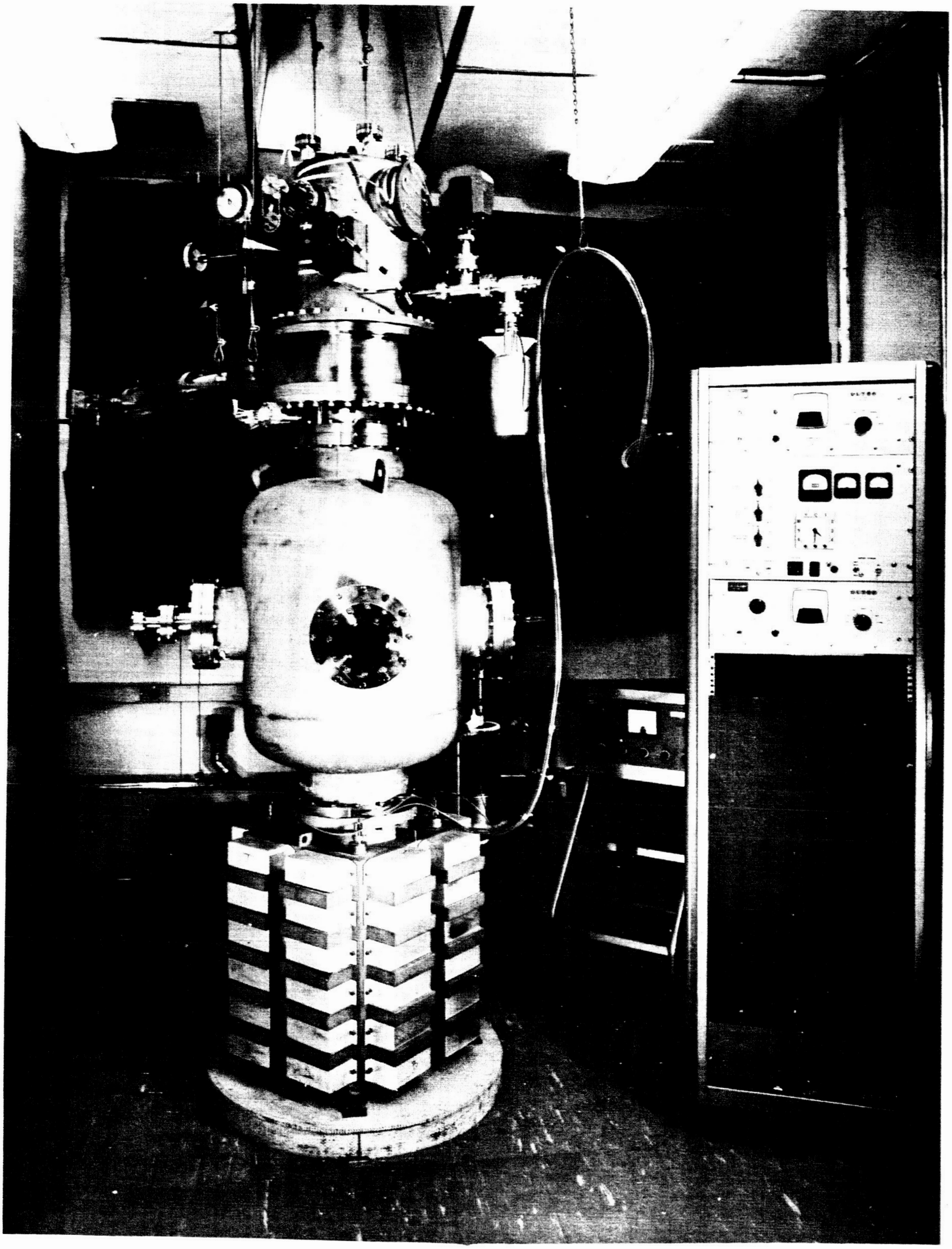

Figure 7 200 LITER HIGH VACUUM CHAMBER WITH ENTRY LOCK

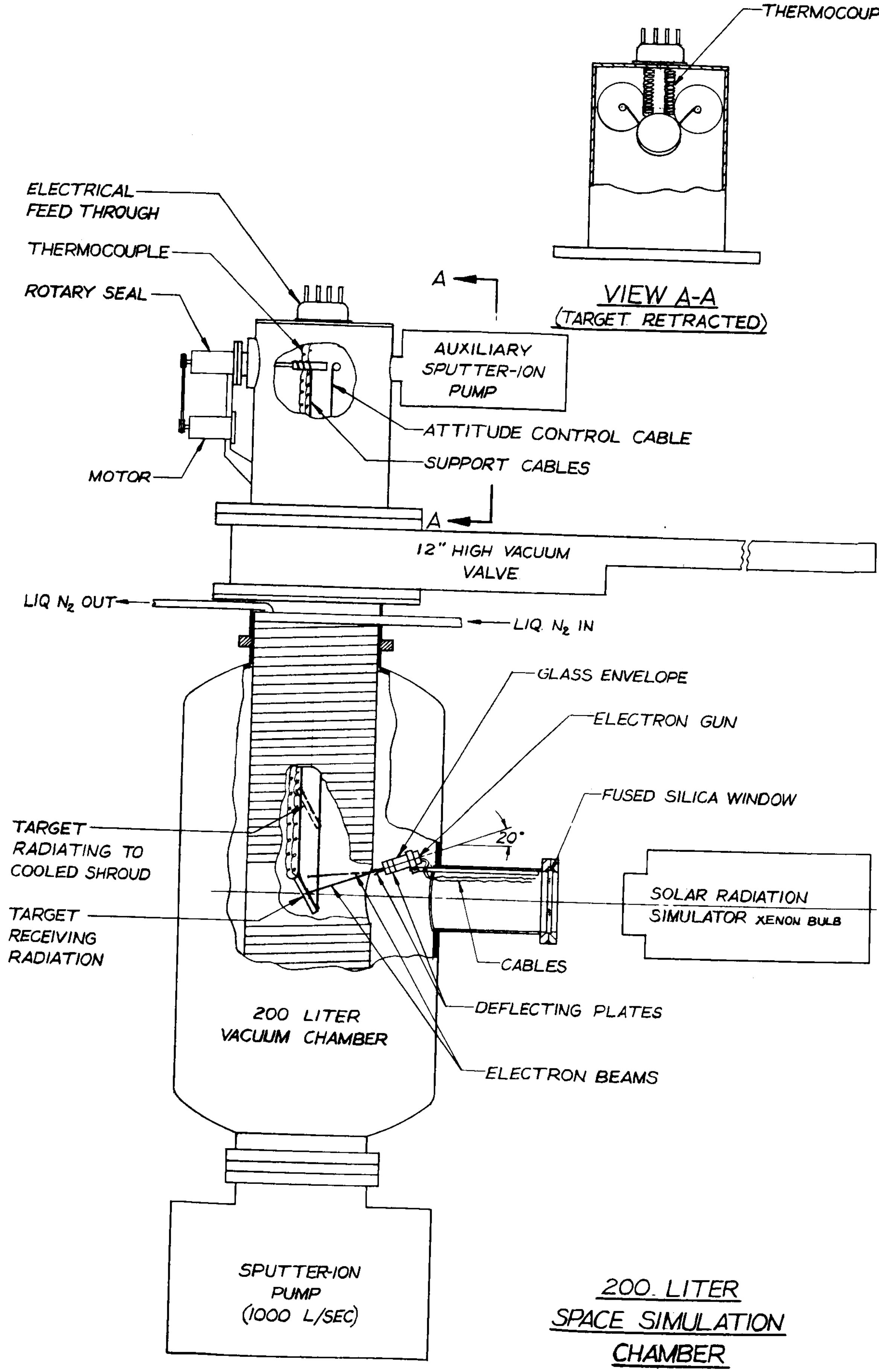

Figure 8 SCHEMATIC DIAGRAM OF 200 LITER HIGH VACUUM CHAMBER

wires insulated from each other by a special Refrasil inorganic high temperature sheathing. As the specimen is wound up or down, the cables extend and retract.

When a test specimen has been attached to the chains and electrical leads, the entry lock is bolted to the top of the chamber using gold O-ring seals and is evacuated by an independent cryopump and Vacion pump. When the pressure has been reduced to the value of the main chamber vacuum the large valve is opened. Depending on the nature of the specimen a bake-out of the entry lock may be made. The specimen can now be lowered into a position opposite the window so that irradiation can be started. Figure 9 shows a number of thermal control coatings opposite the 8 inch diameter fused silica window installed for a screening test.

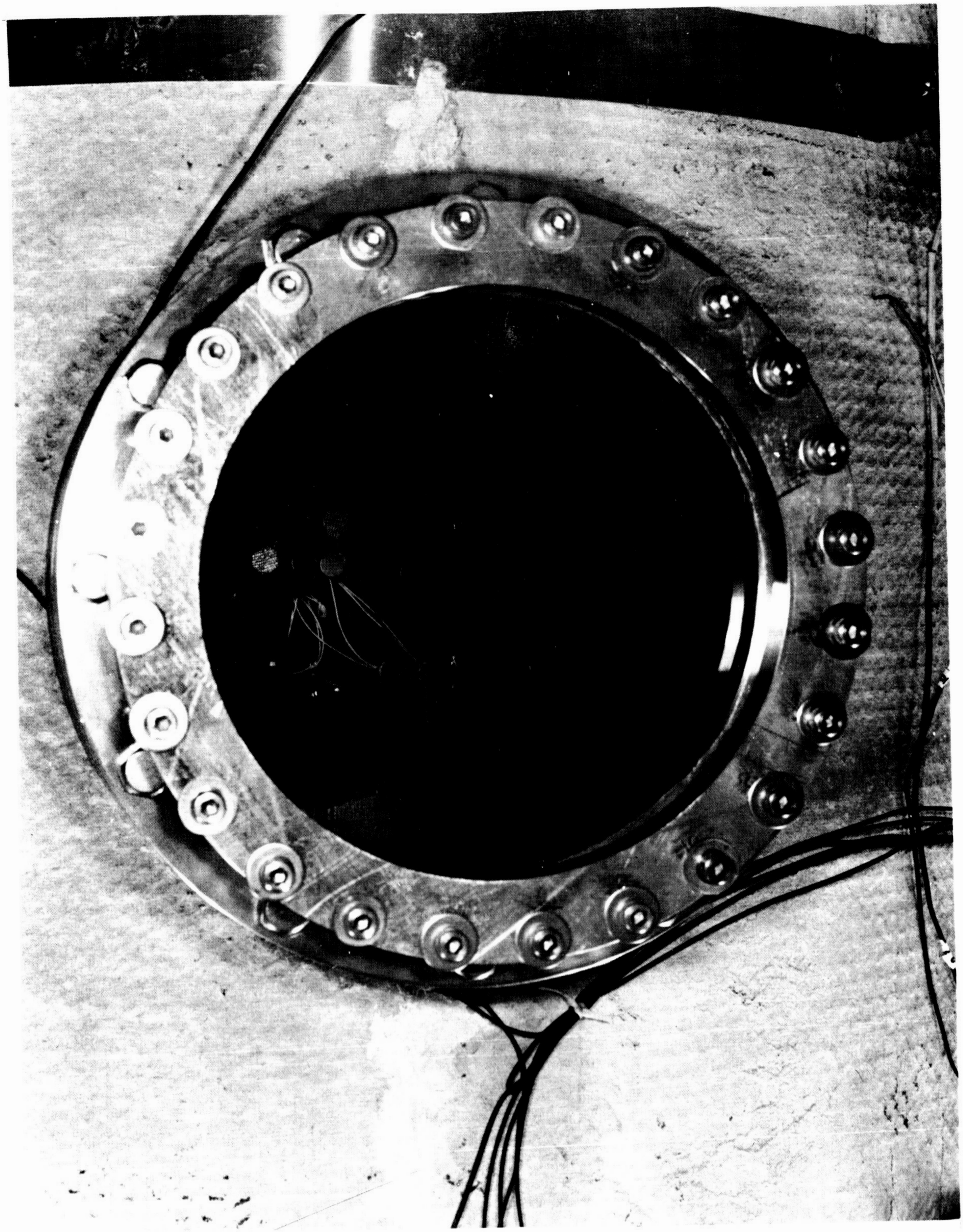

Figure 9 THERMAL CONTROL SYSTEMS IN VACUUM CHAMBER

D. THE SOLAR RADIATION SIMULATOR

A 5 kw high pressure Xenon lamp supplied by Hanovia, Inc., is used as a solar radiation simulator. The accessory optical system consists of a fused silica lens. It has been found that in practice it is necessary to supplement the ultraviolet radiation of the high pressure Xenon lamp to obtain a satisfactory intensity in this region of the zero air mass solar spectrum. High pressure mercury lamps (type GE AH-6) are used for this purpose and one is mounted in a parabolic reflector just to the side of the main Xenon lamp. The total flux emitted by the lamps was measured with a single junction thermopile at a distance of 30 inches from the lamp. The thermopile, mounted on an optical bench was moved across the radiation beam and the emf output was recorded at intervals of one cm. The window of the vacuum chamber was interposed between the lamp and the thermopile. The results of these measurements are shown in Figure 10. Accordingly, the intensity of the radiation is higher than one Sun for a beam diameter of 15 cm. The flux value was adjusted to one Sun value by increasing the diameter of the beam by the use of the adjustable fused silica lens.

The absolute spectral irradiance of the lamp combination was determined by the transfer method in the region of 0.25 to 2.6 microns. A standard tungsten filament lamp calibrated at the National Bureau of Standards was used as the source of standard radiance. The lamp was operated at its maximum temperature of calibration, with the brightness temperature of the filament at 0.665 microns of 2573°K using the spectral emissivity values for tungsten. The true temperature of the filament was found to be 2828°K.[5] A curve was then constructed using the Planck relation for 2858°K, and the spectral emissivity values describing the standard spectral radiance of the source. The absorptance of the lamp window was also taken into account in defining this spectral radiance.

Using a Perkin-Elmer Model 13 spectrophotometer, the spectral irradiance of the solar simulator was compared with the standard radiance source over the range of 0.25 - 2.6 μ. In order to cover the entire spectral range two detectors in the monochromator were necessary. In the 0.25 - 0.7 μ range an RCA photomultiplier tube type 6903 was used and from 0.7 to 2.6 μ a thermocouple detector was employed. A curve showing the spectral intensity at 144 cms from the 5 KW Xenon lamp together with the mercury arc lamp is shown in Figure 11. A curve of Solar spectral irradiance after Johnson [6] is included for comparison. There is a large peak in the infrared region which departs from the desired Solar irradiance. The effect of this peak however, is to make the test that much more conservative.

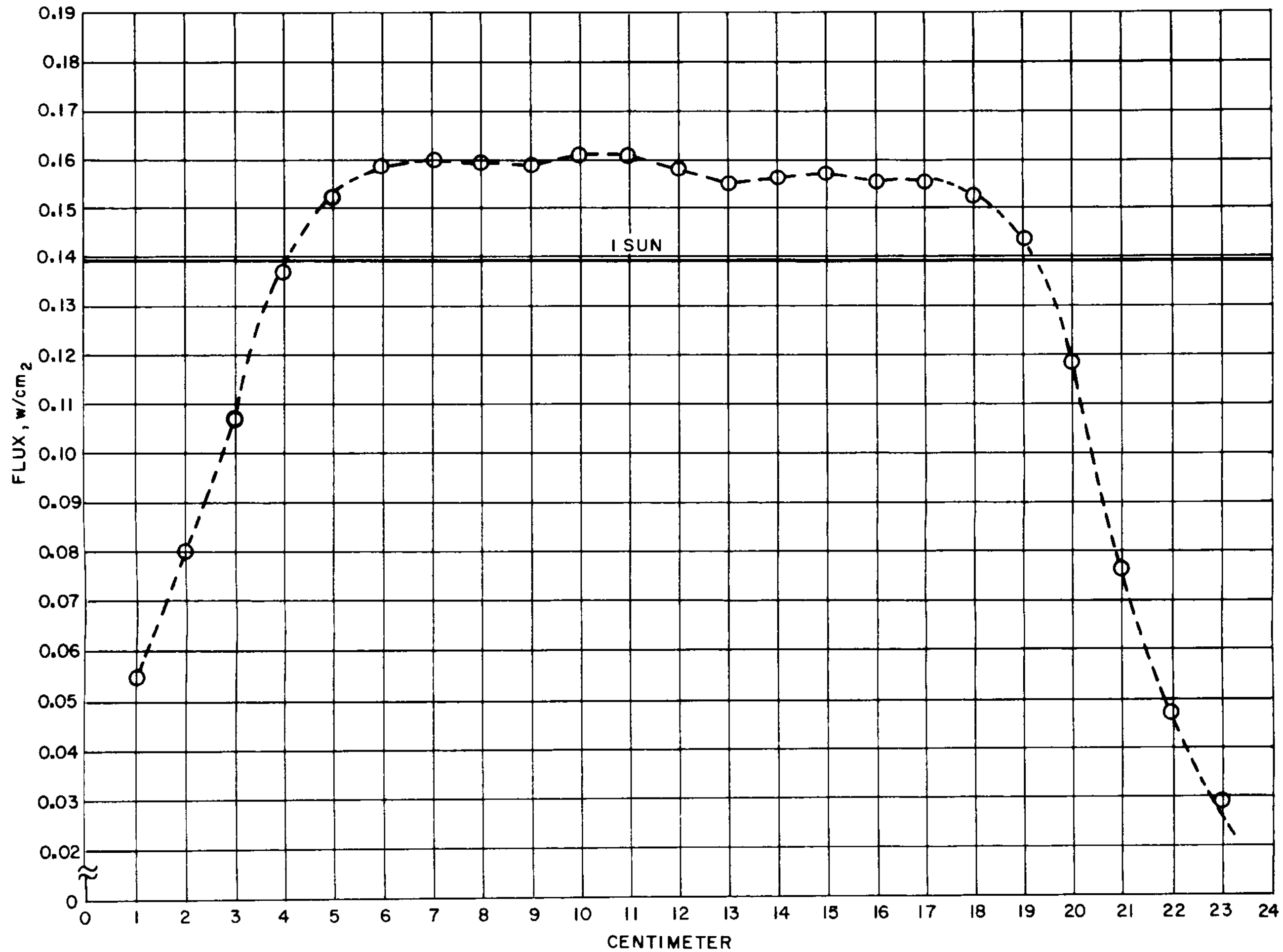

65-5450

Figure 10 FLUX DISTRIBUTION OF SOLAR SIMULATOR BEAM

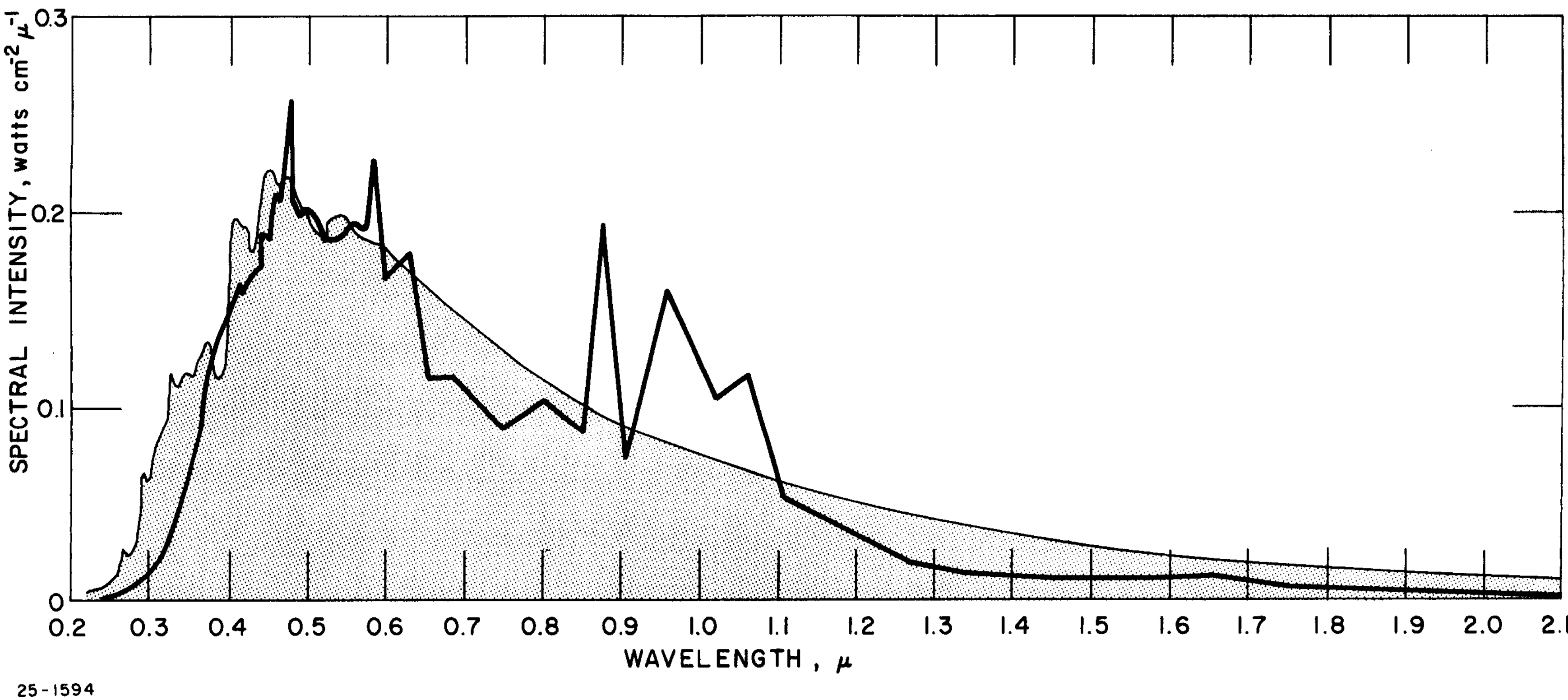

Figure 11 SPECRTAL IRRADIANCE

E. ASCENT HEAT SIMULATOR

A simple, quick method was established for testing a large number of samples for their resistance to ascent heating. The schematic diagram of the ascent heat simulator is shown in Figure 12. Nitrogen gas is used since the partial pressure of oxygen is negligible at the elevation where the maximum temperature is reached. The gas is made to pass through a ceramic tube wound on the outside with kanthal wire for electrical resistance heating. The tube is filled with pebbles in order to increase the heat transfer surface area. The sample, mounted on a steel rod, is placed at the outlet of the tubular heater. The support rod is held by two ball bushings allowing it to be moved along the axis of the furnace. The movement of the rod is accomplished by an adjustable pivot point level system which is activated by a specially designed variable rpm cam. A counter weight keeps the sample support in contact with the cam. Thus the rotation of the cam moves the sample in and out of the tubular heater at a predetermined rate. The temperature of the heater, the pivot of the lever, and the rpm of the cam are controlled in such fashion that the time temperature history of the sample surface approximates closely the ascent heating curve shown in Figure 13.

The performance of the simulator was analyzed and compared with the computational data from the ascent heating study. The known weight, specific heat, and measured temperature rise of a sample determine the net energy received by it irrespective of available energy quantities. In Table VII the first 3 lines give the heat input needed for 0.0015 pound Al, Be, and Teflon samples which cause the temperature to increase by 1000°F. The fourth line gives the corresponding value for a sample of Apollo material being tested in the pebble bed heater and reaching 1100°F. A comparison of the heat inputs show that the total magnitude of heat flux from the pebble bed heater is of correct order. It should be noted, however, that the shear stresses are much lower than those expected during ascent.

TABLE VII

ENERGY REQUIREMENTS

All samples weigh 0.0015 pound and are exposed to a ΔT of 1000°F		
Al	0.339	Btu/sample
Be	0.85	Btu/sample
Teflon	0.39	Btu/sample
Avco 5026	0.52	Btu/sample

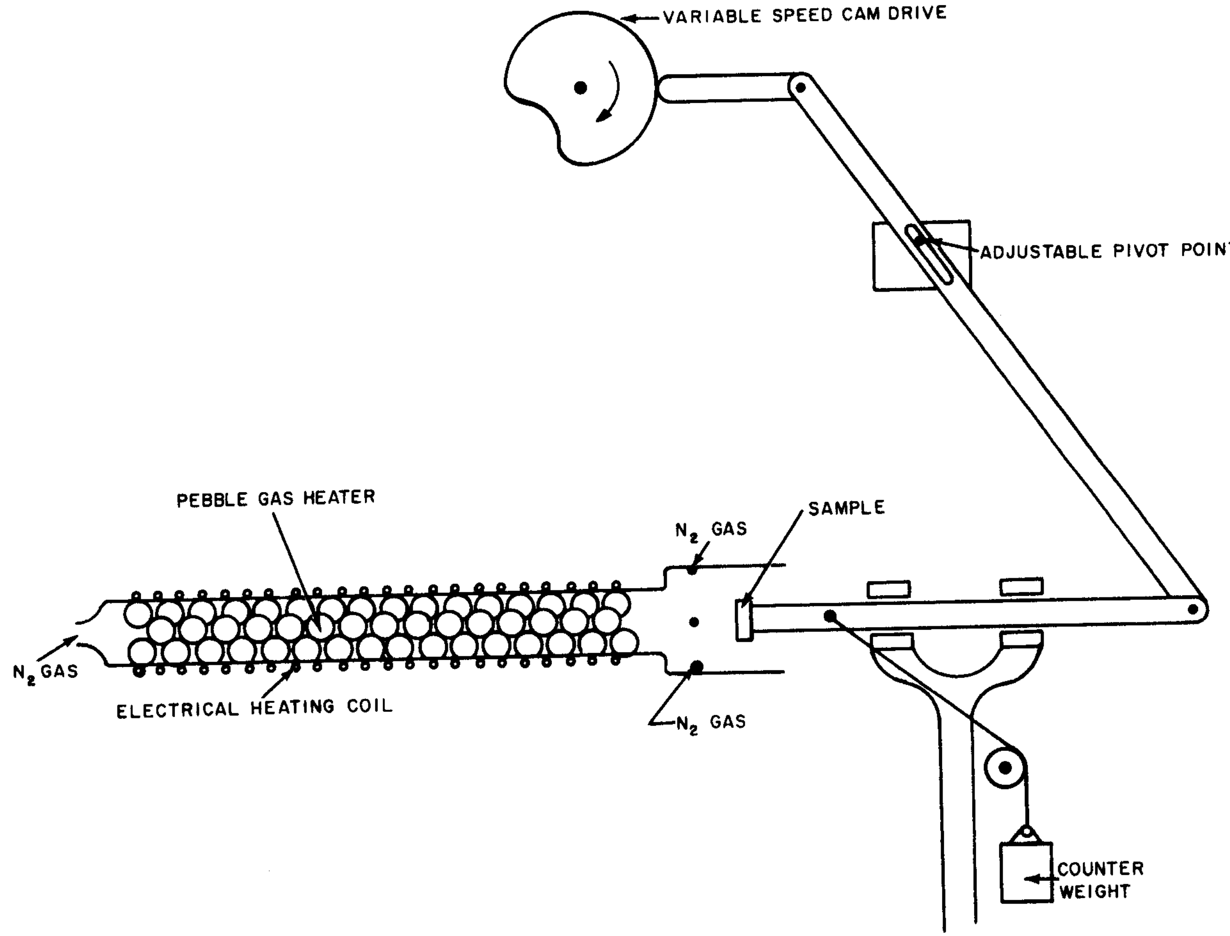

65-5449

Figure 12 PEBBLE BED HEATER

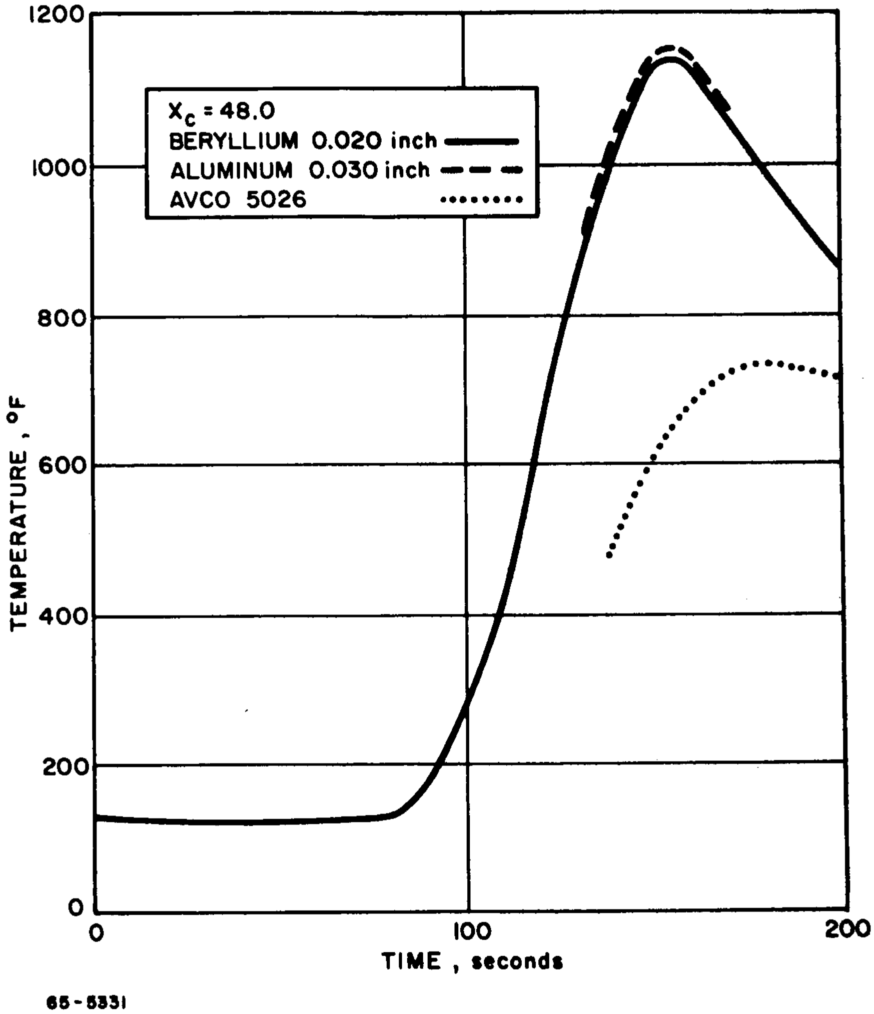

Figure 13 SURFACE TEMPERATURES DURING ASCENT

1. Test Results

Preliminary tests of coated samples exposed to the heated air stream from the pebble bed heater indicated that the thermal decomposition of the 5026-39 H/CG ablator was detrimental to the optical properties of the coating. For example, the α and ϵ of an aluminum painted sample increased from 0.21 and 0.18 to 0.6 and 0.5 respectively. A photograph of this sample before and after exposure to the simulated ascent heating is shown in Figure 14. In addition, the preliminary tests showed that the pressure increase beneath an impervious layer of aluminum foil, over the ablator material, is large enough to rupture the foil.

Pore sealed and moisture vapor barrier coated specimens of 5026 material were coated with refractory thermal control coating and tested in the pebble bed heater. The results showed that upon exposure to the established heating cycle with a 1150°F peak temperature, thermal decomposition products of the substrate appear to penetrate the thermal control coating and deposit on its surface a dark charlike coating. This is not entirely surprising since the underlying polyvinylidene chloride based coatings are thermoplastic and under the influence of heat would be expected to soften, flow, and decompose by a dehydrohalogenation process leaving behind a black charry residue.

Another set of experiments were performed in order to define the maximum temperature to which the pore-sealed 5026 material can be heated without causing failure of the thermal control coating. Specimens with and without pore sealer, but with no vapor barrier coating, were provided with the PAK (78-6A) coating, consisting of aluminum pigments in a K_2SiO_3 binder. Instead of the established heating curve (pebble bed heater), the samples were heated to consecutively increasing temperatures for 2 minutes, beginning at 600°F. The results are shown in Figure 15 a-e.

It was found that at 600°F, no harmful decomposition took place. However, a slight shrinkage of the honeycomb filler occurred as was evidenced by the apparent protuberance of the honeycomb walls. At 700°F the shrinkage was more pronounced, but the integrity of the aluminum coating was still preserved. At 750°F the honeycomb filler shrunk so much that the coating cracked and had a tendency to peel. In addition, it appeared that pyrolytic decomposition products escaped through the cracks and deposited on the surface of the coating. This degradation at elevated temperature is consistent with the TGA curve of the 5026 material (Figure 16).

The change in radiative parameters is shown in Table VIII.

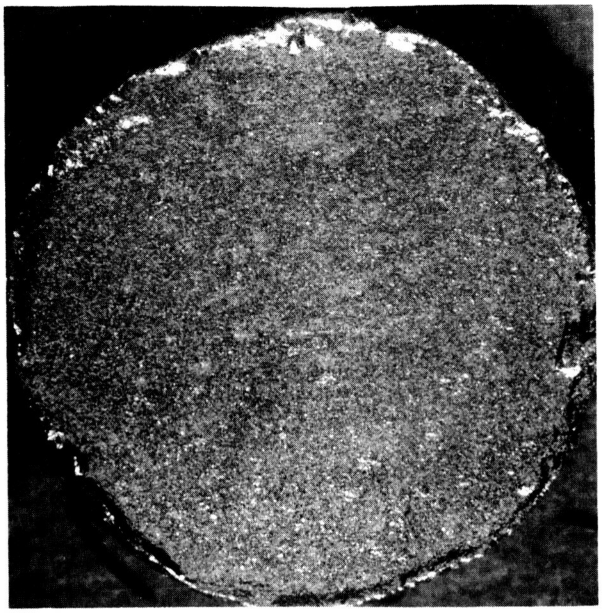

a. Before

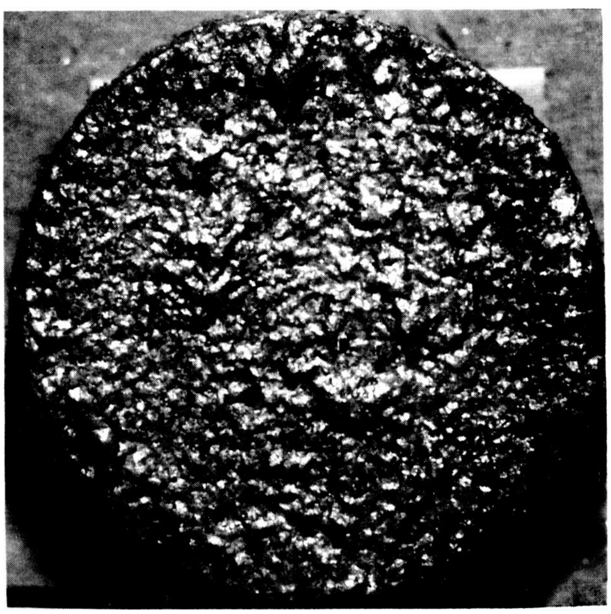

5X

b. After

Figure 14 SAMPLE EXPOSED TO PEBBLE BED HEATER

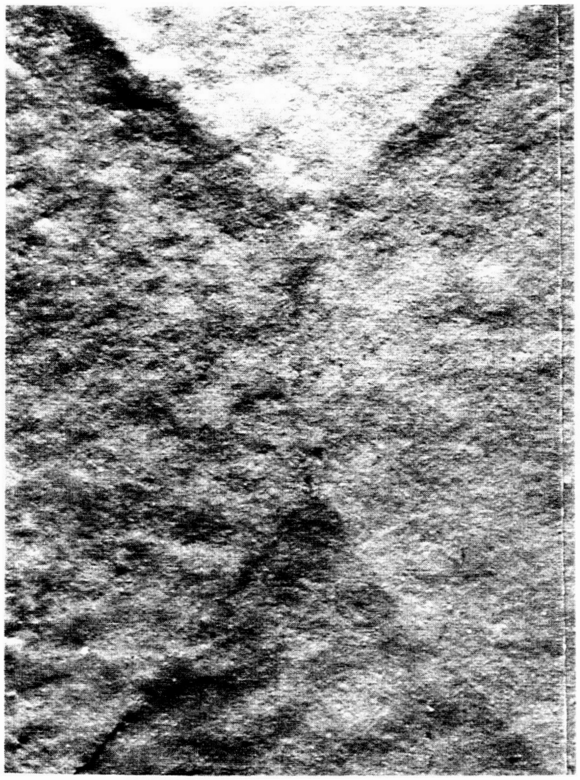

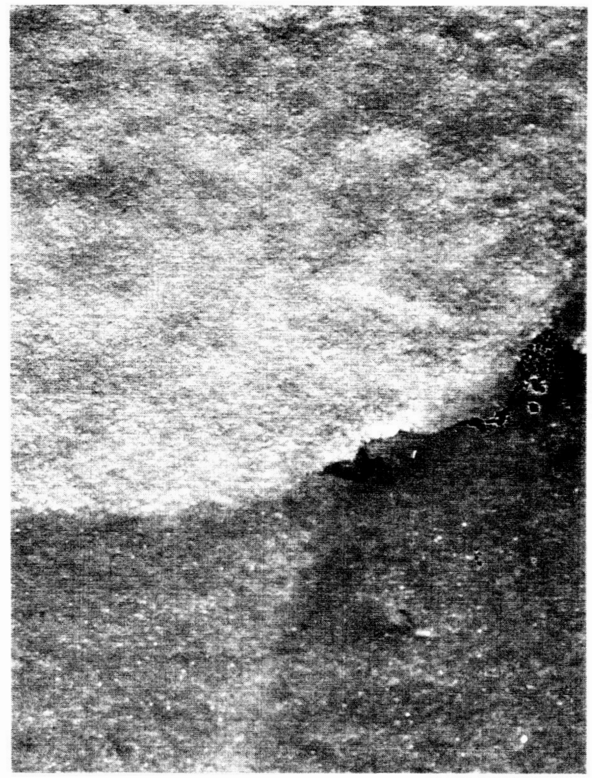

c. $700^{o}F$

d. $750^{o}F$

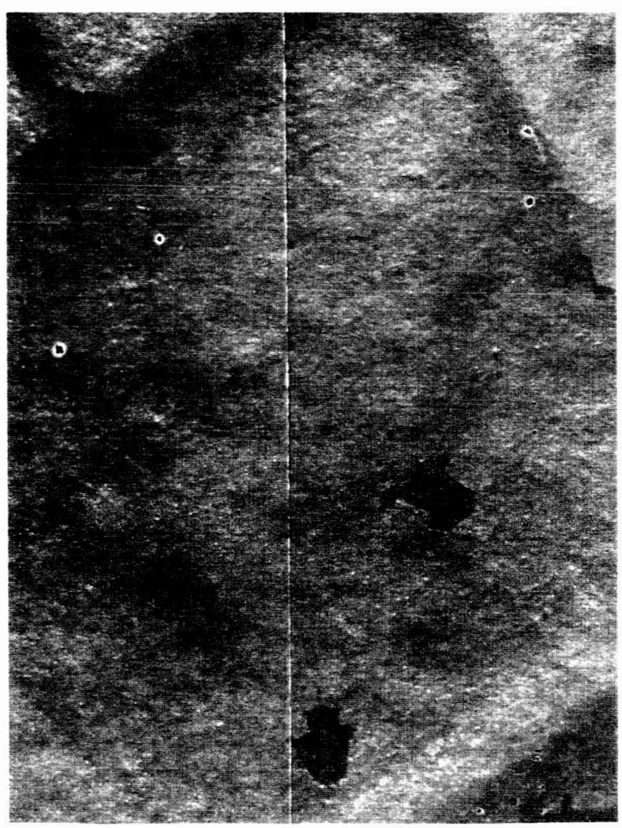

10X

e. $800^{o}F$

BED HEATER AT VARIOUS TEMPERATURES

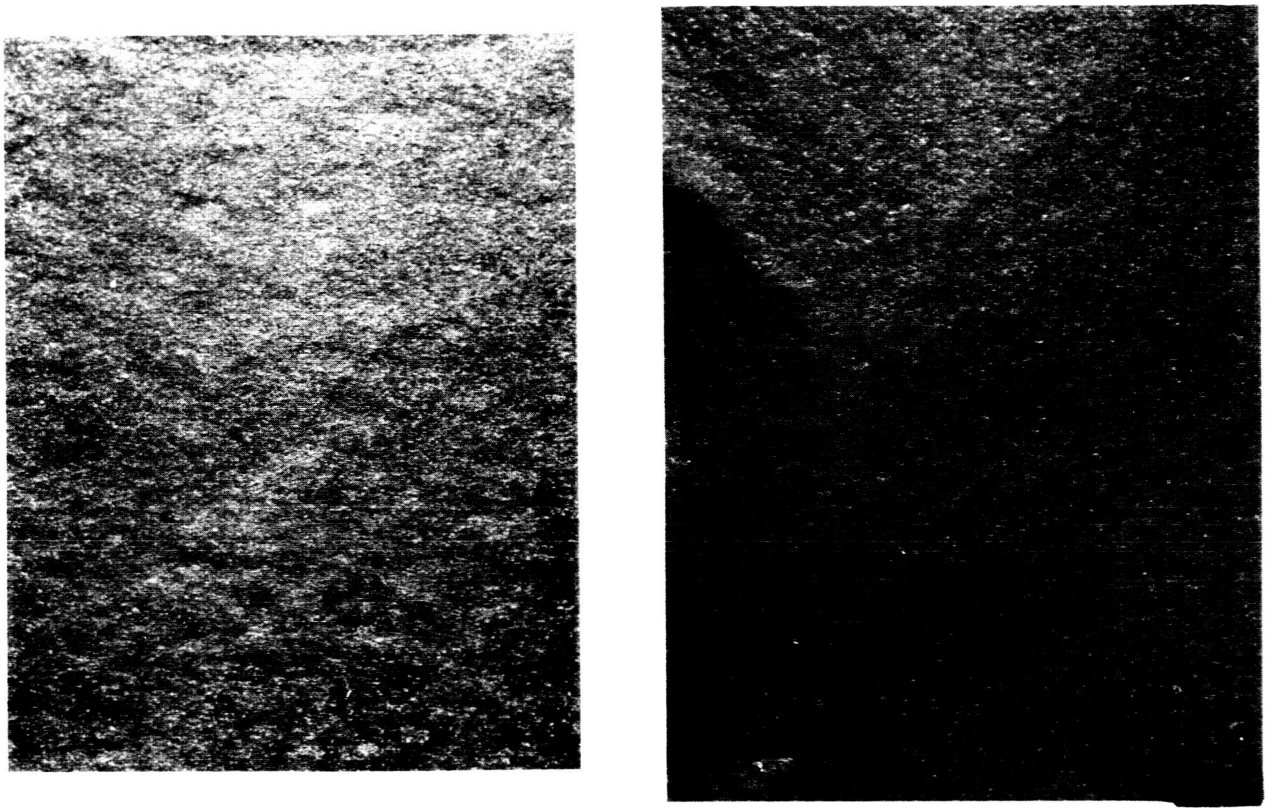

10X

a. Original

b. $600^{\circ}F$

Figure 15 SAMPLES EXPOSED TO PEBB

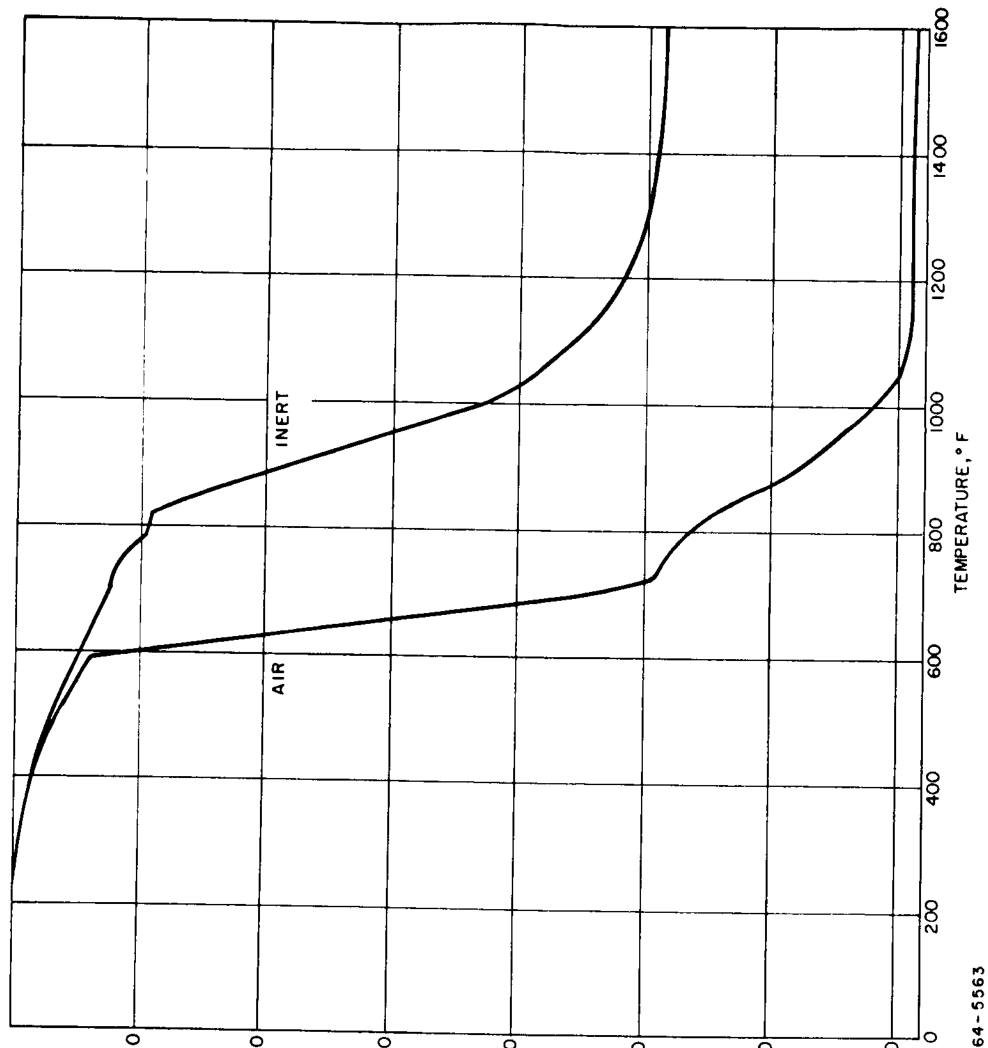

Figure 16 T.G.A. CURVE FOR 5026

TABLE VIII

EFFECT OF SIMULATED ASCENT HEATING ON OPTICAL PROPERTIES OF PAINTED 5026 ABLATOR MATERIAL

Temperature °F	Before Exposure		After Exposure	
	α	ϵ	α	ϵ
600	0.15	0.25	0.18	0.28
700	0.15	0.31	0.21	0.33
750	0.17	0.30	0.23	0.35
800	0.18	0.32	0.30	0.44

Ascent heating tests were performed in which an aluminum-silicone paint (Heat-Rem No. 170) was applied directly to the basic 5026 ablator material (without pore sealer or vapor barrier) and to the 5026 material with the specified pore sealer. The results showed that the optical properties of the samples without pore sealer were only slightly affected by the ascent heating test (before $\alpha = 0.27$, $\epsilon = 0.30$, and after $\alpha = 0.29$, $\epsilon = 0.29$) whereas the α of the pore sealed sample changed considerably (before $\alpha = 0.25$, after $\epsilon = 0.53$).

Because the ascent heat effect was alleviated by the sublimable coating no further tests were performed.

F. HOT AND COLD CYCLING

Controlled hot and cold baths were assembled to test the stability of the candidate coating systems toward the thermal cycling that they would experience in space. The hot bath consists of glycerol, thermostatically controlled at 250°F. The cold bath is a mixture of solid carbon dioxide and alcohol maintained at a temperature of - 110°F. The samples were enclosed in a copper envelope and submerged alternately in each bath. One cycle consisted of one hour in the hot bath followed by one hour in the cold and each test consisted of three such cycles.

The Apollo heat shield material in its standardized form has three coatings. The first, a pore sealer, consists of a filled, amine-cured epoxy novolac resin. The second, the moisture vapor barrier, is a grey pigmented polyvinylidene chloride coating while the third, involves the same base resin but with a titania pigment and has no functional role. These coatings were not intended to and do not withstand elevated temperatures.

During the thermal cycling of thermal control coated heat shield samples, it was observed that after two cycles between - 150 and + 250°F, numerous small blisters appeared on the surface. On investigation, it was found that these blisters form on the moisture vapor barrier coating. The thermal control coating follows the same change in surface contour and thus its radiative parameters are altered. The surface blistering effect is shown in Figure 17 (a) through (d) where (a) represents the pore-sealed surface of 5026 material, (b) is the same as (a) plus the grey pigmented moisture vapor barrier, (c) is the same as (b) plus the titania pigmented coating, and (d) represents all three coatings plus an aluminum filled silicone-based thermal control paint. The changes in radiative parameters as a consequence of surface blistering are significant in that the α and ϵ values of (d) before thermal cycling were 0.22 and 0.24 respectively, while after they were 0.38 and 0.44. Interestingly, when the same thermal control coating was applied directly over the pore sealed 5026 material (without vapor barrier coating) and the composite thermally cycled, no blistering occurred and the radiative properties were unaltered (Figure 18).

The blistering may be the result of the following two phenomena. First, gases may be released by the 5026 material during heating which are restrained by the impermeable moisture vapor barrier. Second, there may be residual solvent left in the moisture vapor barrier which expands or vaporizes upon application of heat. Accordingly, the blistering can be avoided by omitting the moisture barrier; its role will be taken over by the thermal control/sublimable coating system which is impermeable by water vapors.

After the completion of this investigation it was learned that the top white coating found to be responsible for the blistering has been omitted in the specifications for the Apollo heat shield.

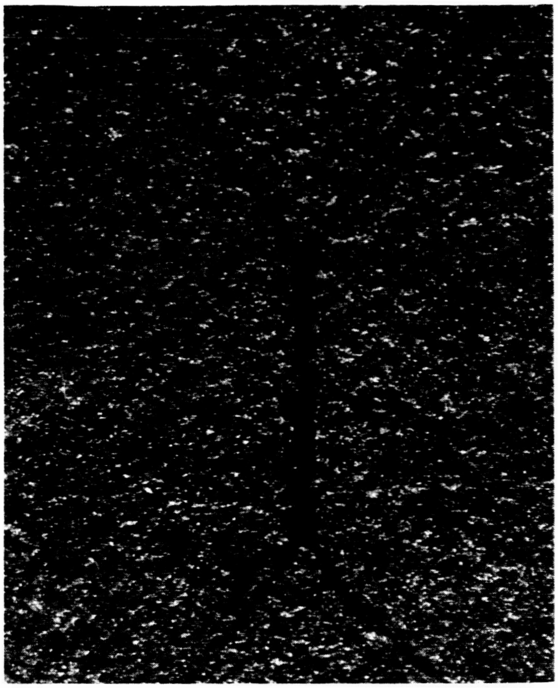

a.

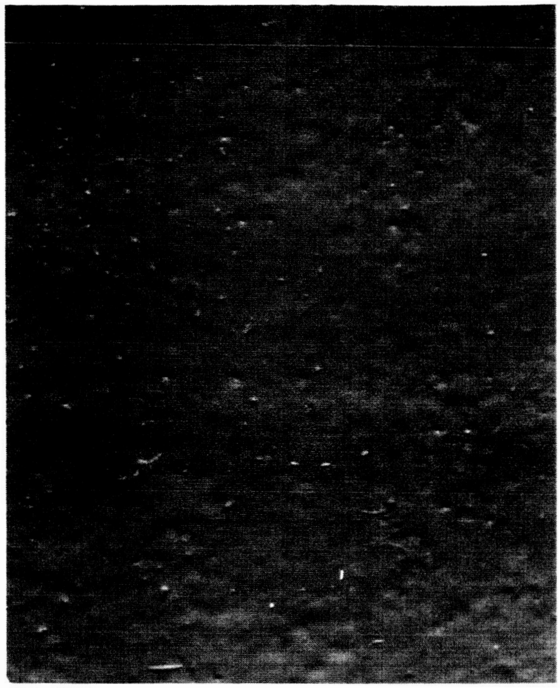

b.

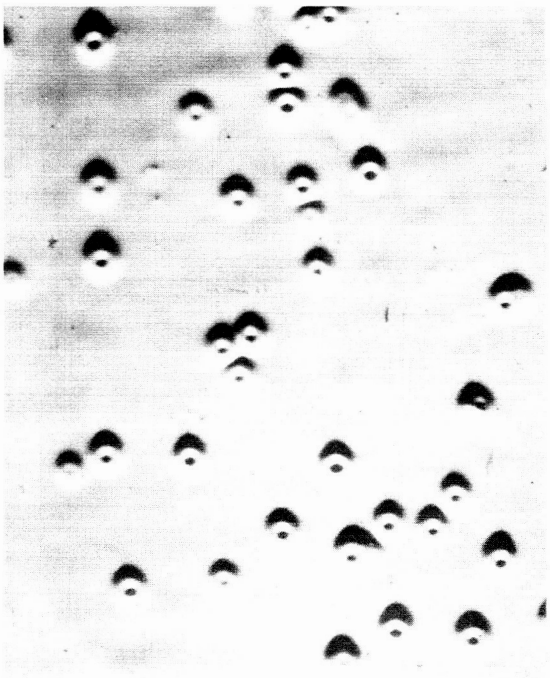

c.

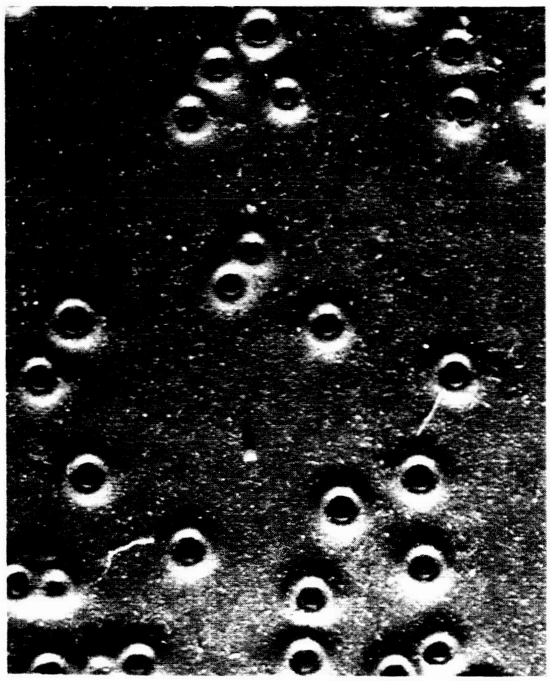

d. 10X

Figure 17 HOT AND COLD CYCLED 5026 (COATED) MATERIAL

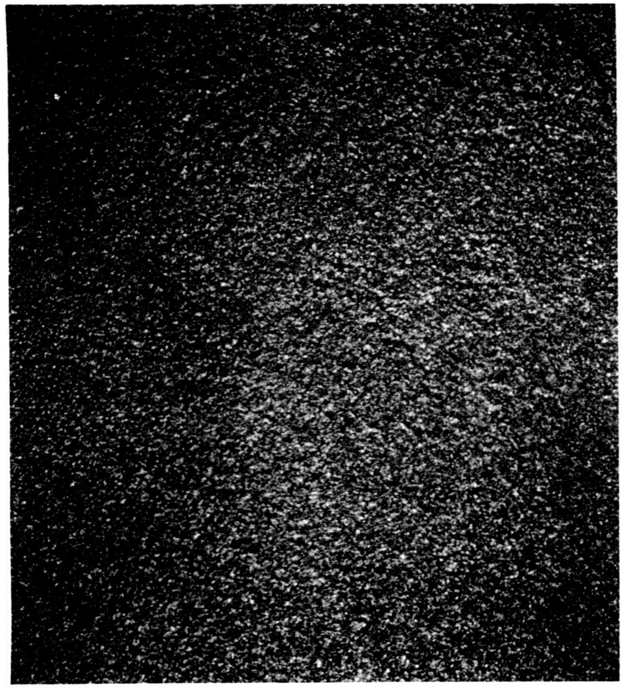

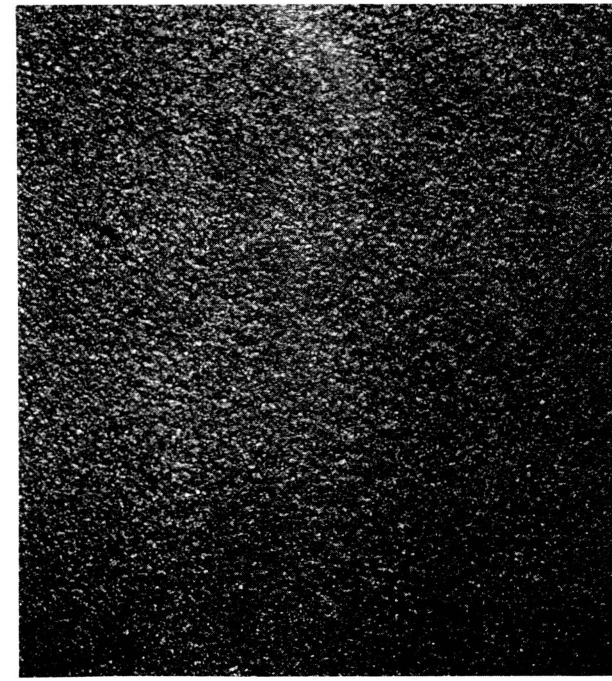

10X

a) Before Thermal Cycling

b) After Thermal Cycling

Figure 18 HOT AND COLD CYCLED SAMPLE (NO VAPOR BARRIER)

The thermal stability of five candidate coating systems was tested by cycling between +150 and -110°F. In these tests the Apollo heat shield material was used without the moisture barrier coating. Two separately prepared samples of each coating systems were tested. The results, shown in Table IX, indicate good stability.

TABLE IX

THE EFFECT OF THERMAL CYCLING ON OPTICAL PROPERTIES

Description	First Sample				Second Sample			
	Before		After		Before		After	
	α	ϵ	α	ϵ	α	ϵ	α	ϵ
Fiberglass - Al - 5026	0.13	0.38	0.13	0.39	0.13	0.37	0.13	0.38
Fiberglass-Heatrem No. 170 - 5026	0.24	0.50	0.25	0.51	0.24	0.52	0.25	0.56
Mylar-Heatrem No. 170 - 5026	0.24	0.50	0.26	0.51	0.26	0.51	0.26	0.52
SiO-Al-Mylar-5026	0.14	0.41	0.15	0.44	0.16	0.44	0.15	0.43
K_2SiO_3 - Al - 5026	0.12	0.40	0.16	0.41	0.14	0.42	0.16	0.43

G. ATTACHMENT STUDIES

The object of this phase of the program was to survey and evaluate commercially available high temperature adhesives and mechanical fasteners for attaching the candidate thermal control coatings to the Apollo heat shield (5026) material.

1. Adhesive Bonding

Based on the thermal control concepts which were considered suitable in view of the optical property requirements, the following adherend combinations were of interest for bonding studies:

5026 material/metal and 5026 material/metallic foil

Both organic and inorganic adhesives were considered, but the survey only included the organics. Over twenty promising candidates have been found.

The following criteria have been established for adhesive selection:

a. The adhesive bond must be capable of withstanding simulated ascent heating and of retaining its integrity during a subsequent hot-cold soak test,

b. Its physical form must permit easy application by conventional techniques; i. e., brush, roller coating,

c. The cure temperature should preferably be below 250°F and cure pressures less than 15 psi,

d. There should be negligible weight loss during the cure cycle,

e. The system must possess a reasonable working (pot) life, and

f. The adhesive should preferably also function as a refractory pore sealer for the 5026 material.

Of the 20 candidates, 11 were selected for study based on previous work conducted by Avco/RAD's Adhesive Group.

Bonded specimens were prepared from machined discs (3/4 x 3/8 inch dia.) of the 5026 material, with and without pore sealer and approximately 50 mil aluminum sheet stock (3/4 inch dia.). Experimental data regarding specimen preparation are given below in Table X.

TABLE X

EXPERIMENTAL DATA FOR BONDED SPECIMEN PREPARATION

No.	Adhesive	Gms		psi	Temp (°F)	Time (Hrs.)
		Part A	Part B			
1	Bloomingdale BXR - 34B-16	20	4	--	200	16
2	Bloomingdale HT 424	--*	--	15-30	325	1
3	Bloomingdale HT 435	--	--	15-30	325	1.3
4	Epoxylite CF 8738	100	25	--	120	24
5	Epoxylite CF 8825	100	9	--	250	1
6	Epoxylite CF 8822	100	36	--	275	3
7	Epoxylite CF 5523	100	40	--	350	2
8	Epoxylite CF 5524	100	220	--	350	3
9	Narmco Metal Bond 302	--	--	15-50	225	3
10	Epon 422	--	--	15-30	350	1
11	Thermo-Resist Glom-on RT	100	40	--	160	4
12	Thermo-Resist Glom-on RT	100	40	--	75	24

* indicates a tape adhesive

The curing conditions reported above are, for the most part, those previously shown to produce the most refractory bonds. It can be seen that six of the eleven adhesives were cured at temperatures greater than 250°F, a non permissible exposure for the Apollo command module. It was felt however, that should any of these six adhesives significantly out-perform those cured at lower temperatures, alternate cure cycles, i.e., longer times at lower temperatures, could be applied.

The eleven adhesives were screened by exposing two bonded specimens of each (with and without pore sealer) to ascent heating as simulated by the pebble bed heater. The specimens were allowed to cool to room temperature and were then subjected to three hot-cold cycles. Microscopic examination of sectioned specimens resulted in the following tentative conclusions:

a. None of the bonds failed during ascent heating in that no delamination was observed.

b. In all instances, some adhesive degradation occurred, but to different extents, as evidenced by charring at the bond line. However, the extent of degradation as it affects adhesive properties is not yet known. The Apollo material experienced only slight darkening close to the adhesive interface. Figure 19 is a cross section photograph of a specimen which was exposed to ascent heating and three thermal cyclings.

c. Nineteen out of the twenty-four bonded specimens remained intact after three hot-cold cycles which indicated that the physical properties of the majority of the adhesives were not completely degraded by the thermal exposure. A large number of these nineteen specimens showed minor cracks at the bond line but the adherends could not be pulled apart manually or easily forced apart with a needle.

d. Based solely on microscopic inspection, adhesives 1, 2, 3, 5 and 12 seemed to be the best. Interestingly, adhesives 11 and 12 consisted of the same material except that number 11 was cured at 160°F for 4 hours and number 12 was cured at room temperature for 24 hours. Both specimens of number 11 delaminated badly during thermal cycling.

2. Mechanical Fasteners

The possibility of using a multilayer system as a thermal control coating depends to some extent on solving the attachment problem.

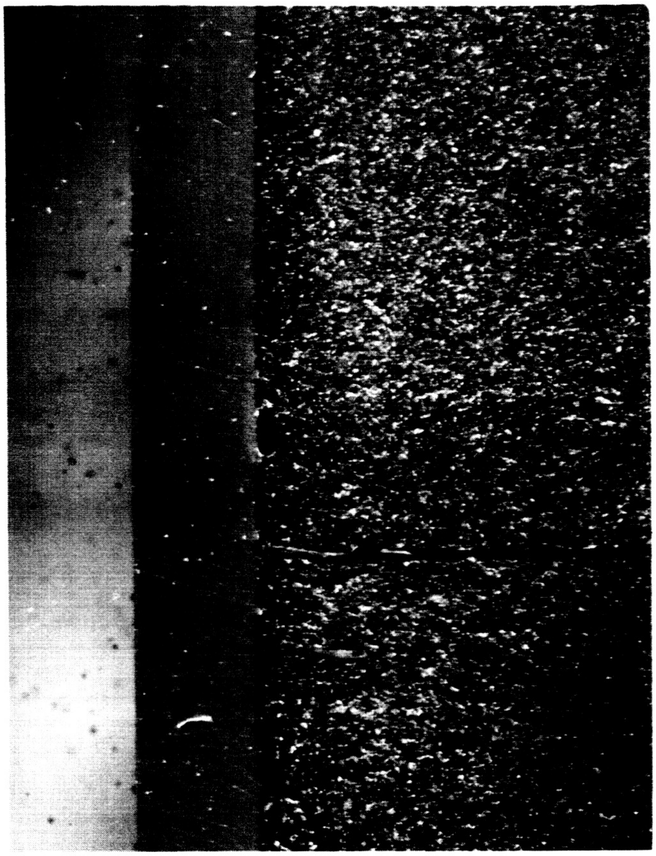

10X

Figure 19 BONDED A1-5026 AFTER ASCENT HEATING AND THERMAL CYCLING

The Tinnerman Fastener shown in Figure 20 is made of nylon but could be made of Teflon and bonded in the ablator material with an adhesive compound. The fastener itself has a high tensile strength in a firm material and the real problem would therefore, be one of integrating the unit with the main Avco ablator material. In a test the above fastener was embedded and bonded in the Apollo material using a room temperature curing adhesive. A tensile force of 240 pounds was required to pull out the fastener.

In reality the required mechanical strength of the fasteners is not very high. During ascent at 0-angle of attack there is no negative pressure and the complete cover is always under positive pressure pressing it onto the conical shaped vehicle. During reentry, the reverse takes place as the suction in the wake tends to pull off the cover. However, the total static pressure up to maximum heating is only of the order of 1 psi (NAS-Memo SEM 062 and RAM-6). Therefore, the suction in the worst case can not exceed 140 lbs/ft^2.

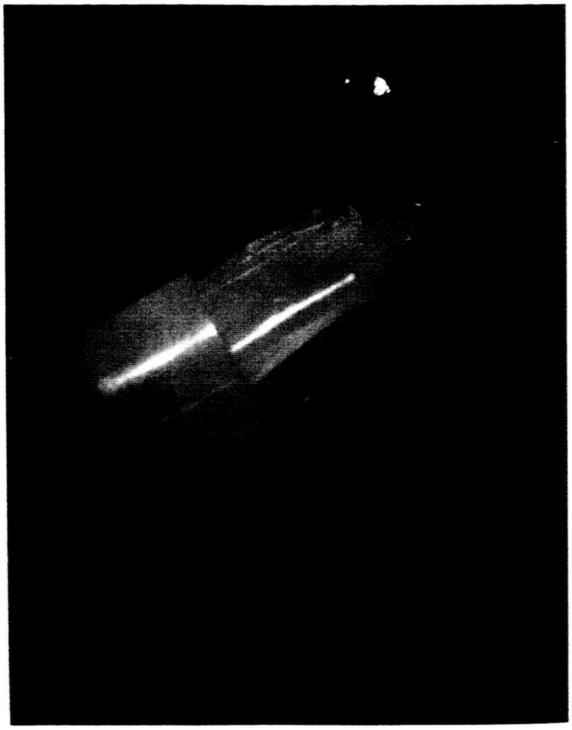

6X

Figure 20 TINNERMAN FASTENER

H. VACUUM STABILITY TESTS

If an impervious film is used as part of the thermal control system a pressure differential of approximately 14 psi will be established across the film once the vehicle is in space. To determine whether this pressure differential would cause rupture of an aluminum foil layer or of the adhesive bond used to attach the foil to the heat shield, the following experiment was performed: A piece of 5026 material was completely covered with aluminum foil. The foil was attached to the heat shield material by a layer of epoxy cement and the seam of the foil was sealed with silicone resin. The composite sample was then placed in a chamber and the pressure was reduced to approximately 1×10^{-5} torr. Additional pressure reduction was not felt to be necessary since its effect on the pressure differential would be negligible. Examination of the specimen after vacuum exposure indicated no rupture of the foil and no adhesive failure. A slight expansion of the silicone rubber was observed but it is felt that it was due to air trapped in the cement itself. The results of these tests indicate that no vent holes or perforations are required if an aluminum foil layer with epoxy cement is used.

Subsequent tests of aluminum foil tape (Y-9050) with a silicone cement exposed to vacuum of 1×10^{-8} torr in the 200 liter chamber also showed no signs of rupture or adhesive failure. Therefore, no vent holes or perforations have been specified for the systems using the Y-9050 aluminum tape.

V. COATING SELECTION

On the basis of the results of the screening tests as well as on the basis of practical considerations concerning the availability and fabricability of the various systems, the following were selected as the most promising coatings.

1) Mylar film on Heat-Rem No. 170 Aluminum Paint

2) 100-13 (EM-32)*Fiberglass cloth on Heat-Rem No. 170 Paint

3) 100-13 (EM-32) Fiberglass cloth on Al Tape (Y9050)

4) Heat-Rem Clear MP Binder on Al tape (Y9050)

5) Si0 on Aluminized Mylar Tape (Schjeldahl)

6) K_2Si0_3 on Al Tape (Y9050)

These six systems were then further evaluated under simulated space environment conditions.

In the initial environmental stability tests, the samples were placedin a 200 liter chamber, which was then evacuated to 7 x 10^{-8} mm Hg, and exposed to simulated solar radiation for 72 hours. In specifying the duration of simulated solar exposure, it was considered that, during the total Apollo mission, the surface of the command module would be exposed to space environment, including solar radiation for 170 hours. A 30 degrees section of the surface would be exposed to the maximum insolution for 1/6 - 16.3 percent of the total time. For another 16.3 percent the insolation will be 70 percent of the maximum and for a third 16.3 percent the incidence solar radiation will be very weak. Therefore 72 hours (42 percent of the total mission time) irradiation with one Sun intensity in the space simulation chamber includes a sufficient safety margin to establish the u. v. and solar radiation stability of the tested coatings.

In the first test, five candidate systems were exposed to the simulated space environment. In addition, a highly polished aluminum disc and a copper disc coated with 3M black were also installed as radiation reference samples. The samples were arranged in a planar configuration as shown in Figure 9 so that all samples would receive uniform radiation. The α and ϵ values of the samples

* Upon examination of fiberglass fabrics, it was found that No. 100-13 and EM-32 were equivalent materials. Since EM-32 fabric from the Exeter Manufacturing Co. was more readily available, this cloth was substituted for the No. 100-13 fabrics. No change in the behavior of systems containing this material were observed.

before and after exposure were used as a measure of the stability of each of the coatings in the space environment. The effect of the exposure on the optical properties of the coatings is shown in Table XI.

TABLE XI

EFFECT OF EXPOSURE ON THE OPTICAL PROPERTIES OF COATINGS

Sample	Before Test		After Test		
	α	ϵ	α	ϵ	α/ϵ
1. Mylar film on Heat-Rem	0.30	0.70	0.35	0.68	0.51
2. Em-32 Fiberglass cloth on Heat-Rem	0.30	0.62	0.27	0.58	0.46
3. Schjeldahl tape	0.14	0.46	0.17	0.48	0.35
4. Heat-Rem binder on Al tape	0.23	0.60	0.25	0.58	0.43
5. EM-32 Fiberglass cloth on Al tape	0.20	0.51	0.20	0.53	0.38

Although the measured α and ϵ values for the systems do not show any gross changes, visible observations showed that samples 1, 3 and 4 yellowed. The discoloration was so pronounced in the case of sample 1 that the sample was removed from further consideration.

In the second series of tests, new samples of the candidate systems were again exposed to vacuum and simulated solar radiation for 72 hours. The sixth candidate system, potassium silicate on aluminum tape, however, was substituted for sample 1. The result of this series is shown in Table XII.

In this test, the solar intensity was found to have increased to as high as 1.45 suns. This increased intensity may account for the increase in α for sample 3 and in ϵ for the sample 4 (Table XII). It should be noted, however, that samples 1, 2, and 5 showed negligible changes even under the increased solar radiation intensity.

As a result of the space environment stability tests, the two most stable candidates with optical properties within the stipulated limits were selected for additional testing. These were:

- EM-32 Fiberglass cloth on Y9050 Aluminum tape
- Potassium Silicate on Y9050 Aluminum tape

to 7 x 10^{-8} torr to approach the space vacuum. An aluminum heater was attached to the metal honeycomb backup structure so that the interior face of the ablator structure could be maintained at 75°F: the temperature maintained by the E.C.S. unit in the command module. Thermocouples were placed at the interface of the ablator material and the thermal control system. Five thermocouples were distributed across the 5 inch surface of the sample to monitor the uniformity of the incident radiation. These thermocouples indicated temperatures within 5 degrees of each other showing that the uniformity of the incident beam was satisfactory.

The performance of the SiO-Aluminum - Apollo structure system is illustrated in Figures 21 and 22. A five inch diameter block of this system was exposed to the simulated solar radiation for 75 hours and was cycled between the hot and cold soak temperatures to obtain heating and cooling curves. The heating curves (Figure 22) show a tendency of the coating to reach a higher equilibrium temperature as the exposure progressed. This behavior was interpreted as indicating that the sample was sensitive to solar radiation and that α was increasing as the exposure time increased. This interpretation was substantiated when the sample was removed from the chamber and found to have obviously discolored; α was found to have increased from 0.13 to 0.20 during the environmental test.

Subsequent measurements of α on the previously exposed sample, however, showed that α was decreasing with time as it was being measured. To verify this observation, the sample was left exposed to the solar radiation of the solar reflectometer at ambient conditions of temperature and pressure for 16 hours. When the sample was examined after this exposure, the area of exposure was readily discernable as a colorless circle in the discolored yellow field (Figure 23). The observations shows that the SiO-Aluminum system discolors to yellow upon exposure to simulated solar radiation in vacuum but that the yellow color becomes transparent if it is exposed to similar radiation in air. To account for this behavior it is suggested that SiO is unstable toward solar radiation and decomposes to Si and O and/or Si and SiO_2. In vacuum, the silicon remains as the metal and serves to discolor the system. In air, however, the silicon is oxidized to silicon dioxide, SiO_2, which is stable and remains colorless. If this suggested mechanism could be substantiated, it could be beneficial to pre-irradiate the SiO film in air to convert it to the stable SiO_2 before exposure in vacuum.

The cooling curves (Figure 22) indicate a tendency for the cold soak equilibrium temperature to increase as the exposure time increased. This was interpreted as indicating a decrease in the infrared emittance of the coating with time of exposure. This was also substantiated by emittance measurements made before and after exposure; ϵ decreased from 0.43 to 0.36 during the test.

The performance of the fiberglass aluminum Apollo structure system under simulated flight heating and cooling conditions is shown in Figures 24 and 25.

TABLE XII

SAMPLES EXPOSED TO VACUUM AND SIMULATED SOLAR RADIATION FOR 72 HOURS

Sample	Before Test		After Test		
	α	ϵ	α	ϵ	α/ϵ
1. EM-32 Fiberglass cloth on Y-9050 Al tape	0.15	0.48	0.15	0.45	0.33
2. EM-32 Fiberglass cloth on Heat-Rem No. H-170	0.27	0.55	0.26	0.57	0.45
3. Heat-Rem binder on No. U-9050 Al tape	0.20	0.46	0.25	0.41	0.60
4. Schjeldahl tape	0.13	0.48	0.16	0.58	0.28
5. Potassium Silicate on No. Y-9050 Al tape	0.16	0.51	0.17	0.55	0.30

The systems of fiberglass cloth on Heat-Rem No. 170, and Heat-Rem binder or Aluminum tape were eliminated from further consideration because their optical properties were higher than desired. In the case of the Schjeldahl aluminized mylar, it was thought that perhaps the observed discoloration was due to the mylar. Consequently, a sample consisting of a layer of 12,000 Å of silicon monoxide on thin aluminum foil was obtained from the G. T. Schjeldahl Co. This system was then tested along with the two previously selected systems.

The tests were designed to demonstrate the effectiveness of the selected thermal control system during actual space flight.

For these experiments, the test sample consisted of a 5 inch diameter block of the 5026 Apollo ablator material mounted on metal honeycomb as specified in the Apollo heat shield design. The ablator was 1-1/2 inches thick, which is a mean value of the thickness of the heat shield over the entire vehicle. The surface of the ablator was covered with one of the three thermal control coating systems selected for further study.

The sample was placed in the 200 liter controlled environment test chamber and was subjected to conditions typical of the Apollo flight.

The space heat sink was simulated by the blackened, liquid nitrogen cooled shroud maintained at $-274 \pm 4^{o}F$ throughout the test. Radiation heating of the sample was provided by the 5 kw Xenon lamp in combination with the 1 kw watt mercury lamp to simulate the solar spectrum. The chamber was evacuated

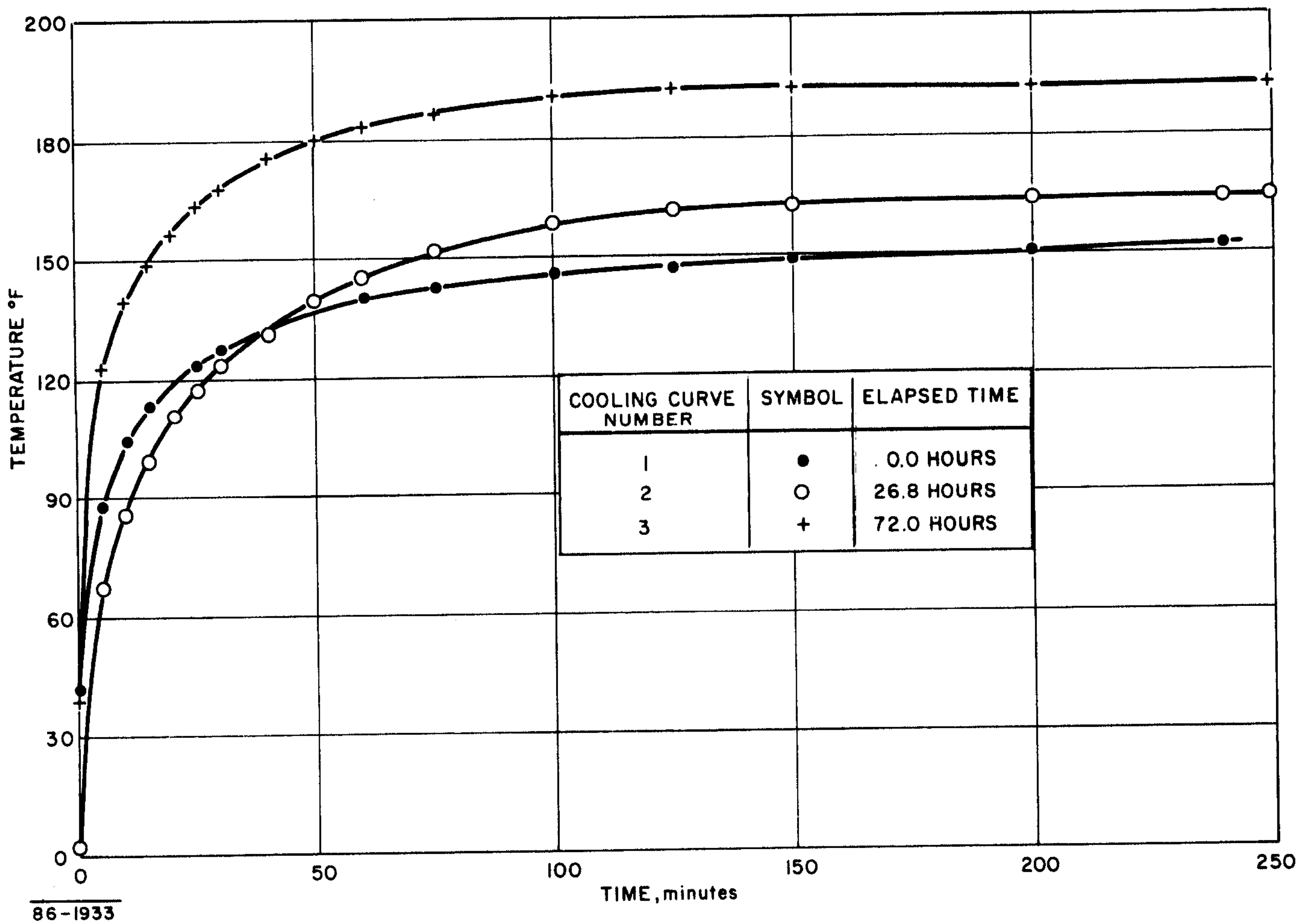

Figure 21 HEATING CURVES -- SCHJELDAHL MATERIAL

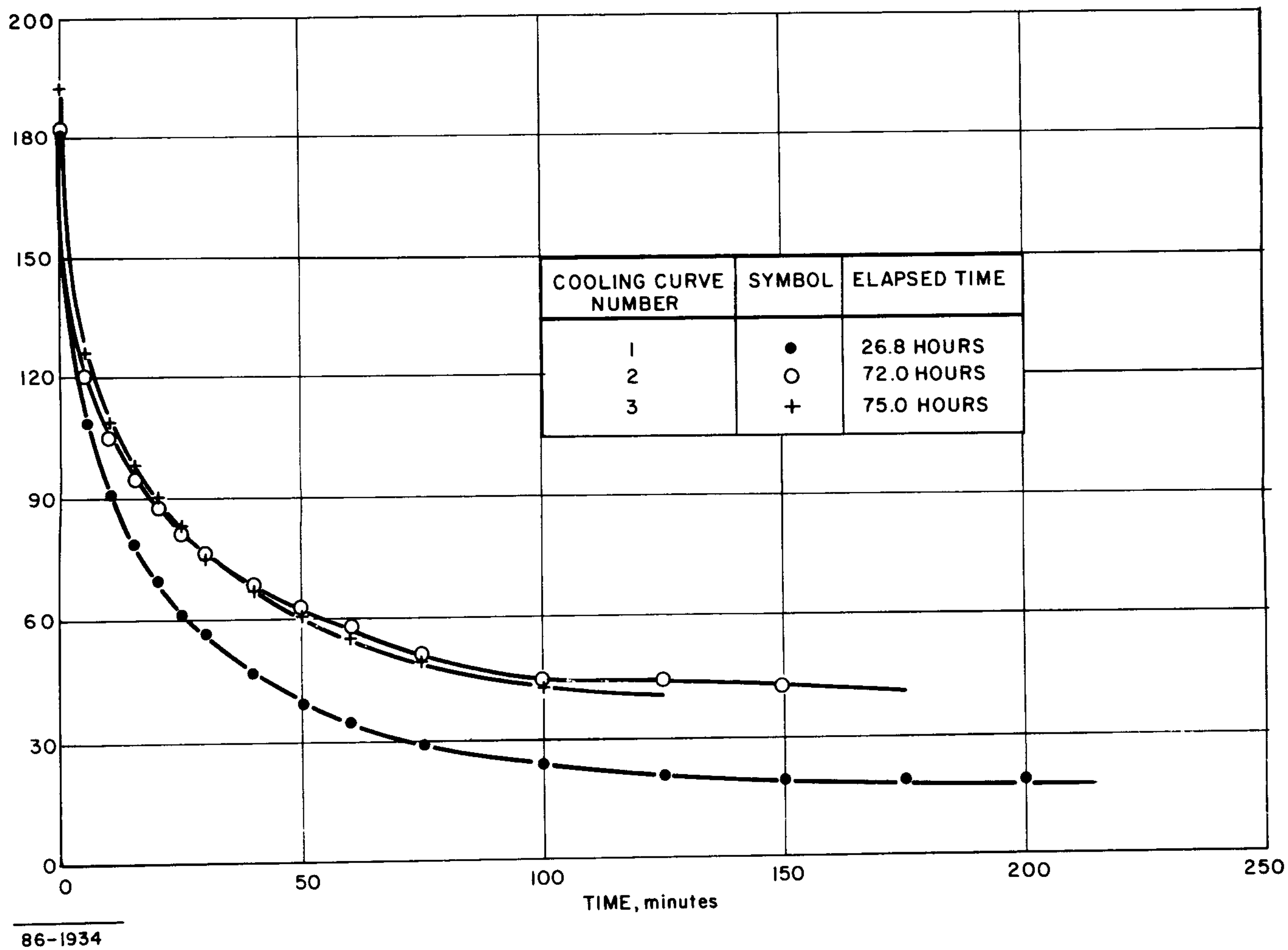

Figure 22 COOLING CURVES -- SCHJELDAHL MATERIAL

Figure 23 BLEACHING OF IRRADIATED SCHJELDAHL MATERIAL

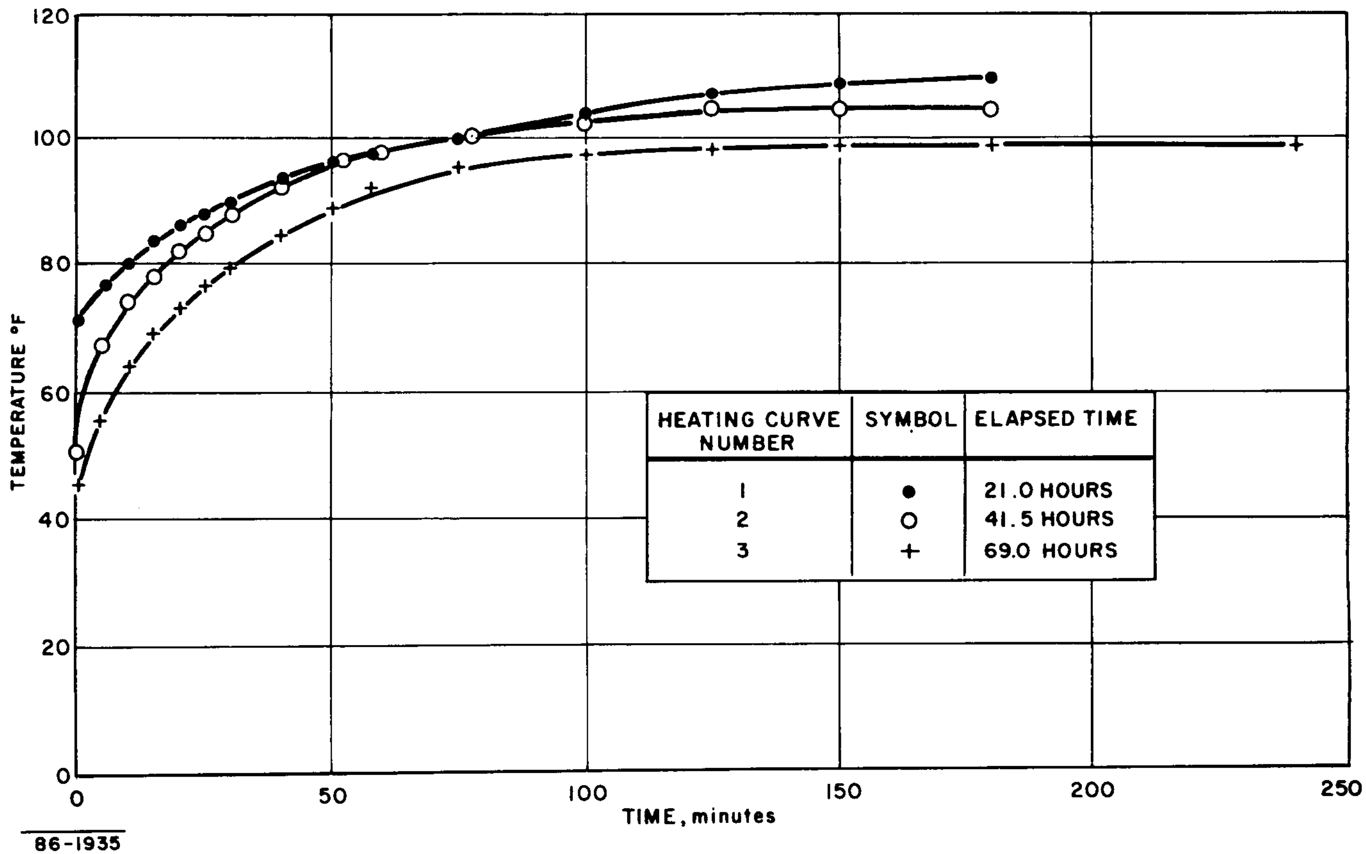

Figure 24 HEATING CURVES -- ALUMINUM TAPE-GLASS CLOTH

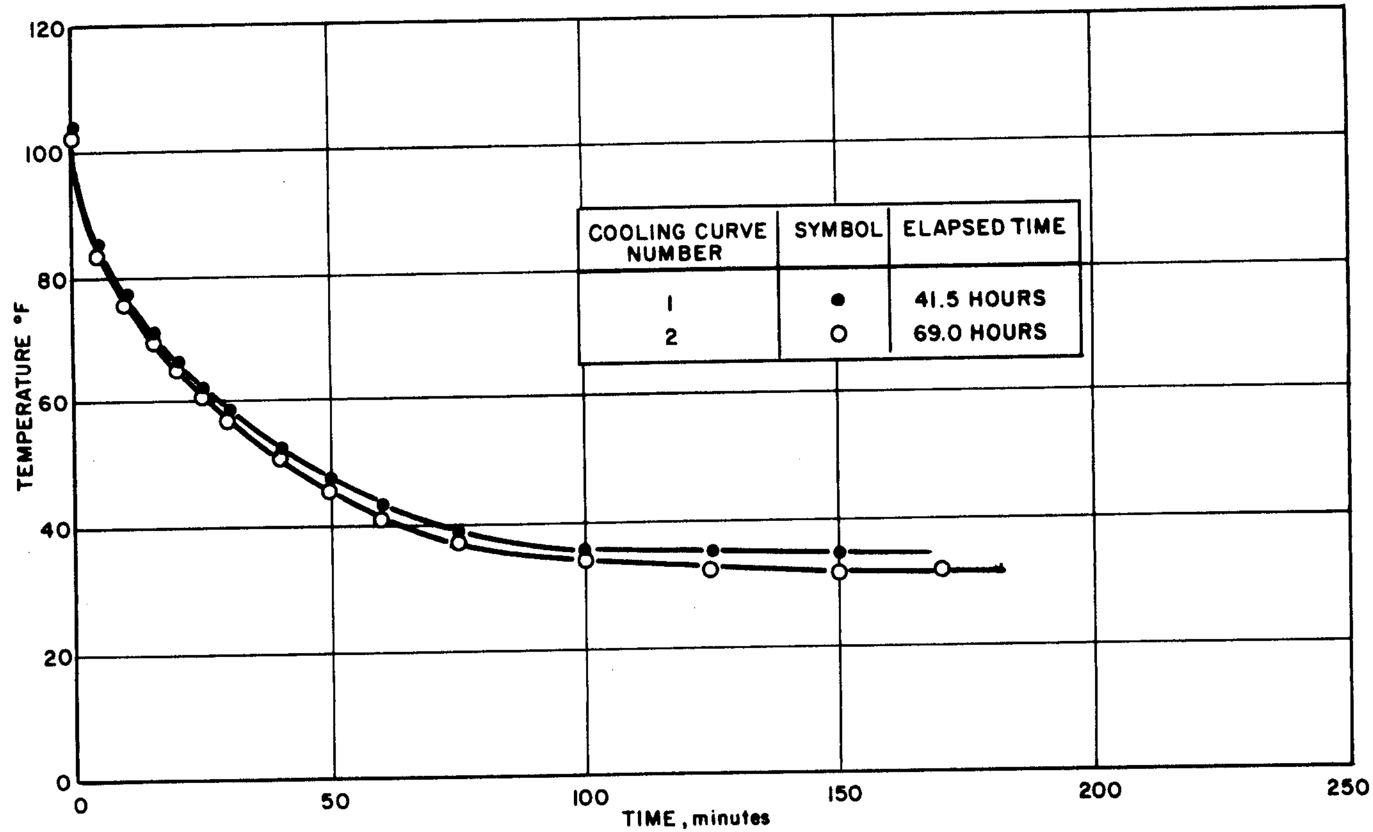

86-1936

Figure 25 COOLING CURVES -- ALUMINUM TAPE-GLASS CLOTH

The curves show that this thermal control system:

1. Would maintain a surface temperature below 110°F for hot soak periods of up to three hours and that the temperature rise would be negligible for continued solar irradiation. The random variations in the maximum hot soak temperatures were not considered indicative of any ultraviolet degradation since they do not show a progressive trend toward either a lower of higher α value. Instead, the temperature differences recorded for each of the four hot soak periods are likely due to small variations in the incident radiation which could lead to the observed temperature differences of $\pm$ 5°F;

2. Would limit the cold soak temperature to above 30°F for shadow periods of up to three hours and to above 20°F for much longer periods.

The effectiveness of the K_2SiO_3 - Al thermal control coating in alleviating the maximum and minimum temperatures in the hot soak and cold soak periods of the Apollo flight is illustrated in Figures 26 and 27. The heating and cooling curves show that this system:

1. Would maintain a hot soak temperature below 75°F for solar irradiation periods of longer than six hours. Heating curve 1 of Figure 25 indicates that the surface would reach an equilibrium temperature about 13°F lower than the equilibrium temperatures recorded for curves 2 and 3. It is believed that this discrepancy was caused by a variation in the attitude of the sample toward the beam of incident radiation rather than by an instability of the coating toward solar radiation. This conclusion is substantiated by the fact that repositioning the sample caused a surface temperature rise and that previous environmental tests had indicated that the system was completely stable toward solar radiation;

2. Would limit the surface temperature to above -30°F for cold soak periods of six hours or longer.

As previously indicated 72 hours of solar irradiation, normal to the surface is an overly severe exposure. In flight, due to the curvature of the vehicle, only a small fraction of the surface can be normal to the incident radiation at a given time. The rest of the vehicle will be irradiated at a more acute angle and will consequently reflect a large portion of the incident radiation. To demonstrate that the acute angle irradiation is less severe than normal irradiation the K_2SiO_3 - Al coated sample was tilted in the environmental chamber to form a 45 degree angle with the incident beam. The equilibrium temperature for the case of perpendicular irradiation was found to be 62°F whereas for the 45 degree irradiation it was found to be 35°F.

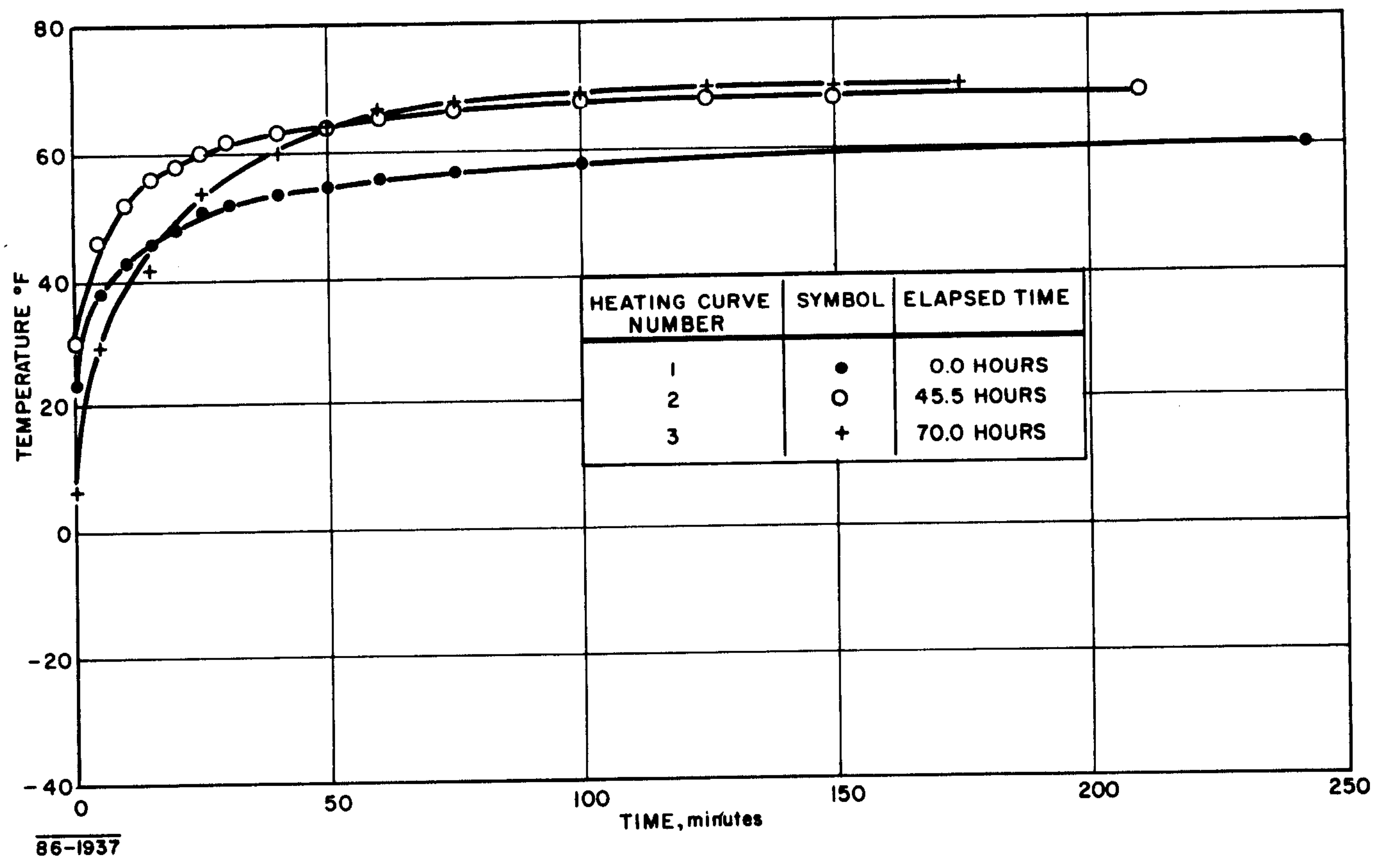

Figure 26 HEATING CURVES -- ALUMINUM TAPE -- POTASSIUM SILICATE

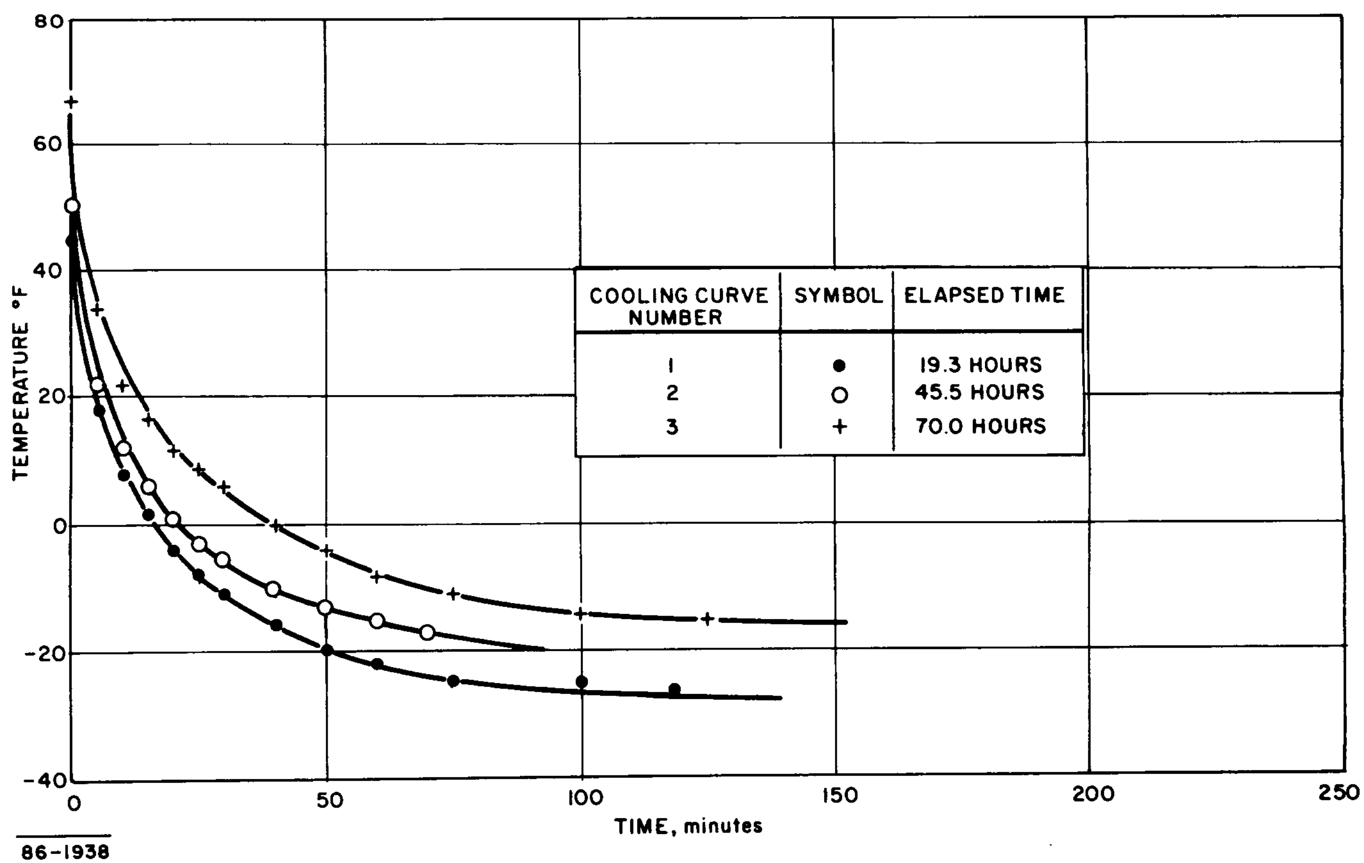

Figure 27 COOLING CURVES -- ALUMINUM TAPE -- POTASSIUM SILICATE

A. SUMMARY OF ENVIRONMENTAL TEST RESULTS

The behavior of each of the six systems under simulated space environment conditions may be summarized in the following way.

1. Mylar Film on Heat-Rem No. 170 Aluminum Paint

The mylar film became embrittled and discolored during the space environment stability test.

2. Fiberglass (EM-32) on Heat-Rem No. 170 Aluminum Paint

This system demonstrated satisfactory stability toward the space environment. Its optical properties, however, were slightly higher than required.

3. Fiberglass (EM-32) on Aluminum Tape (Y9050)

This system proved to be stable toward the space environment and demonstrated that it would maintain the maximum and minimum temperatures well within the stipulated temperature extremes of $150^{o}F$ and $-150^{o}F$.

4. Clear Heat-Rem (MP) Resin on Aluminum Tape (Y9050)

The resin of this system discolored during the environmental stability tests.

5. Silicon Monoxide on Aluminized Mylar Type (G. T. Schjeldahl Co.)

This system discolored during the environmental stability tests. A variation of this system in which the SiO was applied directly on aluminum foil was also tested under the simulated space environment. It also discolored and in addition allowed the surface temperature of the Apollo heat shield to rise above the stipulated $150^{o}F$ maximum.

6. Potassium Silicate on Aluminum Tape (Y9050)

This system demonstrated that it was stable toward the space environment and capable of maintaining the temperature extremes of the heat shield well within the stipulated levels.

The environmental tests indicate that of the six systems evaluated, two systems meet the stipulated requirements for the Apollo thermal control system. These are systems 3, fiberglass cloth on aluminum tape, and 6, potassium silicate on aluminum tape. Complete descriptions of these systems follow.

B. DESCRIPTION OF THE QUALIFIED SYSTEMS

1. Aluminum - Fiberglass System

This system consists of the 3M company's (Y-9050) Heat Reflective Tape covered with the Exeter Manufacturing Company's EM-32 Fiberglass Cloth. The Y-9050 is a lamination of 0.0005 inch aluminum foil to a 0.002 inch glass cloth coated with a silicone adhesive. The foil is highly reflective to radiant heat, while the glass cloth contributes strength and flexibility to the laminate. It has a tensile strength of 75 lbs/inch of 1 inch width, 5 percent elongation, and an ASTM adhesion rating of 22 oz/in. The adhesive is specially compounded for high temperature performance. The tape is readily available in widths up to 12 inches and can be obtained in widths up to 36 inches if required.

The EM-32 fiberglass cloth is available in 250 yd. rolls, 38 inches wide. It is 0.005 inch thick and weighs 1.9 oz/yd^2. It is a leno weave with 30 ends of 16 picks per inch. For this application no lubricant or finishing compound must be specified.

The Y-9050 tape is applied directly to the Apollo heat shield material so as not to wrinkle or contaminate the surface of the tape. The EM-32 fiberglass is spread over the tape and bonded to the tape at 1 inch intervals in each direction. Potassium silicate (Sylvania PS-7) is the adhesive used for this purpose. An enlarged photograph showing the weave of the cloth and the aluminum tape underlayer is shown in Figure 28. When prepared in the described manner the composite should have an α of 0.17 ± 0.02 and an ϵ of 0.47 ± 0.02. It should weigh 0.08 lb/ft.^{2}

2. Aluminum - Potassium Metasilicate

This system is composed of the Y-9050 aluminum tape described for system 1, covered with a thin layer of potassium silicate, PS-7, produced by Sylvania Electric Products, Inc. This grade of potassium silicate is characterized by its outstandingly high purity and high total solids content. It is produced primarily for use in the manufacture of TV picture tubes and cathode ray tubes where it acts as a bonding agent to prevent disturbance of the phosphor during processing. The purity of this solution is important because of the influence of contaminants on the optical properties of the cathode ray screens, and in the present application, on the optical properties of thermal control coatings. This high purity solution is readily available in quantities up to 4500 gallons, shipped in stainless steel tank trucks or in 55 gallon drums.

The Y-9050 tape is applied directly to the Apollo heat shield, taking care not to wrinkle or contaminate the surface. The potassium silicate solution is applied to the aluminum tape by a spraying process. The solution is

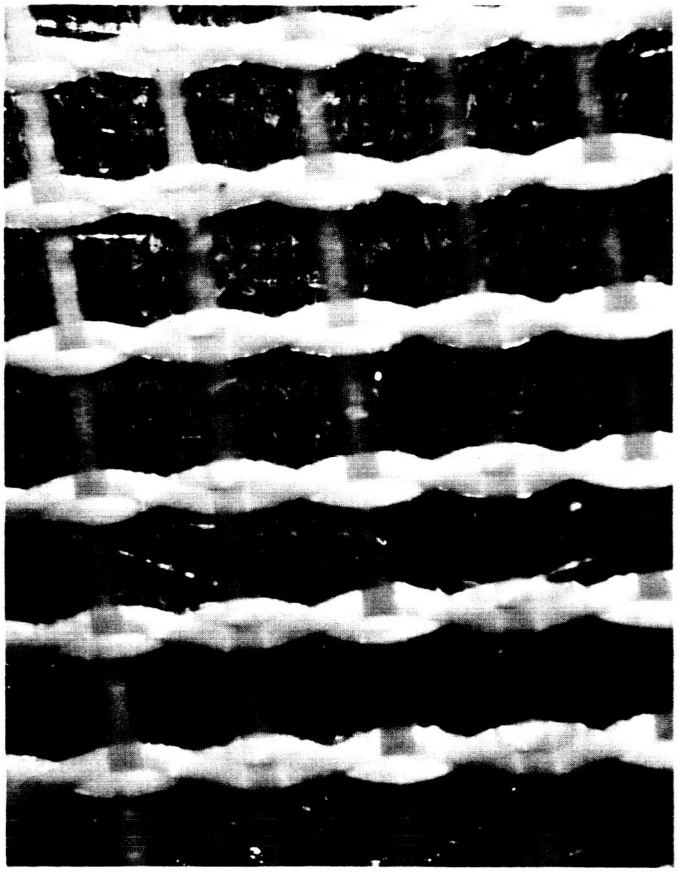

11X

Figure 28 ALUMINUM TAPE -- FIBERGLASS CLOTH SYSTEM sprayed without dilution, as received from the supplier. A De'Vilbiss Spray Gun, type P-MBC-526 with a 704 nozzle tip is used at a distance of 7 1/4 inches from the tip to the surface being sprayed. A transformer pressure of 19 pounds and a pot pressure of 15 pounds is maintained throughout the process. Each pass is made at a spraying rate of 3 inches per second and the optical properties are controlled by the number of passes. A graph showing the variation in optical properties as a function of the number of spray passes is shown in Figure 29. An enlarged photograph of the composite surface is given in Figure 30. This photograph illustrates that the potassium silicate does not form a continuous coating on the aluminum tape. Rather it is present on the tape in evenly distributed dots. The size and distribution of these dots regulates the ϵ of the surface. When this system is prepared, using three spray passes it should have an α of 0.14 ± 0.02 and an ϵ of 0.40 ± 0.12. It should weigh 0.07 lb/ft^2.

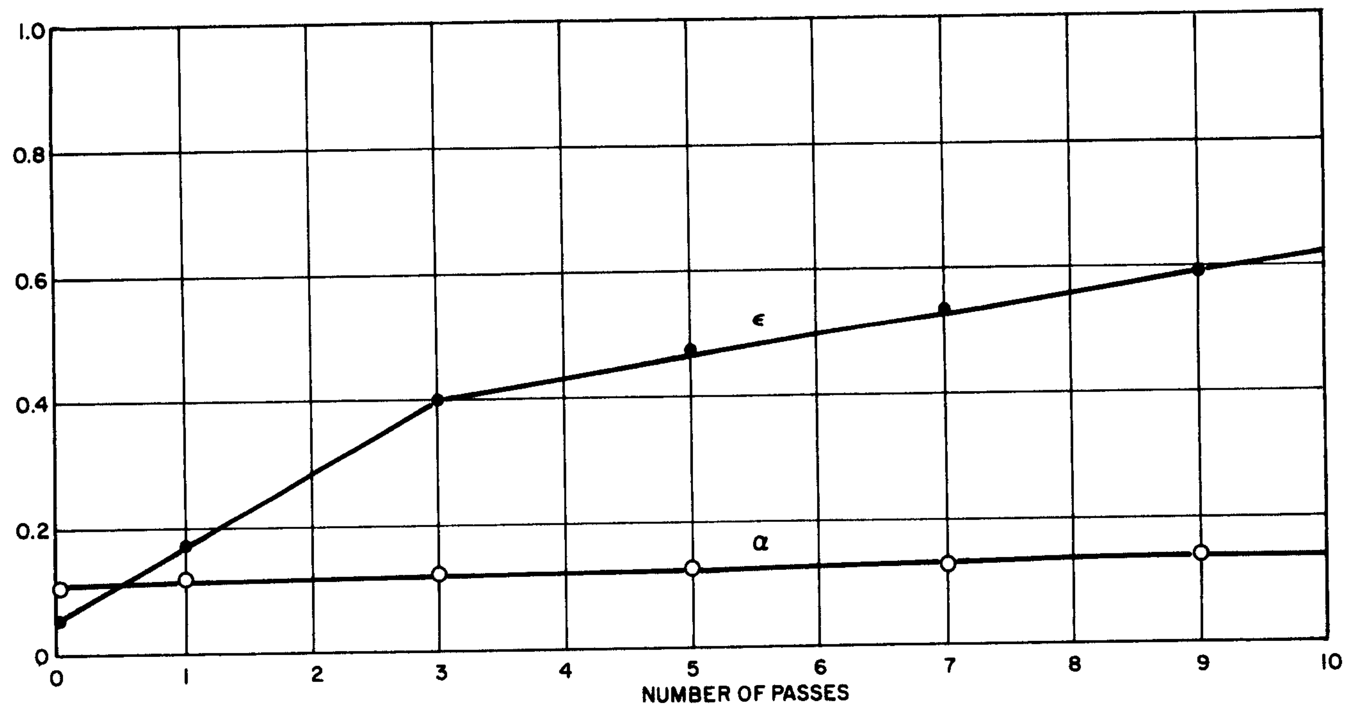

86-1939

Figure 29 NUMBER OF PASSES VERSUS OPTICAL PROPERTIES

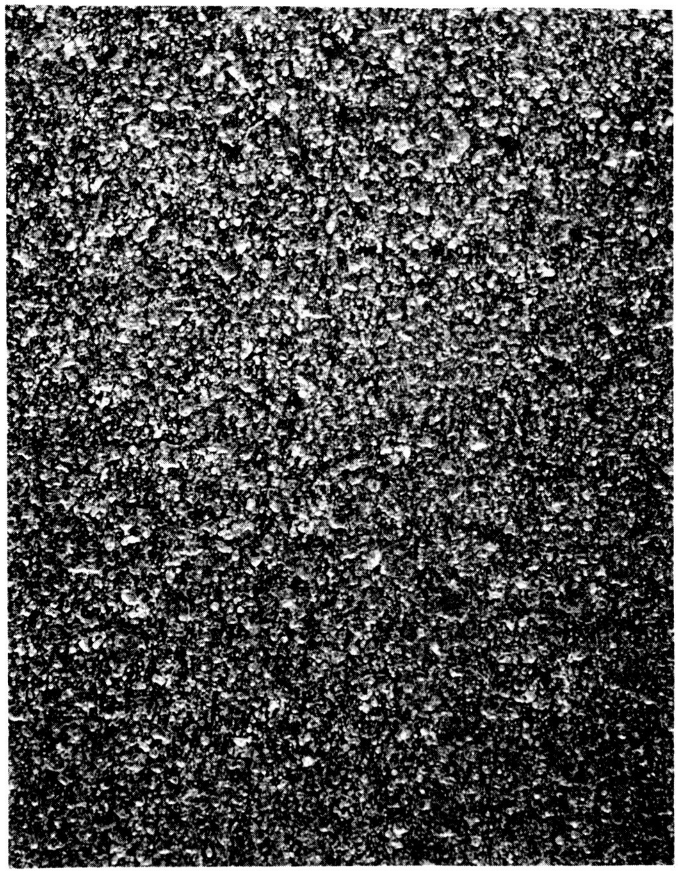

Figure 30 ALUMINUM TAPE -- POTASSIUM SILICATE SYSTEM

VI. DEVELOPMENT OF THE SUBLIMABLE COATING

Preliminary ascent heating and thermal cycling tests performed on the first generation coatings with Apollo ablator material (designated 5026) substrate showed that thermal decomposition and degassing of the substrate and/or its applied moisture barrier would adversely affect the optical properties of the thermal control coating. Further, it was learned that liquid and solid particles in the exhaust of the S4B retrorockets and the abort tower separation rockets, may deposit on the thermal control coating and may adversely affect its radiative properties.

Accordingly, even if the contamination from the moisture barrier decomposition could be completely eliminated, the thermal control coating may still not have the desired optical characteristics after the ascent third stage separation. Therefore, the research effort was reoriented from the refractory coating requirement toward an approach which would solve both the thermal degradation and contamination problem.

A possible solution to this combined problem was found by the use of a sublimable coating over the thermal control coating. A satisfactory sublimable material would absorb a large fraction of the ascent heat, thus keeping the thermal control coating underneath at a relatively low temperature. Further, if present in a thick enough layer, the volatile coating would prevent the deposition of the exhaust contamination on the thermal control coating, provided contaminants do not migrate to the thermal control coating during sublimation. Removal of contaminants during sublimation has not been verified by testing to date. This resolution is required before it can be established that the sublimable coating technique is a satisfactory solution to the contamination problem.

The most important requirements for such a sublimable coating are:

1) It must remove contaminants during sublimation, leaving a clean thermal control coating without presence of any contaminants; *

2) It should be a clean ablator as well as sublimer since any residue from nonvolatile products of ablation would affect the radiative properties of the thermal control coating;

3) It should have a high heat of ablation to minimize the required weight of the coating. This generally implies a high temperature of the triple point since melting drastically lowers the heat of ablation;

---

*Because the contamination problem had not been defined when this contract was initiated, an extensive program involving testing of sublimable coatings under simulated contamination conditions was beyond the scope of this contract.

4) The coating material should ablate at relatively low temperatures since the flux rate and enthalpy during ascent are low; the lower the temperature at which ablation starts, the lower the temperature of the thermal control coating, and the lower the temperature of the surface of the main heat shield during ascent.

5) It should have a high vapor pressure at relatively low temperatures so that it will vaporize quickly in space. Conversely, too high a vapor pressure may increase fabrication problems and could require increased coating thickness to withstand the ascent heating; too high a vapor pressure would also affect the prelaunch behavior of the coating.

Accordingly, a major effort was put forth for the selection, development, application, and testing of potential sublimable coatings.

TABLE XIII

LOW TEMPERATURE ABLATORS

Material	MW	ρ (lb/ft^3)	C_p (Btu/lb °F)	K (Btu/HR FT °F)	M.P. (°F)	H_{sub} (Btu/lb)	H_{fus} (Btu/lb)	q*L at H_s/RT_o = 30 (Btu/lb)
Teflon $(C_2F4)_n$	$(100.02)_n$	136.1	0.26	0.14	1300*	750		1050
Paradichloro-benzene $C_6H_4Cl_2$	147.01	95.7	0.22	0.14 (75° F)	127	200	53.5 (128° F)	83
Camphor $C_{10}H_{16}O$	152.23	62.5	0.44	0.117	354	151.5		474

*sublimation point

A. COATING SELECTION

Initial evaluation was done on the compounds listed in Table XIII since experience at Avco/SSD had shown these to be clean ablators and to have fairly high heats of sublimation. The thermal properties listed in the table show that the sublimation point of teflon is too high since the minimum peak heating temperature on the command module is about 500°F. Further the paradichlorobenzene melts instead of sublimes when the ambient pressure is over 0.2 psia.

B. ANALYTICAL EVALUATION

In order to establish the feasibility of this approach an analytical evaluation was made.

Using the value of H_v-151 Btu/lb from the literature, calculations were made to establish the camphor thickness necessary to keep the ablator temperature below decomposition values. As shown in Figure 31 the calculations indicated that although the camphor had completely vaporized at 140 seconds the outermost layer of the heat shield would not heat above 500°F with a camphor thickness of 0.1 inch. With only 0.05 inch thick camphor coating, complete vaporization would take place after 120 seconds and the now exposed surface would reach a peak temperature of 700°F. These calculations were performed for the highest temperature region of the command module surface, location X_c=48.9. At cooler portions the peak temperature would be lower and some camphor would remain on the surface after ascent.

A similar evaluation was made for Teflon. The surface temperatures of a 0.1 inch and 0.05 inch Teflon coating as well as the temperature of the ablator underneath are shown in Figure 32. While the surface temperatures are not much lower than that of an unprotected surface (1160°F), the ablator surface reaches only 620°F, with a 0.05 inch thick Teflon coating, and less than 500°F with a 0.1 inch Teflon coating. A thermal control coating covering the ablator would reach approximately the same low temperatures. Very little of the original Teflon coating would vaporize during ascent; thus most of this layer would become part of the thermal control coating system.

Because of its low vapor pressure and chemical stability, Teflon could be used as a permanent component of a thermal control coating system. A pigmented Teflon coating or a thin layer of Teflon over an aluminum surface has been considered and efforts to prepare such a coating are described elsewhere.

A high vapor pressure compound e.g. camphor, could not be incorporated into a coating system since on vaporizing, the optical characteristics would change. Calculations were made to determine how much time would be required to vaporize a unit thickness of camphor in space completely exposing the underlying thermal control coating.

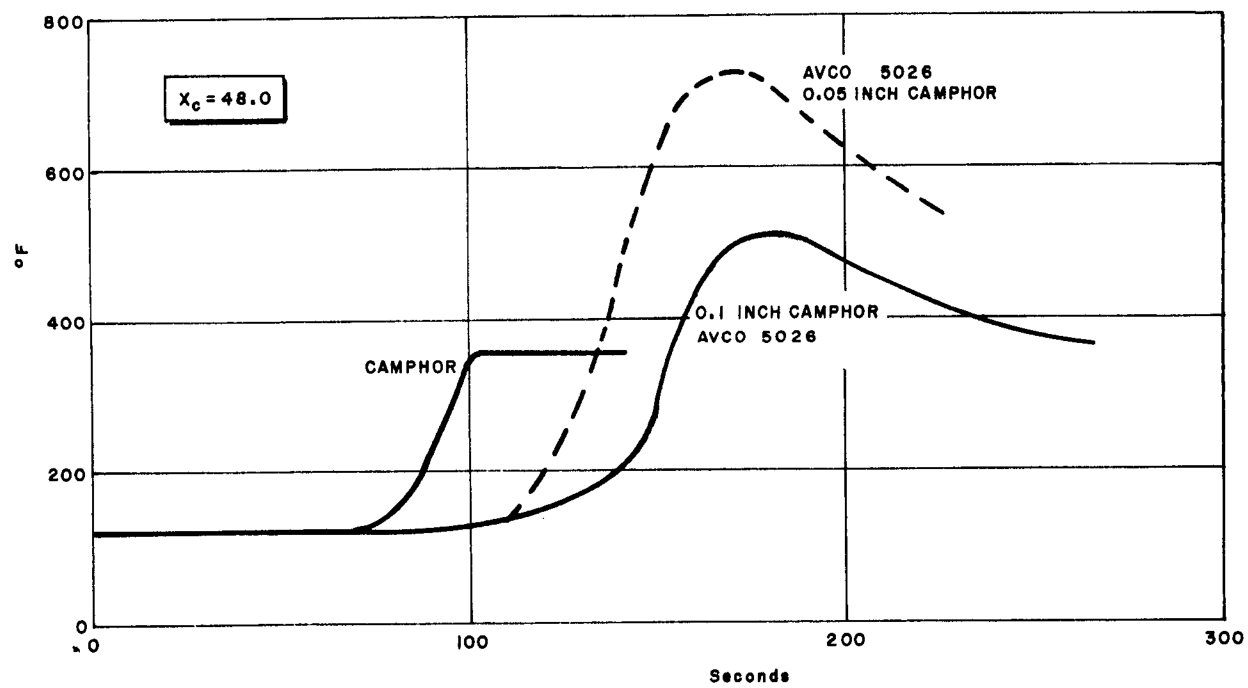

65-5328

Figure 31 SURFACE TEMPERATURE OF CAMPHOR AND AVCO 5026

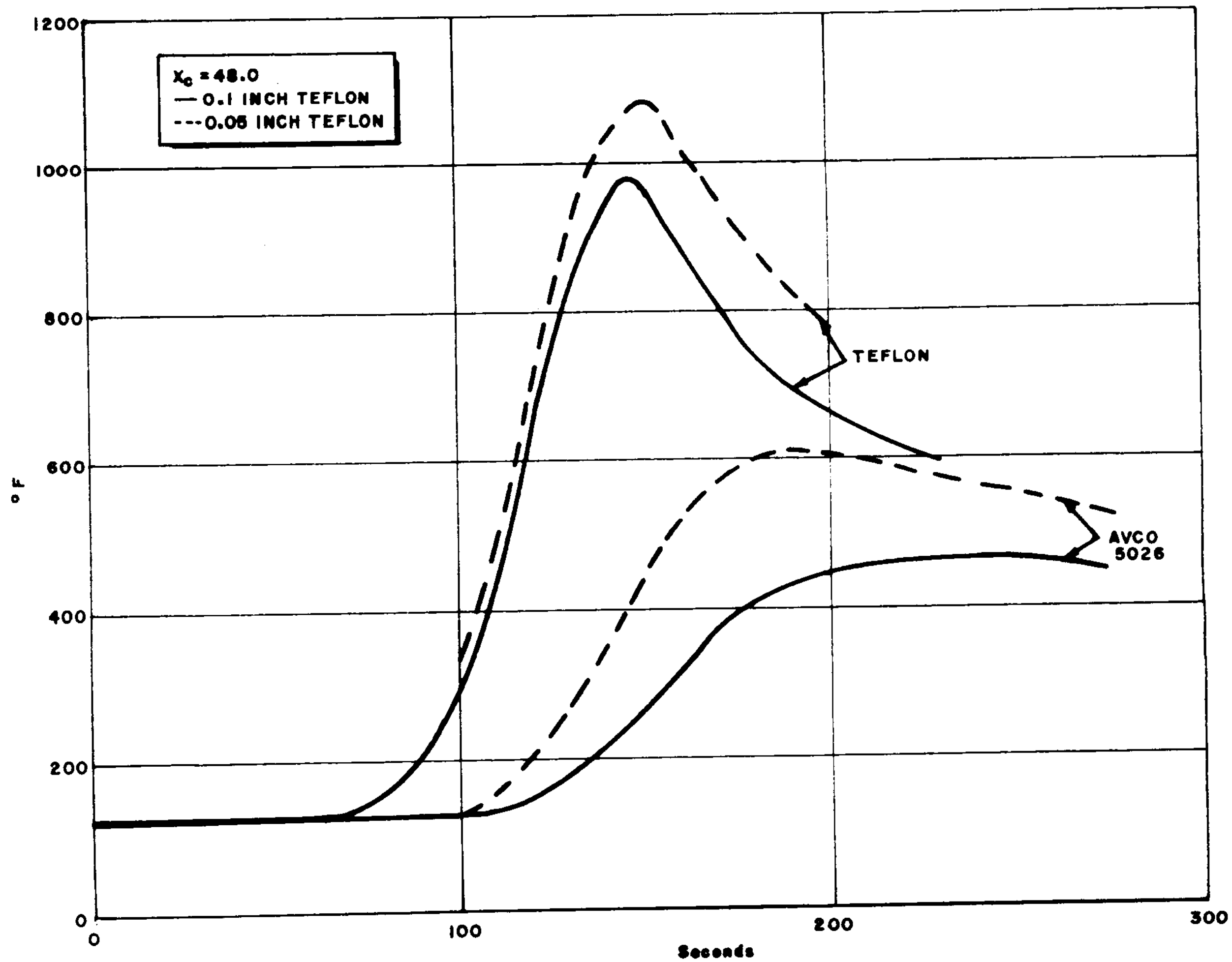

65-5329

Figure 32 SURFACE TEMPERATURE OF TEFLON AND AVCO 5026

Based on average values for α, ϵ and α/ϵ, and assuming that the vehicle can freely rotate about its major axis during flight, it was calculated that a realistic coating surface temperature is about 55 °F. However, if the vehicle is locked in a fixed attitude with respect to the Sun, then that portion of the surface which is being irradiated may reach a temperature of 150 °F and the portion in the shadow, 0 °F. Consequently, three temperatures were selected for the calculations 0 °F, 55 °F and 150 °F to be made from the following equations:

$$\mathrm{Log}_{10} P_s = \frac{A}{T_s} + B$$

$$G_{max} = 0.0583\, \alpha\, P_s \sqrt{\frac{M}{T_s}}$$

where

A+B are constants

T_s absolute temperature, °K

P_s Sublimation Pressure in mmHg.

M Molecular weight of subliming species

G_{max} mass flow rate $g/cm/sec^2$

α accommodation coefficient

The accommodation coefficient is an efficiency factor which relates actual rates to theoretical rates calculated from kinetic theory. Sherwood and Johannes determined α for five organic compounds including camphor and benzoic acid. α ranged from 0.14 to 1.00 in these compounds and was a mild function of temperature. The measured value of α for camphor was 0.18. The value of α will tend toward unity as the ambient pressure decreases; thus increasing the rate of mass flow in space over the experimental values from the laboratory test where the ambient pressure was about 10^{-5} mmHg.

The calculated values of mass flow rate and time for vaporization of 0.1 inch thick coating are given in Table XIV. Table XV compares the calculated mass flow rates for five other sublimers with those for camphor.

C. EXPERIMENTAL DEVELOPMENT

Pure camphor meets all the thermal requirements set forth previously so that further considerations such as processability and mechanical properties became more prominent along with experimental verification of the heat of ablation and rate of sublimation. Paradichlorobenzene, as an alternate sublimable coating, was also tested along with the camphor because of its known easy handling qualities.

As a first approximation, small strips of aluminum were coated with paradichlorobenzene by repeatedly dipping the aluminum in the molten material. This technique was not satisfactory since the material crazed appreciably upon cooling and solidification. Crazing was eliminated by introducing 4 percent by weight of molten, low molecular weight, (1500) polyethylene to the molten paradichlorobenzene. Using this composition, it was found that satisfactory specimens could be cast.

TABLE XIV

CALCULATED MASS FLOW RATES FOR CAMPHOR UNDER VACUUM AS A FUNCTION OF SURFACE TEMPERATURE

Temp. °F	Ps mm. Hg	G_{max} g/m^2. min.	Time (min.) required to Vaporize 0.254 cm Camphor Layer
0	6.89×10^{-3}	3.35×10^{-3}	76.0
55	1.03×10^{-1}	4.71×10^{-2}	5.39
150	3.45	1.455	0.174

Attempts were made initially to spray Camphor solutions using a standard paint spray unit. The results were unsatisfactory in that much Camphor was lost during evaporation of the solvent. The remaining Camphor also tended to form macrocrystalline regions resulting in the development of a large number of cracks. To overcome macrocystallization, molten polyethylene was again used as a diluent and was added to the molten Camphor. Discs were cast in small aluminum dishes with the polyethylene content varied from 2 to 10 percent. Visual examination of the discs indicated that the 4 percent loading was optimum, and this casting was considered satisfactory. However, it did not exhibit the good surface homogeneity characteristic of the Paradichlorobenzene 4 percent PE casting.

TABLE XV

CALCULATED MASS FLOW RATES FOR SUBLIMERS UNDER VACUUM AS A FUNCTION OF SURFACE TEMPERATURE

Compound	Density lbs/ft^3	G_{max} – g/cm^2 – min			α	Hsub Btu/lb.	q*L at H_s/RT_o = Btu/lb.
		0°F	55°F	150°F			
Camphor	63	9.94×10^{-2}	1.25	45.6	0.18	151.5	474
p-dichlorobenzene	95	5.66×10^{-2}	2.27	284		200	83
Naphthalene	71	7.24×10^{-3}	0.281	33.1	0.88	243	85
Benzoic Acid	79	9.31×10^{-4}	2.55×10^{-2}	1.83	--	--	--
Anthracene	78	2.48×10^{-5}	9.15×10^{-4}	0.101	--	--	--
Oxalic Acid	102	5.24×10^{-6}	5.35×10^{-4}	0.220	--	--	--

Thin slices of the Camphor/PE castings were placed into aluminum dishes and were heated for 72 hours at 65°C to completely volatilize the Camphor. The remaining polyethylene did not form a continuous film upon volatilization of the Camphor, but consisted of chunks of a porous (foam-like), flexible, three-dimensional structure with much too low a vapor pressure for volatilization in space.

Further experiments with the Camphor 4 percent PE mixture demonstrated that it could be melt-sprayed onto an aluminum surface. Spraying pure camphor with air atomization gives a spongy coating with low density, poor cohesion, and thus very low shear strength. This latter weakness would make it inoperable as an ascent heat shield since the rate of mass loss from spallation would be far too high.

These processing problems made it mandatory that a broader look be taken at sublimers in general. The high vapor pressure of camphor is both an asset and debit. A high vapor pressure at the triple point prevents melting and thus maintains the availability of the heat of vaporization as a part of the heat of ablation.

Work done at Avco/RAD shows that two of the higher vapor pressure materials p-dichlorobenzene and naphthalene, melt and flow when heated at pressures higher than 0.2 psia while camphor did not show a melt phase at atmospheric pressure (14.7 psia) well above its triple point pressure of 7.5 psia. This sharp difference in behavior may permit transpiration cooling for camphor and could account for the much higher q^*L that camphor exhibits compared to p-dichlorobenzene and naphthalene despite a somewhat smaller heat of vaporization.

This analysis indicated that since no other sublimer was found with a higher vapor pressure at a given temperature than camphor and with at least as high a vapor pressure at the triple point, the major component of any sublimable ascent heat shield material should be camphor.

The poor mechanical properties of a sprayed camphor coating can be related directly to its high melting point (350°F) and the placement of its triple point (Figure 33). Because of its high melting point the spray freezes almost immediately upon exit from the riser tube and thus little or no flow takes place to consolidate the sublimer surface. This results in a sponge-like morphology of low density and little strength. The placement of the triple point on the steep portion of the vapor pressure-temperature curve allows only a very limited liquidus region on the temperature scale. The rapid oxidation of the camphor at temperatures near the boiling point and the boiling point of 410°F make it imperative that a more practical route to sprayability be employed. Addition of a lower temperature sublimer to form a binary mixture will decrease the melting point and give more processing latitude.

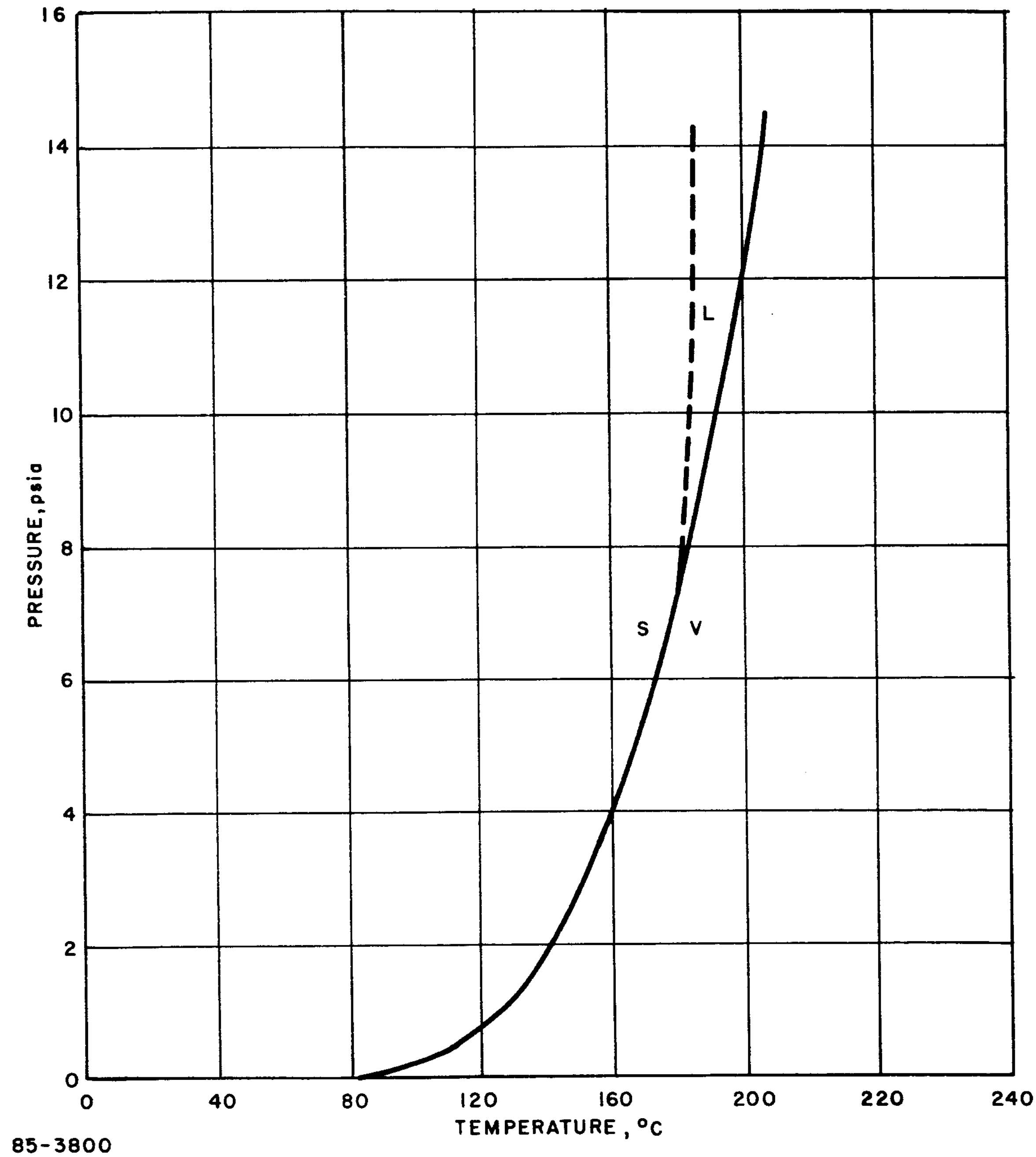

Figure 33 CAMPHOR PRESSURE-TEMPERATURE PHASE DIAGRAM

Since evaporation rate is of primary concern p-dichlorobenzene and naphthalene with the next highest sublimation rates to camphor at 0 °F were investigated first. Binary mixtures of these with 75 percent camphor formed eutectics which are liquid at room temperature. Increasing the camphor to 95-98 percent returned to mixtures to the morphological problems of pure camphor.

It was considered that relatively less compatible sublimers such as oxalic acid or benzoic acid might be able to act as nucleating agents during the crystallization of the mixture. This would prevent the formation of the large crystals and improve the morphology and consequently the strength. Table XVI shows the improvement in tensile strength of cast samples obtained through this technique. Despite the obvious improvement in strength, the much lower vaporization rates of the pure acids, and the association of the vapor phase might give a serious negative deviation from Raoults law.

During a further literature search for promising additives to the camphor coating it was found that camphene and camphor form a series of solid solutions with melting points between 43 °C and 178 °C. This wide range of melting points should allow considerable control over the rate of vaporization of a camphor-camphene coating.

It was found that binary mixtures with 50 percent and 25 percent camphene are much easier to spray and the 10 percent camphene mixture, though plagued by the high temperature of the freezing point, is still much more processible than pure camphor.

The addition of oxalic or benzoic acids improved the crystal morphology and the strength substantially. (Table XVI). However, the lower vaporization rates would have a deleterious effect on the time for complete evaporation of sublimable residue. Consequently, small amounts of benzoic acid were added to camphor and camphene to form a ternary mixture. If the control of crystal growth can be obtained at low concentrations i.e. < 5 percent of the benzoic acid the slight lowering of vaporization rates may be acceptable. Table XVII compares the density, spray rate, and processability of six ternary mixtures based on a camphor-camphene binary mixture. The results show that processability is good to excellent for all of the ternary mixtures except the 90-9-1 mixture where it was fair, as was the 75-25 percent binary mixture. The spray rate increases with decreasing benzoic acid content but drops abruptly at 0 percent. The density on the other hand decreases monotonically with decreasing benzoic acid content. The density and presumably the strength depend greatly on the spraying technique. Highest densities are obtained with a course spray at short distances and with above ambient pot pressures as will be discussed later.

Thus, the material selection has been based upon performance in three areas namely, (a) thermal (ablative characteristic of ascent heating and vaporization at selected temperatures in space), (b) mechanical (shear strength and qualitative

TABLE XVI

MECHANICAL PROPERTIES OF BINARY AND TERNARY MIXTURES

Compounds	Tensile Load	Type of Failure	Remarks
75 percent Camphor 25 percent Oxalic acid	18 pounds	Tension	Small crystals; adhesive failure
75 percent Camphor 10 percent Naphthalene			Partial liquid at room temperature
75 percent Camphor 10 percent Naphthalene 15 percent o-nitrophenol			Partial liquid at room temperature
85 percent Camphor 15 percent Oxalic Acid	66 pounds	Shear	Medium sized crystals; cohesive failure
85 percent Camphor 15 percent Naphthalene	3.1 pounds	Tension	Medium sized; poorly defined crystals;adhesive failure; very soft.
90 percent Camphor 10 percent Naphthalene			Too soft to test
75 percent Camphor 25 percent Benzoic Acid	19.75 pounds	Tension	Medium sized crystals, almost total cohesive failure
75 percent Camphor 25 percent Naphthalene	2.1 pounds	Tension	Small crystals; adhesive failure

TABLE XVII

PROCESSABILITY OF TERNARY MIXTURES BASED ON CAMPHOR-CAMPHENE BINARY MIXTURES

Camphor (percent)	Camphene (percent)	Benzoic Acid (percent)	av.	Spray Rate	Remarks
75	20	5	0.90	12.3 gm/min	Fast; easy to control; no nozzle clogging; very good strength
75	23	2	0.885	20.6 gm/min	Fast; easy to control; no nozzle clogging; good strength
75	24	1	0.835	35.0 gm/min	Very fast; easy to control; no nozzle clogging; good strength
75	24.5	0.5	0.783	52 gm/min	Extremely fast; easy to control; no nozzle clogging; fair strength
75	25	0	0.41	10.3gm/min	Fast; fairly critical distance adjustment; no nozzle clogging; poor strength
50	49	1	0.41	22 gm/min	Fast; easy to control; no nozzle clogging; poor strength
90	9	1	0.89	--	Fast, not so easy to control; some nozzle clogging; fair to good strength

hardness), and (c) processability (ease of spray application and machineability). The material with the best composite of properties is the ternary mixture of 75 percent camphor, 24.5 percent camphene, 0.5 percent benzoic acid, which shows a laminar heat of ablation as high as that of camphor; a vapor pressure that is higher than that of pure camphor; processibility that is very good, and shear strength that should be adequate. It is a clean ablator of micro-crystalline structure which is readily machineable.

D. PERFORMANCE TESTS

The tests procedures and results which will be discussed in detail are those which can give a quantitative value for the performance of the candidate materials. The thermal tests are heat of ablation in the Model 500 low enthalpy arc, rate of vaporization (both under one sun radiation and no radiation or simulated shadow), and definition of material as clean ablator. The mechanical test data are primarily shear strength though morphology was also noted; the processability tests give values of spray rate and resulting product density as well as a qualitative description of spray behavior.

The ablation tests were performed in the Avco/RAD Model 500 plasma generator. This machine produces a subsonic jet of air 1/2 inch in diameter which exhausts directly into the atmosphere. Gas enthalpies and heat transfer rates (flat faced cylinders) which can be generated, cover the range of 600 to 10,000 Btu/lb and 25 to 1300 $Btu/ft/sec^2$, respectively. The enthalpies generated during ascent heating are lower than the minimum listed above, but the low slope of the enthalpy- q^* curve makes extrapolation to the desired levels possible without introducing significant error.

Laminar ablation tests were conducted on camphor, benzoic acid, 75 percent camphor, 25 percent camphene mixture; and a 75 percent camphor, 24 percent camphene, 1 percent benzoic acid mixture. The camphor and the ternary mixture were tested over a range of conditions, but only a single sample of the benzoic acid and the binary mixture was tested. The results obtained are: $H = 680$ Btu/lb and $q_c = 25$ $Btu/ft/sec^2$. The single samples dished making it impossible to get recession rates and to calculate ablation data. Camphor also dished at this low enthalpy level; accordingly higher values of H were required to obtain ablation results. The test results are presented in Figures 34 and 35. For the camphor and the ternary mixture respectively where:

H = stagnation enthalpy referenced to absolute zero

q_c = cold wall heat flux measured with a flat faced water cooled calorimeter

S = recession rate

q^* = laminar thermochemical heat of ablation

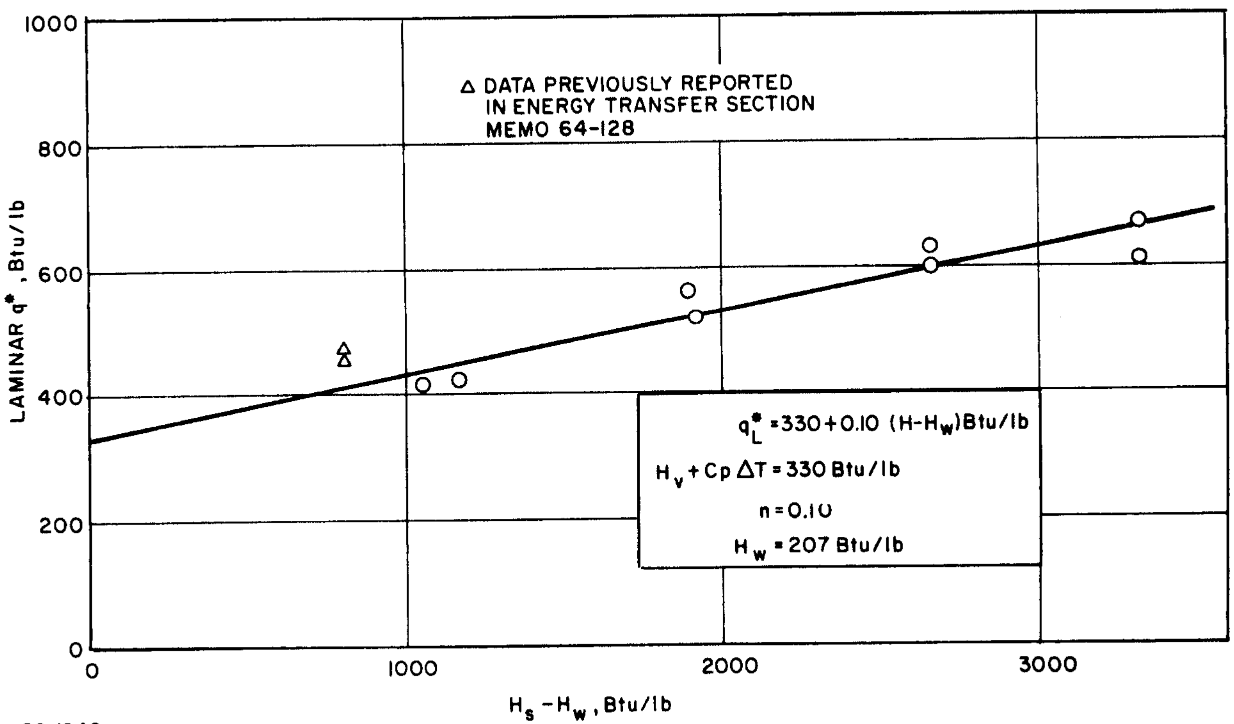

86-1940

Figure 34 LAMINAR q* VERSUS ENTHALPY FOR CAMPHOR

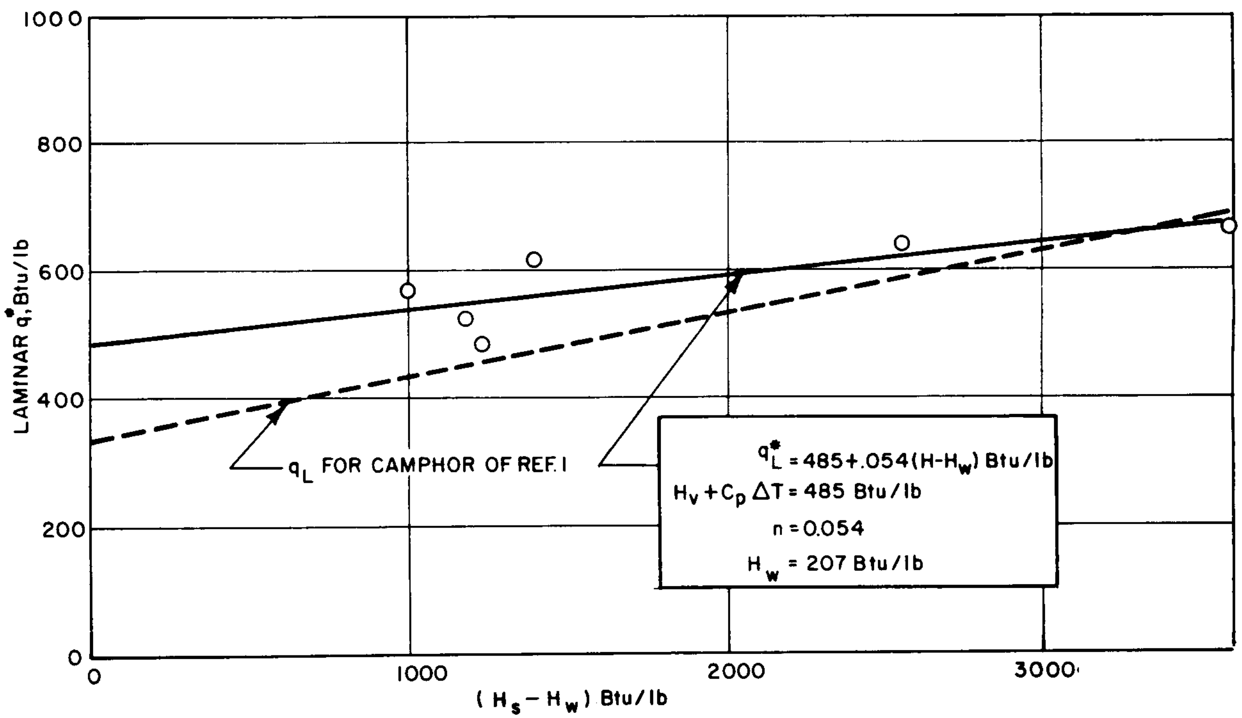

86-1941

Figure 35 LAMINAR q* VERSUS ENTHALPY FOR TERNARY MIXTURE

q^*L = least squares fit of the q^* vs $(H - H_w)$ data

H_w = wall enthalpy

n = slope of the q^*L curve

H_s = heat of sublimation

C_p = specific heat

T_s = ablation temperature

Two data points previously obtained at AVCO for camphor (obtained by identical tests) are included and show good agreement with the present data.

Ablation theory for a subliming material gives the equation

$$q^* = H_s + C_p \Delta T + n (H - H_w)$$

and when

$$H = H_w$$

$$q^* = H_s + C_p \Delta T$$

Therefore the intercept values of Figures 33 and 34 give the experimentally determined $H_s + C_p \Delta T$ term as 356 Btu/lb and 485 Btu/lb for pure camphor and the 75-24-1 percent ternary mixture respectively. The value of 356 Btu/lb for camphor is somewhat higher than the value calculated using handbook values of C_p = 0.39 Btu/lb°R, H_s = 155 Btu/lb and T_s = 860°R. The front surface motion pictures taken during the tests showed some liquid blown off the edge of the sample. The samples gave the appearance that the camphor was boiling at the surface. A larger amount of flow was shown by the benzoic acid sample and some material was removed as a liquid. The camphor-camphene binary mixture showed behavior similar to the pure camphor.

E. SUBLIMATION TESTS

To assure protection against retrorocket exhaust deposition on the thermal control coating, the sublimable coating should survive the ascent phase and retain its integrity above 600, 000 feet altitude. Beyond this stage, however, it should vaporize quickly and without leaving any residue in order to completely expose the thermal control coating. Theoretical mass flow rates of camphor and the ternary mixture were presented in Tables XIV and XV. Vaporization experiments were performed in order to compare the calculated values with experimentally determined vaporization times.

The vaporization chamber shown in Figure 36 was connected to a high capacity vacuum system consisting of mechanical forepumps and mercury diffusion pumps. A 1 x 1 x 1/8 inch Apollo heat shield material with a 0. 1 inch sublimable coating was mounted 0. 5 inch away from a heater consisting of a fused silica plate wound with Nichrome wire. The heater was calibrated for irradiating samples at fluxes of any desired intensity. The surface temperature of the sublimable coating was measured with a thermocouple.

The first set of measurements was performed using pure camphor as a sublimable coating. The experiments were conducted at two conditions of temperature and vacuum. At 4.0×10^{-4} mm of Hg and 40° F, all of the camphor coating vaporized in five minutes. In this case, the sublimation chamber was immersed in liquid N_2 to condense the camphor vapors along the walls. The heat flux incident on the subliming surface was regulated at 0. 0345 cal/cm^2 min the solar constant. The second run was made at 1.3×10^{-3} mm of Hg and -40° F whereupon only 12. 5 percent (0. 205g) of the camphor sublimed in two hours. During this run, the heater was not used, and the chamber was immersed in an alcohol-dry ice trap.

The theoretical and experimentally determined mass flow rates for camphor at + 40 and - 40° F are given in Table XVIII, together with data of Fishell and Wilson,[7] at -0. 4 and 75. 2° F. It can be seen that above 0° F, the experimental data suggest that any remaining camphor will vaporize in an acceptable length of time. It should again be noted that the time calculations are based on the assumption that no camphor was vaporized during ascent heating. A discrepancy appears to exist between the data of Avco/RAD and that of Fischell and Wilson in that Avco's experimentally determined mass flow rate at + 40° F is greater than that of Fishell and Wilson's at + 75. 2° F. All other factors being equal, this apparent anomaly can be explained by the fact that these authors used compression molded disks of camphor for their studies, while Avco's coatings were applied using a melt-dipping technique. There is evidence in the literature which shows that for the same material, highly compacted (compression molded) specimens can have mass flow rates 15 times lower than that of specimens prepared by other techniques.

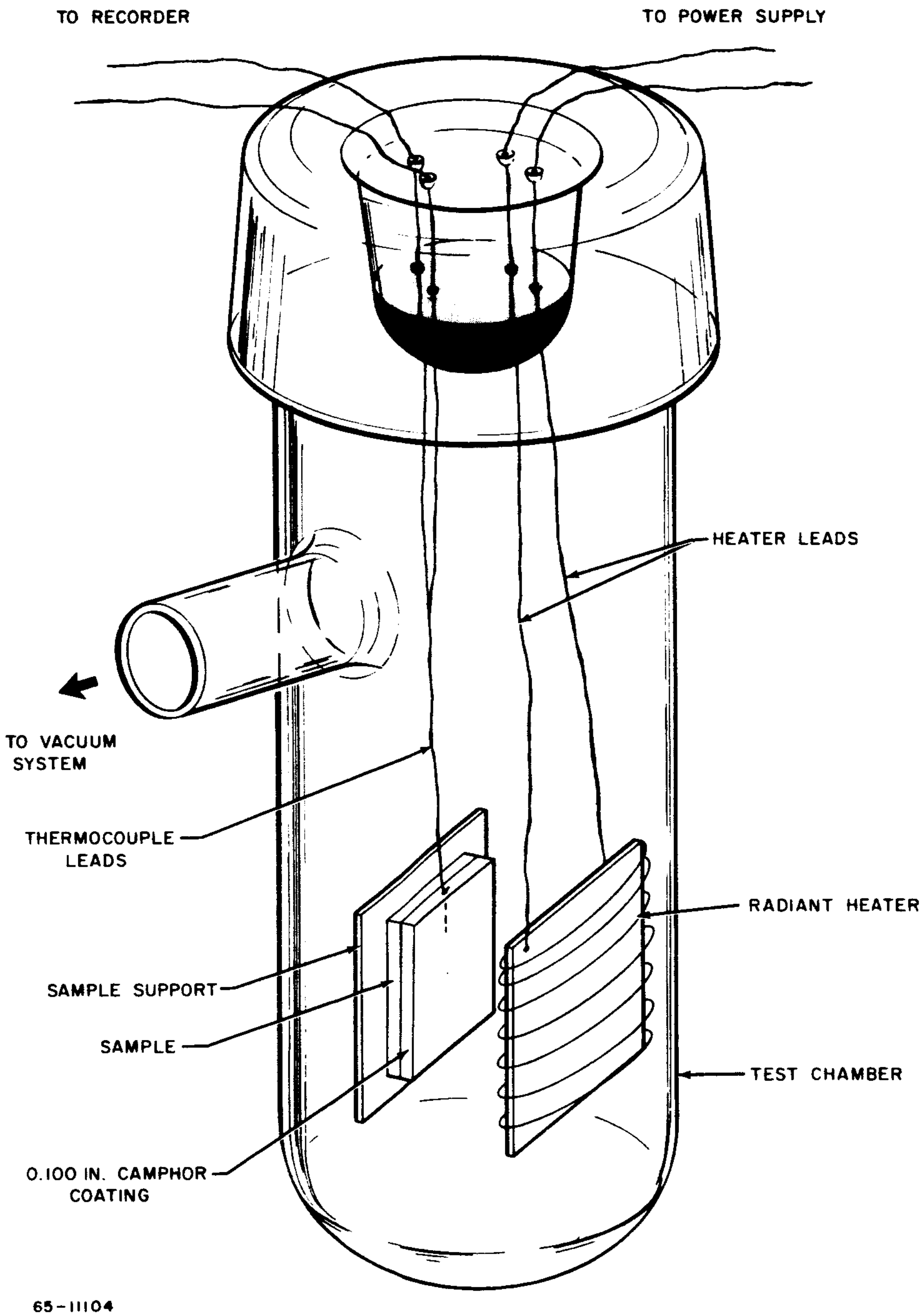

Figure 36 CAMPHOR VAPORIZATION TEST APPARATUS

TABLE XVIII

EXPERIMENTAL AND THEORETICAL MASS FLOW RATES FOR CAMPHOR UNDER VACUUM AS A FUNCTION OF SURFACE TEMPERATURE

Temperature °F	P_s (calc.) mm. Hg.	G_{max} gm/cm^2 min.		Time (min.) required to vaporize 0.254cm camphor/cm^2	
		Theoretical	Experimental	Theoretical	Experimental
-40° F	6.21×10^{-4}	17.6×10^{-4}	2.65×10^{-4}	144.5	958
-0.4° F*	----	1.8×10^{-2}	0.43×10^{-2}	14.1	59
+40° F	5.19×10^{-2}	13.5×10^{-2}	5.07×10^{-2}	1.88	5
+75.2° F	----	6.0×10^{-1}	0.90×10^{-2}	0.42	28.2

*Data of R. E. Fischell and L. Wilson, J. Spacecraft, 2, No. 3, p. 376, May-June 1965

The data also indicates that at -40°F 16 hours would be required to vaporize the entire 0.1 inch thick camphor coating. It is to be realized, however, that surface temperature as low as -40°F immediately after ascent heating will only be reached on the cold side of the command module if a fixed orientation of the vehicle toward the Sun is constantly maintained. Since such an operation is not contemplated, sublimation rates at temperatures below 0°F need not be considered. The experimentally obtained vaporization rates contain another conservative parameter in that the vacuum was only in the order of 10^{-3} mm of Hg. It is obvious that in the hard vacuum of space the vaporization rates will be much higher.

Further screening tests were performed on benzoic acid, camphor, camphor-benzoic acid, camphor-camphene and a mixture of camphor-camphene and benzoic acid. The samples were irradiated by a flux equal to one sun and at a pressure of 10^{-5} torr. The results of these tests are the first six materials in Table XIX, and are expressed as coating thickness decrease per unit time (cm/min). The addition of camphene significantly speeded up the sublimation process which was predictable from the lower sublimation point of camphene. A more detailed investigation was made of the vaporization rates of the ternary mixtures containing 0.5 to 2 percent benzoic acid and various percentages of camphor and camphene. The results of these tests are the last five materials in Table XIX, where vaporization rate measurements were performed under a radiant flux of one sun and a pressure of 10^{-5} torr and also in shadow conditions at the same pressure. The addition of high percentages of camphene again markedly increased the vaporization rate. Increasing the percentage from ~ 24.5 percent to 49 percent more than doubled the rate both in the Sun and shadow position. If a mixture of 90 percent camphor 9 percent camphene-1 percent benzoic acid 0.254 cm thick were left in the shadow position (the worst possible condition) the coating would vaporize in about 81 minutes. The same coating would take only 10 minutes to disappear in sunlight. Thus no problems should be experienced from coatings of this type lasting so long that they might affect the thermal balance of a spacecraft.

An essential criterion of the sublimable coating is that it should volatilize without any residue. Samples of the fiberglass-Al tape-5026 system and the Potassium Silicate-Al tape-5026 system were coated with the ternary sublimable coating mixture after their α and ϵ values were measured. Following this, the sublimable coating was completely vaporized in the vacuum system shown in Figure 36. The measurement of radiative parameters after the vaporization proved that the sublimable coating vaporized completely without deteriorating the thermal control surface.

TABLE XIX

VAPORIZATION RATES

Mixture	Thickness Decrease (cm/min x 10^{-2})	
	Shadow	Sun
Benzoic Acid	----	0.70
Camphor	----	1.85
90 Percent Camphor - 10 Percent Benzoic Acid	----	2.08
90 Percent Camphor - 10 Percent Camphene	----	2.60
75 Percent Camphor - 25 Percent Benzoic Acid	----	2.09
75 Camphor - 20 Percent Camphene - 5 Percent Benzoic Acid	----	2.30
90 Percent Camphor - 9 Percent Camphene - 1 Percent Benzoic Acid	0.31	2.63
75 Percent Camphor - 23 Percent Camphene - 2 Percent Benzoic Acid	0.33	2.61
75 Percent Camphor - 24.5 Percent Camphene - 0.5 Percent Benzoic Acid	0.48	3.01
65 Percent Camphor - 34 Percent Camphene - 1 Percent Benzoic Acid	0.51	3.42
50 Percent Camphor - 49 Percent Camphene - 1 Percent Benzoic Acid	0.98	6.17

F. STRENGTH TESTS

The shear strength tests were performed on a standard tensile testing machine with modified grips since the normal core shear samples could not be made with maximum density with Avco/RAD's spraying apparatus. The test pieces were machined to 1 x 1-1/2 x 1/4 inch in a manner similar to the density samples and tested in the grips shown in Figures 37 and 38. Initial tests were done in a crude manner from cast samples. A schematic diagram of the jig is shown in Figure 39. The sample material was melted and poured into the polystyrene cup with the bottom nail in place. When the cup was filled the upper nail and cap were put in place and the sample allowed to freeze. A notch was then cut through the polystyrene tube so that only sample material was holding the two nails together. The nails were placed in the grips of a tensile testing machine and stressed under tension. In one sample the notch was not cut entirely through the polystyrene tube so that the upper nail pulled out with the sample failing in shear. Table XX shows the results of the preliminary testing with the cast samples. This test, though crude, shows a significant difference between binary mixtures with oxalic or benzoic acids and all the other mixtures tested in this set of samples. Table XXI compares the ultimate shear stress values with close control over the sample, size, and shape with the refined sample holder. Any of the ternary mixtures appear to have adequate shear strength except the 50-49-1-percent mixture which is too low. The binary 75-25 percent camphor-camphene mixture, 90-9-1 ternary mixture and mixtures containing 75 percent camphor with any benzoic acid content from 0.5 to 5 percent gives sufficient strength to eliminate this as a factor in choosing the optimum composition.

The shear stress regime which the sublimable coating encounters is not particularly severe, but the coating has to maintain its integrity through this loading to ensure proper performance of the underlying thermal control coating. Unexpectedly, rapid loss through shear failure and consequent spallation would subject the Apollo heat shield to too high a temperature, causing degradation and staining of the thermal control coating in addition to the possibility of contamination by the rocket exhausts.

Initial tests were primarily qualitative since the pure camphor samples had macroscopic defects. The cast material displayed gross cracks from contraction during freezing while the sprayed material was spongy and with poor consolidation. These gross defects were not seen in the mixtures so that quantitative tests were then used to distinguish the better candidates from those of poorer quality.

The maximum density of each of the ingredients was known from literature data so that a good approximation of the consolidation was available by comparing the experimentally determined density with the calculated maximum. A small

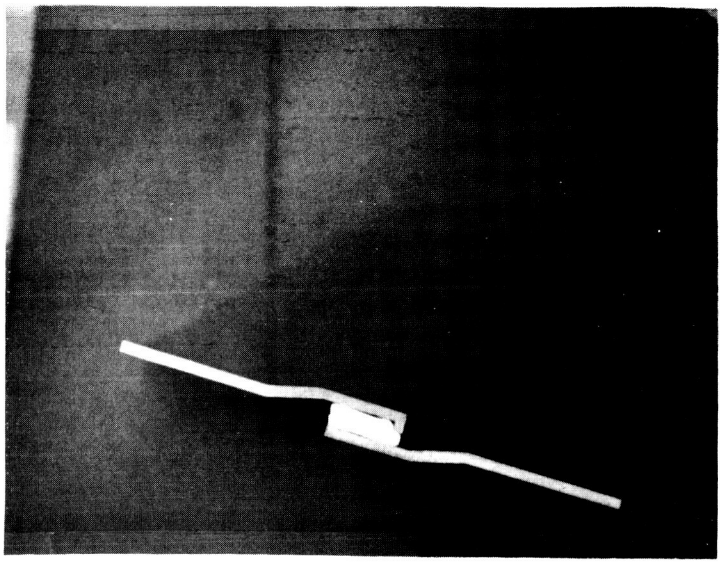

Figure 37 TEST GRIPS

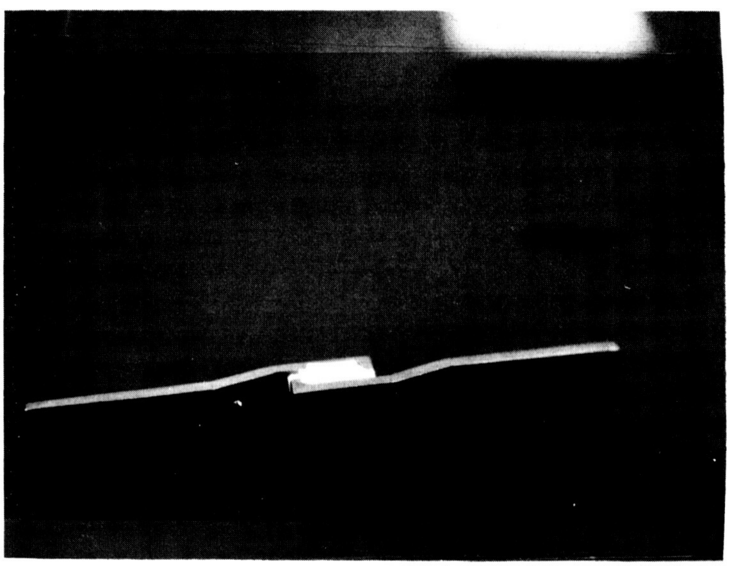

Figure 38 TEST GRIPS

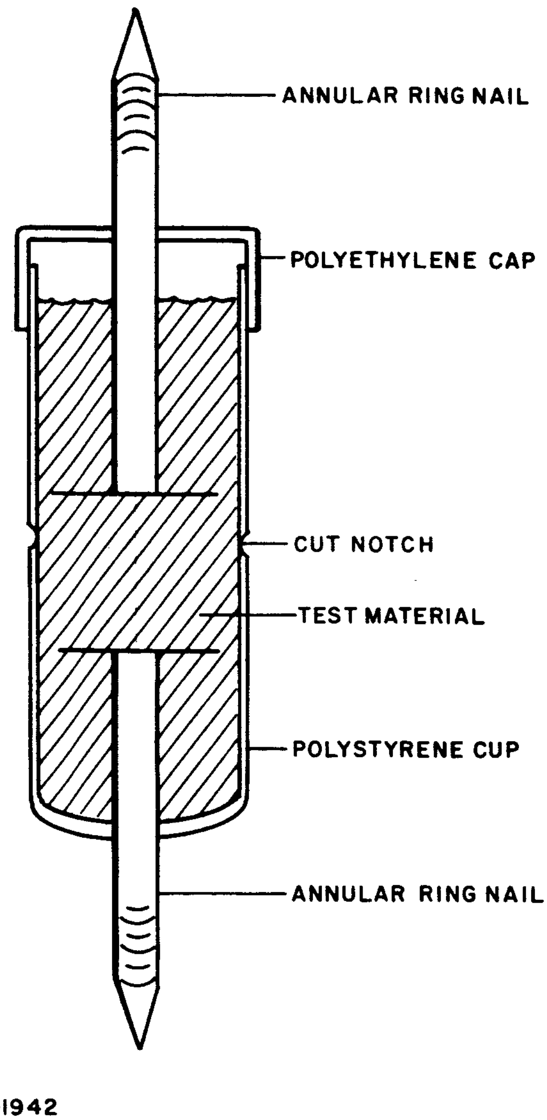

Figure 39 TEST JIG

piece of the material was cut and filed into the shape of a rectangular parallelepiped of about 1 x 1 x 1/4 inch. The piece was measured with a micrometer and weighed on an analytical balance. The density was then calculated from these data. Some of the earlier candidates were so poor mechanically, that this crude method indicated greater accuracy than was inherent in the sample uniformity. The most recent materials, the ternary camphor-camphene-benzoic acid mixtures have sufficient strength and compactness that the samples can be cut to size on a standard milling machine using a four flute cutter.

TABLE XX

MECHANICAL PROPERTIES OF CAST BINARY AND TERNARY SUBLIMABLE MIXTURES

Composition	Tensile Load	Type of Failure
75 Percent Camphor; 25 Percent Oxalic Acid	18 pounds	Tension
75 Percent Camphor; 10 Percent Naphthalene; 15 Percent Acenaphthene		Partial liquid at room temperature
75 Percent Camphor; 10 Percent Naphthalene; 15 Percent O-nitrophenol		Partial liquid at room temperature
85 Percent Camphor; 15 Percent Oxalic Acid	66 Pounds	Shear
85 Percent Camphor; 15 Percent Naphthalene	3.1 pounds	Tension
90 Percent Camphor; 10 Percent Naphthalene		Too soft to test
75 Percent Camphor; 25 Percent Benzoic Acid	19.75 pounds	Tension
75 Percent Camphor; 25 Percent Phenanthrene	2.1 pounds	Tension

TABLE XXI

SHEAR STRENGTH OF SPRAYED SUBLIMABLE MIXTURES

Composition	Ultimate Shear Strength (pounds/inch^2)
75 Percent Camphor; 25 Percent Camphene	71.9*
75 Percent Camphor; 24.5 Percent Camphene; 0.5 Percent Benzoic Acid	63.7
75 Percent Camphor; 24 Percent Camphene; 1 Percent Benzoic Acid	61.0
75 Percent Camphor; 23 Percent Camphene; 2 Percent Benzoic Acid	75.4
75 Percent Camphor; 20 Percent Camphene; 5 Percent Benzoic Acid	91.4
50 Percent Camphor; 49 Percent Camphene; 1 Percent Benzoic Acid	poor
90 Percent Camphor; 9 Percent Camphene; 1 Percent Benzoic Acid	43**

*Appeared to show crushing failure rather than shear failure

**Lateral movement of jig may give distorted value

G. SPRAY PROCESS DEVELOPMENT

The properties that make camphor promising as a low temperature ablator also make it difficult to apply. For example, the narrow liquidus range and high vapor pressure near its triple point, which contribute to its high heat of ablation, require precise temperature control in order to maintain the camphor liquid in the melting pot as well as in the heated conduction hoses. The narrow liquidus range limits the temperature of the molten camphor to a few degrees above its freezing point. This causes the molten camphor spray to freeze into small particles before it contacts the substrate surface and results in a weak, sponge-like coating. In addition, the high vapor pressure of camphor near its deposition temperature requires rapid cooling of the coating to avoid excessive loss of camphor immediately after deposition.

Normal paint spray equipment was tried first with a camphor solution after it was apparent that casting was not feasible due to the macroscopic morphology of the resulting mass. The gross cracks between the large crystals due to the contraction in freezing added to the problems of holding a liquid on the curved surface of the command module, making it imperative that a better coating method be developed. The solution spraying was an equally poor answer since the high vapor pressure of the sublimer (camphor and paradichlorobenzene were tested almost exclusively by this method) made the technique extremely inefficient due to vaporization of the sublimer as the solvent was removed.

Coupled with this was the fact that the material was still liquid upon reaching the surface to be coated, accordingly the method was quickly abandoned. Because of the ease of application of a spraying technique, melt-spraying was attempted next. The first equipment assembled to test the practicability of melt-spraying as a fabrication method was very crude. In essence, it was a half pint tin can fitted with a copper riser tube through its top, and a copper coil with the end placed to give an atomizing effect when air was blown through it. Heat was applied by placing the can on a hot plate and a hot air gun was aimed at the coil to prevent freezing of the camphor in the riser tube.

This arrangement produced more homogeneous and dense coatings than the solution spraying but the spraying rate and droplet size could not be controlled satisfactorily. The temperature control was not sufficient to prevent freezing in the riser tube or violent boiling in the pot. It was also found that the metals in the tin coated pot catalyzed the oxidation of the camphor thus causing discolorations.

In a modification of the apparatus a smaller diameter copper tube was used instead of the tin pot. Winding electrical heating tape around the tube achieved sensitive temperature control but accidental freezing still occurred. The oxidation of the camphor was prevented by nickel plating the copper container. When, however, the ternary mixtures, containing benzoic acid were sprayed with this apparatus, the nickel coating was attacked by the benzoic acid causing discolorations.

A third apparatus was built of stainless steel to eliminate the contamination problem (Figure 40). In addition, the pot was so designed that it could be pressurized and the atomizing air adequately preheated. The air preheating prevented freeze up problems and the pressurization made control over the spray particle size possible. The substantial improvement in sprayability as the technique changed from air atomization toward semi-airless spraying suggested complete airless spraying.

The apparatus assembled, consists of an electrical tape heated stainless steel pressure pot capable of holding 1000 psig at 500° F, a heated teflon lined stainless steel braided hose, and a normal deVilbiss airless spray gun wrapped in heating tape. The pot, hose, and spray gun with their associated variacs for temperature control are shown in Figure 41. The spray from the airless unit did not have the same geometry as that of the air or semi-airless atomized units. The last two always gave a full cone spray with complete atomization at the end of the riser tube. The airless nozzle is a slit and the resulting spray is that of a fanshaped sheet. Complete atomization does not seem to occur at pot pressures up to 90 psig, though satisfactory spraying can be done at pressures as low as 50 psig. Even at the higher pressures an unatomized stream remains at the edges of the spray at distances of 4-6 inches from the nozzle while in the center, complete breakup of the film emerging from the nozzle occurs at about 1/2 inch. Figure 42 illustrates this phenomenon. The samples made from this unit have a much smoother surface than any nonairless samples. The highest sample densities were obtained using this spraying equipment. Specific gravities of 0. 935 and 0. 930 were measured compared to a theoretical specific gravity of 0. 945-0. 960 depending upon whether the benzoic acid content is 5 or 0. 5 percent respectively. The previous maximum was 0. 91 for a 75-20-5-percent ternary mixture. The difference in specific gravity may be a function of the distance of the spray head from the surface to be sprayed. The 0. 935 value is for a distance of 1 1/2-2 inches and the sample sagged some when held in a vertical position as the thickness increased. The 0. 930 value was obtained with a 4-5 inch spraying distance and showed no sag. Thin samples made on a rotating drum with the gun held stationary gave very smooth homogeneous films. This indicates that a properly designed jig could spray to closely controlled thicknesses; this can not be achieved with a semi-airless unit. The latter did give a dense coating but resulted in macroscopic, uncontrolled thickness variations. These variations would necessitate spraying a heavier than required coating with subsequent machining to final dimensions. The airless spraying technique, in contrast, yields homogeneous, high density coating. Further it is eminently suitable for scale-up to large surfaces, with little if any modifications.

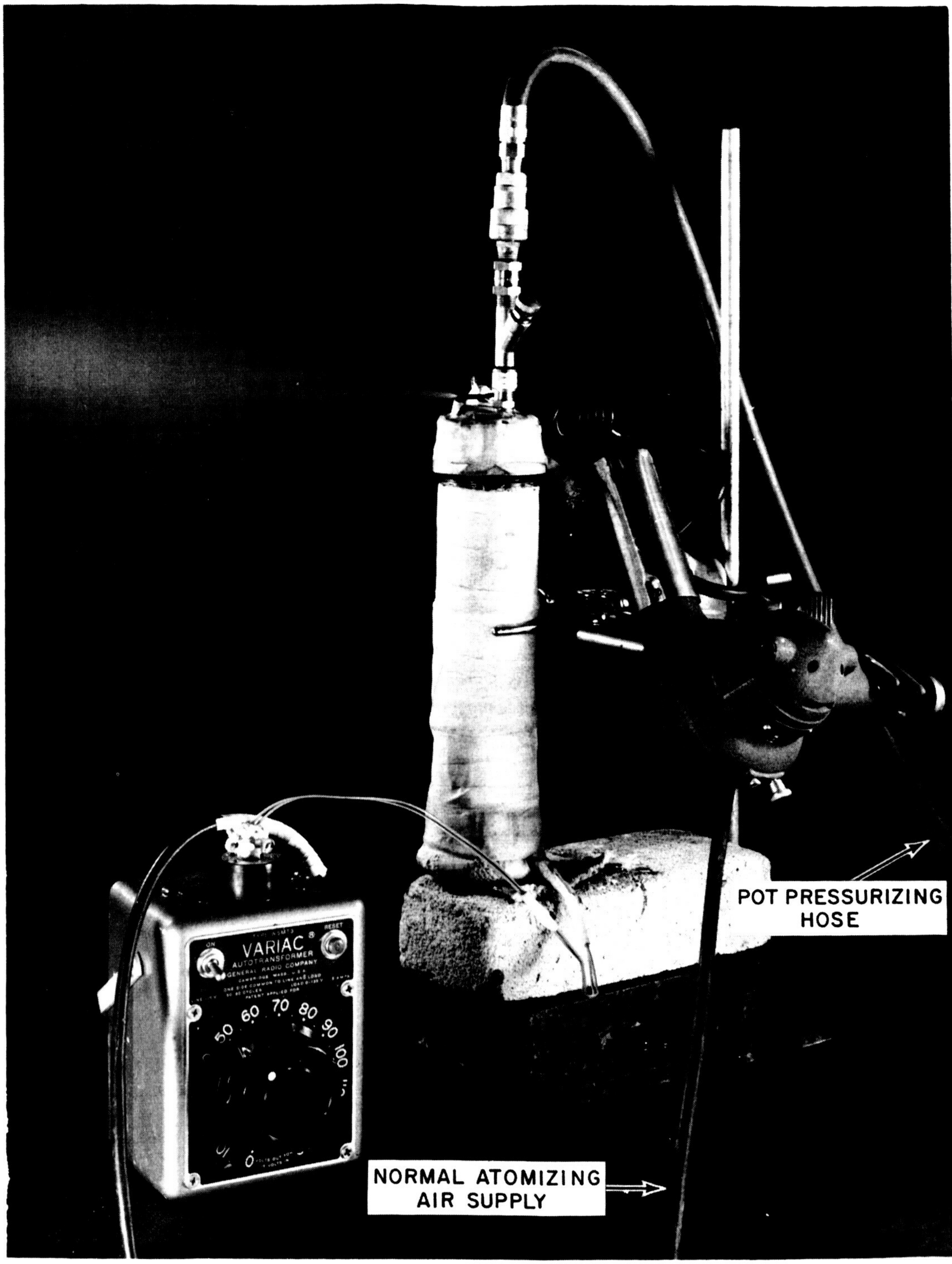

Figure 40 THIRD GENERATION SPRAY APPARATUS

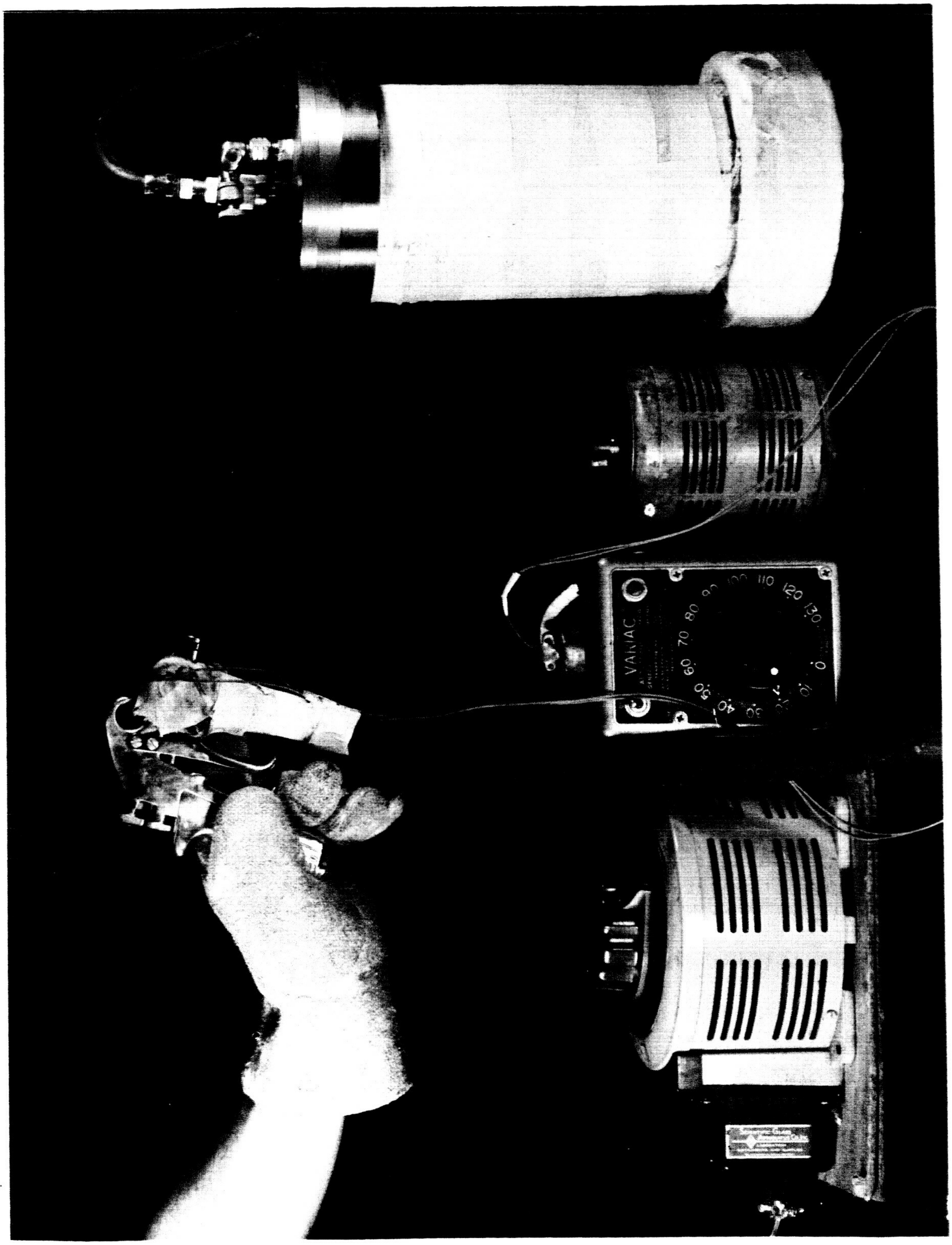

Figure 41 HEATED AIRLESS SPRAY UNIT

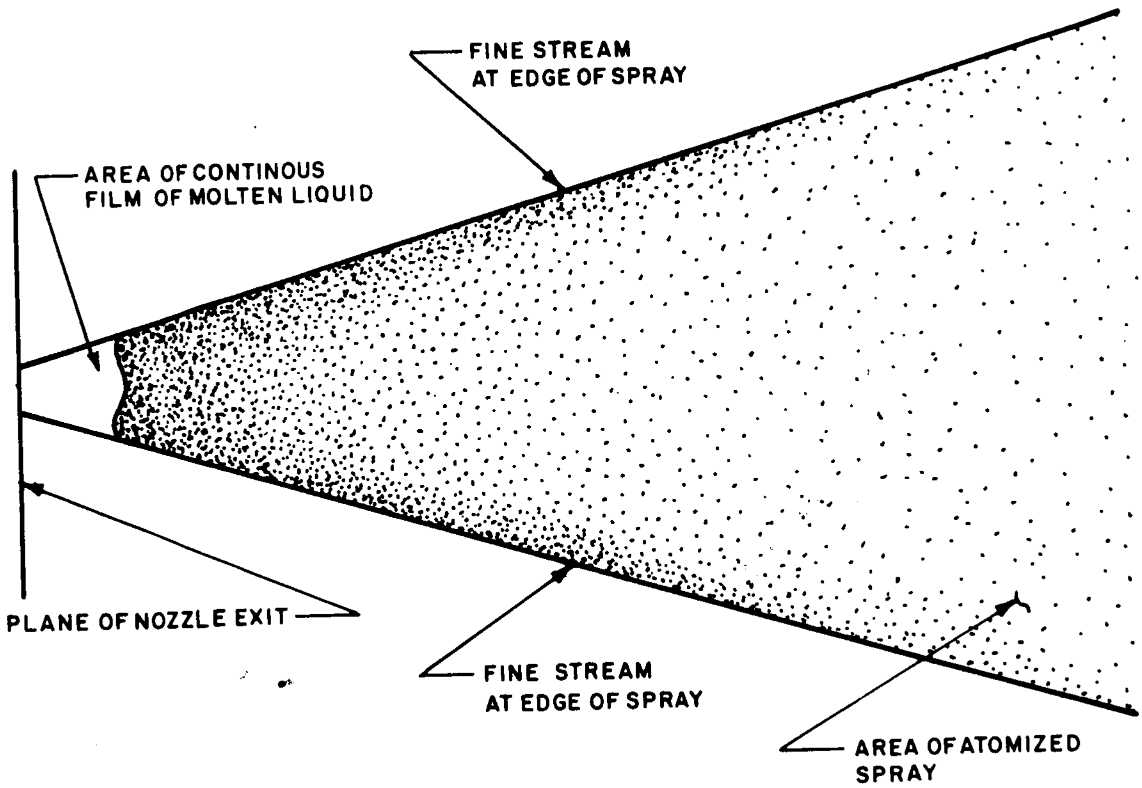

FILM AT LEFT IS ONLY 15 – 30 MILS THICK IN DIRECTION NORMAL TO PAPER AND GRADUALLY EXPANDS TO ~ 1/4 INCH AT RIGHT END

86-1943

Figure 42 SPRAY CONFIGURATION OF AIRLESS NOZZLE

H. SUMMARY

A sublimable coating has been developed to protest the thermal control coating during ascent against thermal decomposition, and may protect it against contaminations from the retro and abort tower separation rocket exhaust. The coating consists of a ternary mixture of the following composition:

75 percent weight	camphor
24 percent weight	camphene
1 percent weight	benzoic acid

This coating is applied to the thermal control coating surface with an airless gun tax spraying technique. The maximum thickness is 0. 1 inch at location 48 and it is graded towards the cooler portions. The total weight is 85 pounds. The residual ternary mixture will vaporize completely after ascent in space vacuum within a short period of time. As stated previously, however, contaminant removal during sublimation has not been verified.

(Page 118 intentionally blank)

VII. VAPOR BARRIER AND GROUND STORAGE COVER

Proper performance of the sublimable coating requires the calculated thickness at all stations of the command module prior to lift off. Long storage on the ground at ambient temperatures may cause premature volatization of the coating and would thus affect its performance. It is important therefore to provide a vapor barrier ground storage cover.

At present it is visualized that a thin film, such as Saran Wrap can be used for this purpose. The film should be removed prior to launching. This, however, may be a somewhat cumbersome operation considering the large number of access panels and the possibility of postponements shortly before a scheduled launch. In the latter case a new protective film has to be applied for further ground protection.

A more practical vapor barrier would be a thin film with high stability at ambient temperatures which would completely and cleanly volatilize during ascent even at the coolest (approximately 500°F) portion of the command module.

Two candidate polymers (both commercially available) appear to have the required characteristics. The first is polymethyl methacrylate. This polymer, which has been studied very extensively, depolymerizes almost quantitatively to the monomer on heating by a rather simple degradation mechanism. It has been found that the depolymerization is affected by the molecular weight, the type of initiator used in the polymerization process, the presence of inhibitors or u.v. absorbers, and the existance of cross linking if any. The depolymerization progresses at a considerably rapid rate at temperatures as low as 320°F. The resin is highly soluble in many solvents and thus spraying is a suitable method of applying a thin coating. Several polymethacrylate resins are available commercially including the methyl, ethyl, isobutyl and n-butyl polymers. This is important since the thermal stability is greatly affected by the substitution group.

The second polymer system, which completely degrades into the volatile monomer is the polyformaldehyde or polyacetal. The thermal stability of these polymers depends to a large extent on the endcapping of the polymer chain. The endcapping is applied to the commercial product in order to reduce the decomposition. If, however, a commercial product without this stabilizer is used, the polymer is decomposed to the gaseous monomer at moderately elevated temperatures. Polyformaldehyde is soluble, however, in only such solvents which also dissolve camphor. An experimental technique will have to be developed for the spraying of polyformaldehyde solution without affecting the sublimable coating. This may be achieved by the use of a selective combination of solvents.

A composite technique may be used to overcome the application problems for this otherwise suitable material. According to one supplier, thin films of the polymer could be obtained. The film would be cut to the shape of individual panels, and access ports, and bonded to the frames with conventional adhesives or by fusing the edges into the camphor coating. This method would result in a complete, pinhole free coating, permitting the opening and closing of various ports providing a good moisture and vaporization barrier. The development work necessary for the successful application of this process, does not appear to be excessive and the required materials are commercially available.

VIII. REFERENCES

1. Buwalda, E. P. and A. R. Hibbs, J. P L. External Publication No. 481 (April 1958).

2. Schatz, E., Thermal Radiation Properties of Binary Mixtures, presented at the AIAA Thermophysics Specialists Conference, Monterey, Calif. (September 1965).

3. Pezdirtz, G. F. and N. T. Wakelyn, Ultraviolet Stability of Some Modified Metal Phosphates, Sixth National SAMPE Symposium, Materials for Space Vehicle Use, Seattle, Washington, (November 1963).

4. Hass, G., L. F. Drummeter, and M. Schach, Temperature Stabilization of Highly Reflecting Spherical Satellites, J. Opt. Soc. of Am., 49, No. 9, pp. 918-924, (September 1959).

5. DeVos, J. C., A New Determination of the Emissivity of Tungsten Ribbon, Physica 20, 690 (1954).

6. Johnson, F. S., The Solar Constant, J. Meteor. 11, 431 (1954).

7. Fischell, R. E. and L. Wilson, Spacecraft Application of Subliming Materials, J. Spacecraft 2, p. 376 (June 1965).